SENSORY SOURCE IDENTIFICATION FROM NERVE RECORDINGS WITH MULTI-CHANNEL ELECTRODE ARRAYS

by

Paul Richard Christensen

B.A.Sc., Simon Fraser University, 1994

THESIS SUBMITTED IN PARTIAL FULFILLMENT OF THE REQUIREMENTS FOR THE DEGREE OF MASTER OF APPLIED SCIENCE

in the School of Engineering Science

SIMON FRASER UNIVERSITY

July, 1997

ABSTRACT

After a stroke or spinal cord injury, the voluntary use of paralyzed limbs may be partially restored with Functional Electrical Simulation (FES). To restore the use of paralyzed hands, it would be beneficial to also recover the sensory signals originating from natural receptors in the individual fingertips. Several approaches are possible for recording sensory nerve activity from multiple sources, including 1) implanting electrodes on individual digit nerve branches in the hand, 2) implanting multiple intrafascicular electrodes in larger nerve trunks in the forearm, or 3) implanting cuffs containing multiple electrodes around the forearm nerve trunks.

The first approach is the least practical because it is surgically more time-consuming and has the greatest potential for nerve damage. In this thesis, I have evaluated the other two approaches with Multi-Contact nerve Cuffs (MCCs) in acute and chronic experiments and with arrays of Longitudinal IntraFascicular Electrodes (LIFEs) in the chronic situation. Hindlimbs and forelimbs of anesthetized cats were used as models for the paralyzed human forearm and hand. Electrical and mechanical stimulation of the individual digits was used to test the selectivity of multi-channel electrode arrays. The results from mechanical stimulation were further analyzed to determine the accuracy of digit identification from features in the recorded neural activity.

The results of electrical digit stimulation tests in acute and chronic situations showed improved levels of selectivity over other investigators' versions of MCCs. As could be expected from their locations and geometries, LIFEs provided more selective recordings and more accurate digit identification than MCCs. In response to mechanical stimulation of the individual digit pads, the digits were correctly identified from their associated neural bursts with 70% to 90% accuracy for MCCs and 80% to 100% accuracy for LIFEs. These results indicate that multi-channel neural recordings are a realistic solution for obtaining sensory feedback information for the control of FES systems in disabled humans.

QUOTATION

This little piggy went to market.

This little piggy stayed home.

This little piggy had roast beef.

This little piggy had none.

And this little piggy went "wee-wee-wee" all the way home.

ACKNOWLEDGMENTS

A lot of Thank You's go out to various groups. My parents, Fleming and Mary, for all the encouragement and support that they have supplied me throughout all my years of school. My brother Brent and friends that have given me support outside of school. Alex Szolnoki and the rest of the members of the Simon Fraser University Science Technical Centre deserve thanks for construction of the various digit manipulators. Kevin Strange, Yunquan Chen, Tiffany Blasak, and Andy Hoffer for assistance, discussion, and support. Mihaela Ulieru for help and discussions on fuzzy logic. Rob Balshaw of the Simon Fraser University's Statistical Consulting Service for some early statistical consultation.

TABLE OF CONTENTS

LIST OF TABLES

LIST OF FIGURES

CHAPTER 1 : INTRODUCTION

Purpose

When a person becomes paralyzed from a spinal cord injury or stroke, there is a loss of voluntary control of the muscles whose motoneurons are located below the lesion. Above the lesion, full conscious control is retained and below the lesion they system works improperly because it does not have normal descending input. At the level of the lesion, the damaged motoneuron cell bodies eventually die forming a "dead zone" of denervated muscles. Even though voluntary control of muscles has been lost, the sensory receptors are still active, but the information may be unable to reach the brain where it is normally needed in the process of executing movements.

One way to restore some voluntary control to a partially paralyzed person is with Functional Electrical Stimulation (FES), whereby select muscle groups may be electrically stimulated to provide some degree of mobility. Because the neural innervations and muscular attachments in the human body are so complex, it is very difficult to return normal function although some crude function may be restored such as standing, some walking, and some reaching and grasping (Nathan, 1993; Franken, Veltink, and Boom, 1994). Normally the stimulation system is controlled by the person through some part of their body that still retains some voluntary motion, such as the contralateral shoulder for quadriplegics (Buckett, Peckham, and Strother, 1980; Nathan, 1993) or the hands for paraplegics (Franken, Veltink, and Boom, 1994).

Currently, several implementations of FES systems are crude due to their open-loop configuration. The user controls a joystick (Buckett, Peckham, and Strother, 1980) or presses a button and a programmed series of electrical stimulations to the muscles is executed to achieve the desired task. However, this type of system does not respond well to disturbances and may cause trouble for the user as the system does not adapt to accommodate changes in surfaces, loading situations, or velocities of movement.

With the use of feedback in a closed-loop FES system, finer control may be achieved so a target force (Haugland and Hoffer, 1994; Crago, Nakai and Chizeck, 1991)

or position (Yoshida and Horch, 1996) may be maintained and fatigue may be reduced (Haugland and Hoffer, 1994). Closed-loop systems inherently accommodate to disturbances through the use of feedback to maintain a target position, force, or trajectory. Lemay et al. (1993) studied the improvements that can be achieved by using closed-loop control over open-loop control systems in a hand neuroprosthesis.

Feedback sensors may be of two types: electromechanical transducers that are mounted external or internal to the body, such as force plates, length gauges and accelerometers, or transducers that tap into the body's intrinsic sensors, such as proprioceptors and cutaneous receptors (Hoffer, 1990; Hoffer and Haugland, 1992). When intrinsic sensors are used, a mapping between recorded activity and force or position must be made because natural activity is not encoded in easily identifiable units. By tapping into intrinsic sensors some of the problems associated with artificial sensors may be avoided, such as loading of the instrumented limb or digit, cosmesis, and changing sensor properties that occur as the transducers change position over time. Crago et al. (1986) examined the different properties that various sensors must have to be effective for feedback in different neuroprostheses.

The work contained within this thesis is a study within the field of FES to increase the amount of information that can be obtained from a single nerve or nerve branch in a chronic situation. Currently, a single channel of whole nerve or single nerve branch activity can be monitored and used as feedback input to an FES system with nerve cuffs (Sinkjaer, Haugland, and Haase, 1994). By using multi-channel nerve cuffs, I hope to obtain more select information from the same number of implanted devices so that eventually more sophisticated FES controllers may be developed. For instance, reaching and grasping tasks may be augmented so that individual finger control may be achieved rather than just the thumb and a grouping of fingers. In such situations, several channels of information could to be recorded and processed to determine when a digit has made contact with an external surface and which digit had reached the surface. After contact, the FES controller could vary its output to the muscle that spans the joint of the limb segment that has made contact with the surface, but continue stimulating other muscles until all of the digits have made contact with the surface. This refined control would

result in less fatigue to the muscles responsible for moving the digits and allow more specific function.

To achieve this future goal, members of the Neurokinesiology Laboratory at Simon Fraser University (SFU) including myself have designed and constructed a Multi-Contact Cuff (MCC) and have studied its performance in long term experiments. The forelimb of the anesthetized cat was used as a model of the human paralyzed forearm and hand because the anatomy, neural innervation, and dimensions are similar in both cases. An anesthetized subject was necessary to remove voluntary or involuntary muscle activity that would occur in an awake animal and which does not occur in a paralyzed person.

The members of the NIH team included Yunquan Chen who helped design the new MCC, developed the theory for the selectivity measure presented in this thesis, and designed and constructed low-noise high-gain amplifiers. Kevin Strange was responsible for design and construction of the MCCs, implanted the MCCs in the chronic experiments, recorded electroneurographic data, and analyzed the electrical stimulation studies in the later stages. Tiffany Blasak provided animal care throughout the experiments. Ken Yoshida designed, constructed, and implanted the Longitudinal IntraFascular Electrodes (LIFEs). Andy Hoffer acted as senior supervisor and oversaw all aspects of the project including cuff and amplifier design, surgeries, and recording protocols. I helped design the new MCC, designed the digit manipulator, assisted in the recordings, and processed and analyzed the collected data in these experiments.

The work contained within this thesis was conducted as part of and supported by a three year National Institutes of Health (NIH) research contract that was awarded to Dr. Andy Hoffer as Principal Investigator. The scope of the NIH contract is to develop new techniques to allow selective recordings from various digit sources and selective stimulation to different muscle groups. I have limited my work to the first year of this contract.

This thesis details my contribution to the different phases in the first year of the NIH contract. A new and improved MCC was developed by the NIH team, implanted and evaluated. The degree of selectivity that could be achieved with the new and improved

MCC was first determined by electrically stimulating different nerve branches in acute experiments and then moved to chronic experiments. An array of LIFEs, which were developed, constructed at the University of Alberta, and implanted at the SFU Neurokinesiology Laboratory by Dr. Ken Yoshida of the University of Alberta, Edmonton, was similarly evaluated in the chronic situation. To conduct the experiments for the project, I developed a two dimensional digit manipulator that is capable of producing mechanical perturbations, in directions normal to and tangential to the digit pad in the forelimb of a cat. The data analysis was conducted off-line using functions and routines in the Microsoft Excel, SPSS, and The Mathworks Matlab environments.

The layout of this thesis presents in approximately chronological order the background science and applications that my colleagues and I developed using the new multi-contact cuff that we designed. A method to test the efficacy of the new recording cuff and any other similar device or multi-channel recording array is also presented. I then discuss the results of three acute experiments that were performed to test the new MCC through direct electrical stimulation of various nerve branches. Subsequently in chronic experiments, the electrical stimulation experiment in the acutes was extended to electrical stimulation of the digits that indirectly stimulated the individual nerve branches in the forelimb, and a mechanical stimulation protocol was used to test the selectivity of the cuff and to determine to what degree individual digit identification could be possible. At the end of this thesis I outline future objectives and other processing techniques that may be applied to similar sets of data.

Sections of the work presented in this thesis will appear in papers accepted for publication at the International Functional Electrical Stimulation Society's second annual conference to be held in Burnaby in August of 1997 (Hoffer et al., 1997; Chen et al., 1997; Strange et al., 1997; and Christensen et al., 1997).

Objectives

At the start of this project, I planned to address and answer the following questions.

To what degree can one make selective recordings with multi-channel electrode arrays?

Other researchers (Lichtenberg and DeLuca, 1979; Struijk, Haugland and Thomsen, 1996; Sahin and Durand, 1996) had shown that it was possible to make selective recordings with a MCC in acute experiments, although the published results had not been spectacular. We developed a new MCC design that was evaluated in acute and chronic experiments that is detailed within this thesis. Prior to the current NIH contract, LIFEs had been used as selective recording and stimulation devices with success and it was decided that the results of selective experiments with this electrode would be compared to our MCC.

To what degree can multi-channel electrode arrays be used to identify individual digits from recorded neural signals?

MCCs and LIFEs were implanted in animal subjects for chronic experiments and electrical and mechanical stimulation experiments were designed to evaluate the selectivity of the two recording arrays. Further mechanical stimulation experiments were used to evaluate whether individual stimulated digits could be identified from associated neural bursts arising in response to the stimuli.

How are selectivity and accuracy of digit identification related?

To determine the expected accuracy of digit identification in a given experiment, the relationship between accuracy in digit identification and selectivity was analyzed.

CHAPTER 2 : BACKGROUND

Neural Anatomy

In order to understand how electroneurographic (ENG) activity recorded by electrodes in the forelimb correlates with sensory activity arising from the individual digits, it is necessary to have some knowledge of the physiology and anatomy of the system.

Neural pathways and anatomy

Typically, a nerve is composed of a few fascicles which are composed of hundreds of axons, the smallest functional neural unit, that innervate tissue, organ, or muscle (see Figure 2.1). Motor nerve axons conduct from the ventral horn in the spinal cord to muscle units in the periphery.

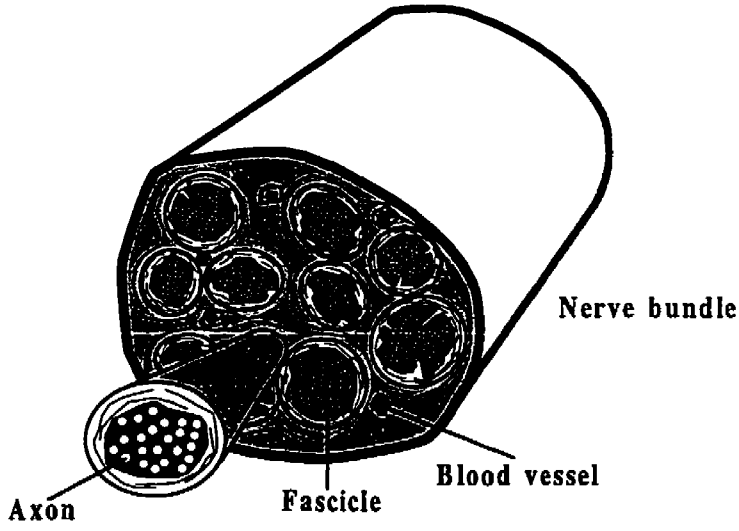

Figure 2.1: Stylized cross section of a nerve

Sensory nerve axons conduct centripetally from the periphery and transmit information generated by individual muscle spindles, Golgi tendon organs, pain or temperature receptors, or mechanoreceptors in skin or joints. Sensory axons collect into one large nerve or several nerves which enter the dorsal horn of the spinal cord where the individual

axons terminate on interneurons, motor nerves, or ascend through various pathways to the dorsal column nuclei in the brainstem or thalamus in the brain (see Figure 2.2).

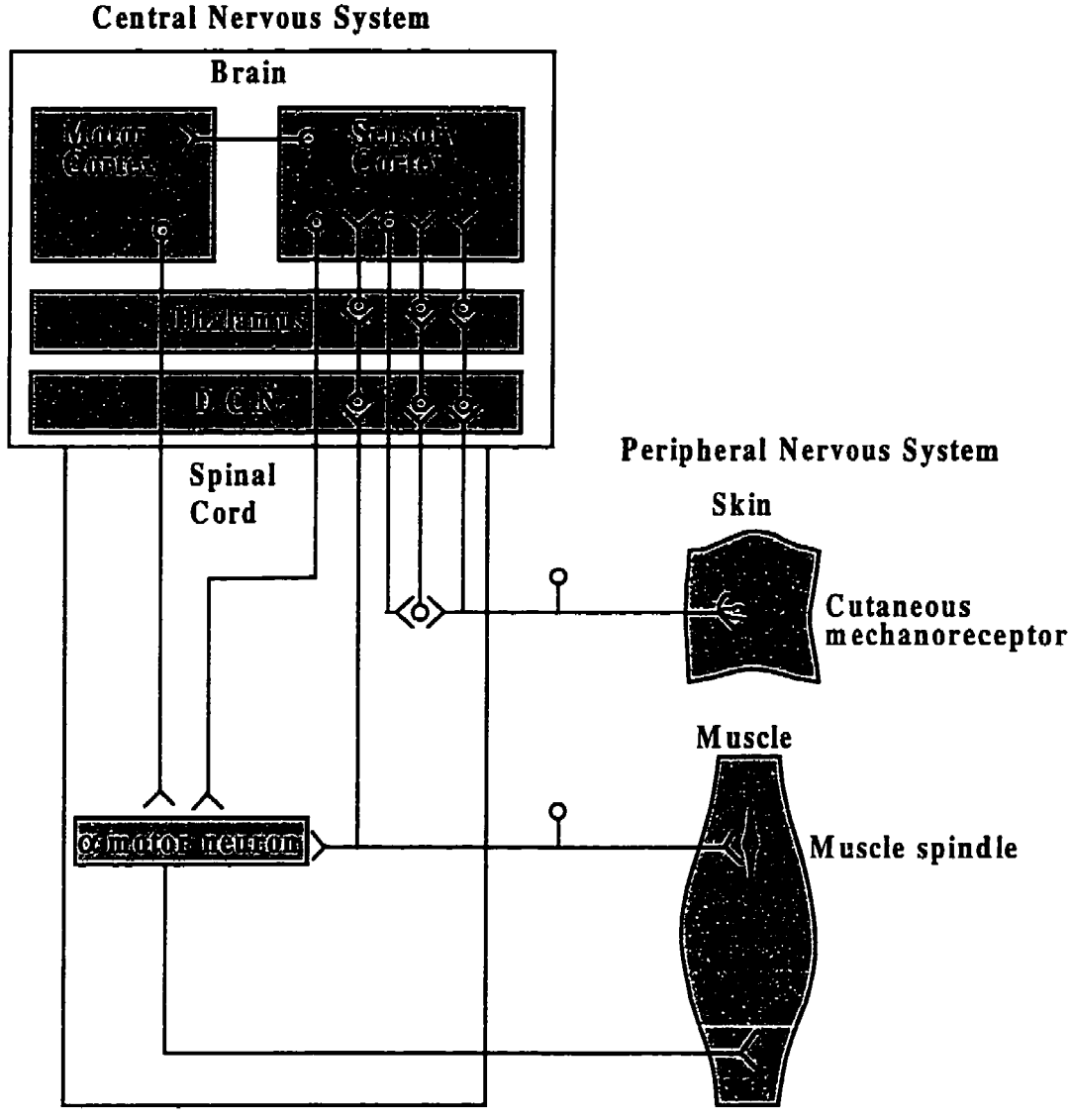

Figure 2.2: Some of the major neural pathways between the cortex and the periphery

Neural receptors

After mechanical stimulation is applied to the digit pads, most recorded neural activity is predominantly from cutaneous receptors and muscle spindles. Activity from muscle spindles is due to stretching of the muscles, whereas activity from cutaneous receptors is normally due to deformation of the skin from contact, vibration, and

movements across the surface of the skin. In this project, spindle activity can be expected from the intrinsic muscles of the forepaw: the lumbricales are innervated by the median nerve and other small palmar muscles are innervated by the ulnar nerve (Crouch, 1969). Activity from cutaneous mechanoreceptors is expected from the time of contact of the mechanical stimulus until it leaves the surface of the digit pad. Direct and indirect electrical stimulation of nerve branches elicits responses in all types of sensory afferent nerves from type I and II muscle spindles to Aβ mechanoreceptors.

Cutaneous mechanoreceptors

Cutaneous mechanoreceptors are responsive to touch and contact on the surface of the skin. As such, they are good indicators of when the skin reaches a surface because they release a burst of activity upon contact and often upon release as well with skin deformation. These types of receptors become active when the skin is rubbed across a surface to determine a texture (Srinivasan, Whitehouse and LaMotte, 1990) or when an object slips across the surface of the skin (Johansson and Westling, 1987). The cutaneous mechanoreceptors are located at the dermis and epidermis junction of the skin and lower in the subcutaneous tissue.

There are four major types of cutaneous mechanoreceptors based on responses to mechanical stimuli and sizes of receptive fields (Rothwell, 1994; Kandell, Schwartz and Jessel, 1991; Westling and Johansson, 1987). FAI, which have Meissner corpuscles as their terminals, are fast adapting receptors whose responses are specific to a small patch of skin (about 10 mm^2). The FAII, which terminate in Pacinian corpuscles, are deep receptors with large receptive fields that are responsive to high frequency inputs like vibrations. The fast adapting receptors are suited to detect the rate of deformation in the skin as they release a burst of activity when the skin deforms upon indentation or release, such as when an object is grasped or released, or when an object slips through the fingers. Superficial SAI units, with terminals in Merkel discs, and deep SAII units, with Ruffini endings, are responsive to prolonged indentations of the skin and to the rate of indentation of the skin. They release a burst of activity when the skin becomes deformed and they

maintain their output discharge with constant deformation of the skin. SAII are also responsive to the direction of stretch.

Muscle spindles

Muscle spindles are transducers that convert muscle fibre length, velocity, and acceleration to trains of electrical impulses. Generally, when a muscle is stretched, the spindles increase their output ENG activity and when it is shortened they reduce their activity. (Kandell, Schwartz and Jessel, 1991).

In this project, some activity from muscle spindles is expected after a normal input has been applied to the digit. This stimulus causes the digit flexor muscles and perhaps other palmar muscles to be stretched. Activity from the radial lumbricales is expected in the median nerve and activity from other palmar muscles in the ulnar nerve.

Neural innervation of the forelimb

From a review of a standard cat anatomy atlas (Crouch, 1969), we can see that, similar to the human hand, the innervation of the cat forepaw is quite extensive with several small branches to each of the digits. Figure 2.3 shows the palmar surface of the right forepaw of the cat. For the purposes of this project, I concentrated on the median and ulnar nerves and their patterns of branching. A review of a human anatomy text (e.g., Palastanga, Field, and Soames, 1994) verified that the median and ulnar nerves follow similar branching patterns in the human forearm and hand, so the general results discussed in this thesis can be transferred to the human.

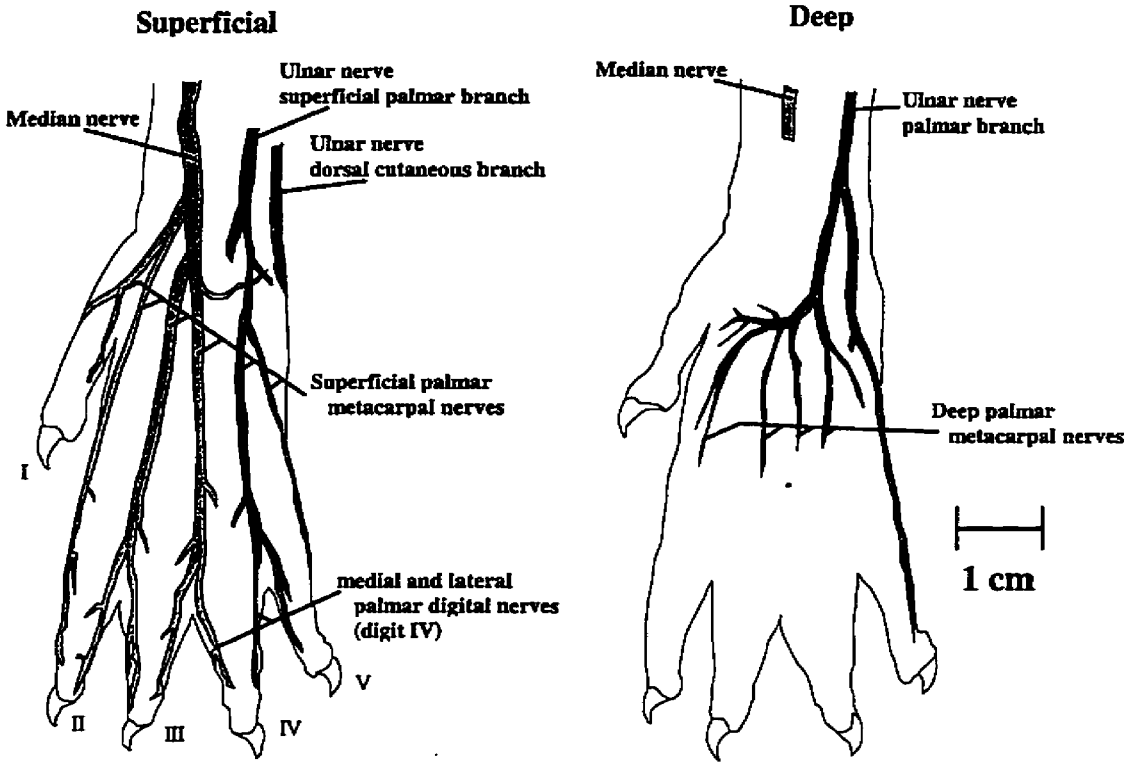

Figure 2.3: Cat forepaw innervation

Median nerve

Following the branching of the median nerve, it can be seen that it innervates the medial aspects of the forepaw. Specifically, it enters the forepaw on the medial side of the wrist and quickly makes three main branches that form part of the superficial palmar metacarpal nerves, the other part being formed from the superficial branch of the ulnar nerve. The first major branch of the superficial palmar metacarpal nerve branches twice more. The first minor branch branches to innervate each side of the skin of digit I and the second branch innervates the medial side of digit II. The second major branch has two branches to the skin on the contiguous sides of digits II and III. The third branch sends two branches to the skin of the contiguous sides of digits III and IV. These final branches are known as the medial and lateral palmar digital nerves. The metacarpal nerves also give branches to the trilobed palmar pad and to the three radial lumbricales muscles.

Ulnar nerve

The ulnar nerve innervates both the palmar and dorsal surfaces of the forepaw. Observing the ulnar nerve, we can see that it innervates the fourth and fifth digits, the surface of the palm, and the volar surface of the wrist.

The palmar branch of the ulnar nerve enters on the lateral side of the wrist and forms two major branches: the superficial palmar branch and the deep palmar branch. The superficial branch enters the palm of the forepaw and also the skin of the ulnar side of digit V and the contiguous sides of digits IV and V. The deep palmar branch bends towards the radial side of the forepaw and gives off deep palmar metacarpal nerves to the short muscles of the palm.

The dorsal cutaneous branch of the ulnar nerve comes from the palmar side of the forearm to the dorsum on the lateral side of the wrist. It divides into two dorsal metacarpal nerves, the first of which innervates the ulnar side of digit V and the second forms digit nerves to the contiguous sides of digits IV and V.

Expected results

From this brief analysis, one should expect to see activity in the recording electrode arrays on the median nerve due to perturbations in digits I through IV and to the palm of the forepaw. Activity in the recording arrays on the ulnar nerve should be seen when a disturbance is present on the palmar or dorsal surfaces of digits IV and V and to the palm of the forepaw. The fact that two small branches innervate each digit may be advantageous because more neural activity may lead to stronger signals and better chances of correct digit identification.

Relationship between neural innervation and implantation sites

One way to obtain selective channels of ENG information would be to implant electrodes into each of the digits and record information from the small nerve branches there. However this technique suffers many drawbacks. It requires very fine surgery skills to implant the electrodes due to the small size of the nerve branches in the digits, and the presence of surrounding small muscles and tendons further complicates the

surgical procedure. Also the highest potential for nerve damage occurs when applying an electrode to a very small nerve as the electrode is very large in comparison to the nerve and may cause mechanical loading on the nerves. Finally, implanting electrodes on five digits is very time consuming.

A second, less invasive technique which requires fewer implanted electrodes and perhaps causes less injury to the nerve involves implanting a Multi-Contact Cuff (MCC) about a large nerve. The cuff can be installed easily about the nerve and the electrodes remain just outside the surface of the nerve. Although the signals detected at each of the electrodes may not provide the same level of selectivity of recordings, the differences in the sets of recorded signals may be sufficient to make source identification possible. Two of these MCCs were implanted on the median and ulnar nerves to form an eight-channel electrode array.

Another way to obtain selective ENG information is to put several small electrodes that record activity from small regions inside a larger nerve. This technique provides very selective information because only a single fascicle's activity is recorded by each electrode. However, this technique suffers from a long surgical procedure as well, and the fine wires may break. Four Longitudinal IntraFascicular Electrodes (LIFEs) were implanted in each of the median and ulnar nerves to form a second type of eight-channel electrode array.

Information Content in Neural Recordings

Several research groups have studied the information contained within neural signals arriving from the periphery for both basic and applied scientific reasons. Johansson and Westling (1984, 1987) have investigated the relationship between grip force and slip in the human fingertips from recordings made in the forearm. Haugland and Hoffer (1994) used the information contained in slip signals in the central footpad of the hindlimb of the cat under general anesthesia as feedback to an FES controller that would prevent slip.

Johansson and Westling (1987) analyzed cutaneous ENG activity arriving from single mechanoreceptors in the fingertips after slips between the index finger and thumb occurred while lifting an object. Microneurographic techniques were used to record activity from individual neurons in the median nerve of human subjects. They discovered that information from cutaneous origin can reflexively modify muscle force in the forearm to prevent slip, without conscious effort. The time scale for the reflex is about 75 ms whereas a conscious effort to prevent slip would require at least 175 ms for the person to realize that a slip is occurring and then take appropriate action.

Milner et al. (1991) studied the relationship between cutaneous neural activity recorded by a tripolar recording cuff implanted around the median nerve in the monkey and the load and grip forces exerted. They discovered that the initial burst in neural activity that occurred when an object was lifted was best related to the rate of change of grip force and when the object was held in position the neural activity was related to the mean grip force.

In an experiment by Haugland and Hoffer (1994), the cutaneous information that is present when a slip occurs was analyzed and used in a closed-loop FES system to control muscle force. In this study, the hindlimb footpad was placed against a block that could slide freely in the vertical direction. Neural signals were recorded from the tibial nerve with a tripolar nerve cuff implanted on the tibial nerve below the last motor branches that innervate the calf muscles and neural activity was recorded and used to control an FES controller for four ankle extensor muscles. When a slip was detected, the muscle stimulator output was increased to increase the force in the implanted ankle extensor muscles which would stop the block from sliding. In this study, it was found that ENG recorded in the tibial nerve provided reliable signals for slip detection.

In a related study by Haugland, Hoffer and Sinkjaer (1994), the relationship between perpendicularly applied force and ENG activity was examined in animals under general anesthesia. A rubber probe (14 mm diameter) was pressed against a constrained footpad with a controlled force, and ENG and displacement recordings were made. The ENG recordings were made using a tripolar cuff electrode placed on the tibial nerve below the last motor branches that innervate the calf muscles. The recorded nerve cuff

signals were amplified and bandpass filtered between 1 and 10 kHz to retain the neural signals while removing low frequency electromyographic (EMG) interference, which was also recorded by the cuff electrode, and other high frequency interference. The results from this study suggested that the total ENG activity in the tibial nerve is related to the applied perpendicular force on the hindpad.

More recently, a two-channel system consisting of two tripolar circumferential cuffs implanted on the median and ulnar nerves in the forelimb was used to examine signals arising from the five digits after electrical stimulation of the digits (Hoffer et al., 1994). This thesis extends the work initiated in the last experiment by evaluating the increased amount of information that can be obtained from a whole nerve by analyzing the information content from multi-channel recording arrays.

Previous Research in Selectivity with Multi-Contact Cuffs

Selective recordings involve the ability to determine the source of an input signal from amongst many possible signal sources. A couple of decades ago and again more recently, different groups studied the issue of making selective recordings using a single recording cuff (Lichtenberg and De Luca, 1979; Struijk, Haugland and Thomsen, 1996; Sahin and Durand, 1996). They used similar preparations, electrode arrays, and recording methods — all groups used anesthetized animals with direct electrical stimulation of nerve branches. This preparation provides signal sources that have no noise contamination from EMG interference and little natural background activity. Recordings of the resulting compound action potentials were made with nerve cuffs located at sites proximal to the stimulation sites.

However, the type of analysis and the definition of selectivity has varied from group to group. The common definition of selectivity has been some sort of measure of the difference in the amplitude of recorded signals that arise from different sources. Sahin and Durand (1996) defined selectivity simply as the observed difference in normalized signals. Lichtenberg and De Luca (1979) used a statistical difference to measure selectivity and more complex mathematical modeling to calculate the centre of electrical

activity in the cross section of a nerve. Struijk, Haugland and Thomsen (1996) used comparisons of ratios of recorded signals to develop a selectivity measure.

Lichtenberg and De Luca

In 1979, Lichtenberg and De Luca studied the question of selective recordings in the sciatic nerve of the rabbit. Six nerve branches - peroneal, plantaris, lateral gastrocnemius, tibial, flexor digitorum longus, and soleus - were stimulated with hook electrodes and recordings were made from five different sites along a 2.3 cm section of the sciatic nerve. The electrode used was a nerve cuff 10 mm long and 2.3 mm in diameter, which had slightly smaller cross section than the sciatic nerve and caused a tight fit about the nerve. Eight wires were placed in the cuff with four in each of two transverse planes separated by 2 mm. Circumferential recordings amongst pairs of wires in the same plane were made, as well as recordings between the longitudinal pairs.

To analyze the data, the recordings made from each pair of electrodes were averaged over all of the stimulation trials and then normalized to the maximum recorded amplitude on a given channel for each nerve branch. Duncan's multiple range test was used to indicate significant differences in the means of the normalized amplitudes as a function of the stimulated nerve branch. In both the longitudinal and circumferential studies, the peroneal nerve could be most easily identified from the other extensor nerve branches with less selectivity present amongst the other nerve branches. Later, the longitudinal data was used to estimate the centres of electrical activity within a cross section of the nerve. The results of the estimates "correlate[d] reasonably well with anatomical data describing the location of the nerve fibres" (Lichtenberg and De Luca, 1979).

Struijk, Haugland, and Thomsen

More recently, Struijk, Haugland, and Thomsen (1996) performed their own selective recordings and analysis. They also studied the sciatic nerve of the rabbit, but only stimulated two branches - the peroneal and tibial nerves. Their nerve cuff was 25 mm long with a 4x2 mm^2 cross sectional area, which is much larger than the typical

sciatic nerve at 3x1 mm^2. Twelve electrode contacts were located in the cuff with four electrodes in each of three transverse planes separated by 10 mm.

Two recording configurations were used in Struijk, Haugland and Thomsen's experiments. In the first, a tripolar configuration was used in which three electrodes in a longitudinal line were configured so that the outer electrodes were shorted together to form a reference for the centre electrode. In the second configuration, the reference electrodes from one longitudinal electrode array were tied to the reference electrodes of the other electrode arrays. That is, all of the outermost electrodes were connected and the four inner electrodes were used as signal sources.

In the analysis of the data, a "selectivity ratio" was defined as the ratio of RMS amplitudes of the recorded CAPs after stimulation of the peroneal or tibial nerves. A "selectivity indicator" was defined as the square root of the product of the two selectivity ratios. Similar results were found for both recording scenarios, with a selectivity indicator of 1.4 for the first configuration and 1.3 for the second configuration.

Sahin and Durand

Sahin and Durand (1996) also studied selectivity with their own electrode array. They conducted studies on the hypoglossal nerve of the Beagle with a tight fitting nerve cuff that would exclude all fluids from inside the cuff. The cuff was 20 mm long, 2.5 mm in diameter, and had twelve contacts in the walls of the cuff. The electrodes were spaced in three transverse planes with 7 mm separation between the planes. Two recording scenarios were used. In the first, tripolar recordings were made along longitudinal sections of the cuff, as in the first Struijk, Haugland and Thomsen case, and in the second, contacts on opposite sides of the cuff were shorted together.

To analyze their data, Sahin and Durand first normalized the recorded CAP data at each contact set by the sum of all recordings at each contact set for a given nerve branch. Next, a "selectivity index" was calculated by normalizing the data from the first step by the sum of the normalized recordings of a given nerve branch. The term "selectivity" then refers to the spread in the selectivity indices of a contact set for various fibre subpopulations. The selectivity was found to be better for the second recording scenario.

Sahin and Durand's conclusion was that selective recordings are possible, "but the effects are small" (Sahin and Durand, 1996).

Previous Research in Selectivity with Longitudinal Intrafascicular Electrodes

Much work with Longitudinal Intrafascicular Electrodes (LIFEs) has already been performed with stimulation of select nerve branches (Nannini and Horch, 1991; Yoshida and Horch, 1993; Veltink, van Alste and Boom, 1989) and selective recording studies performed by Horch and others. Goodall, Lefurge and Horch (1991) studied the information content in ENGs recorded with LIFEs implanted chronically in the radial nerve in the forelimb of cats by stimulating different cutaneous receptors in the digits. More recently Yoshida and Horch (1996) used the ENG recorded in the peroneal and lateral gastrocnemius nerves in the hindlimb to control the position of the ankle by stimulating the tibial nerve to the lateral gastrocnemius muscle in a rabbit with the joint placed under different loads. McNaughton and Horch (1994) classified individual action potentials recorded by LIFEs in the radial nerve after stimulation of individual mechanoreceptors using linear discriminant functions, neural networks, and other classification techniques.

CHAPTER 3 : ELECTRODES

Multi-Contact Cuffs

The Multi-Contact Cuff (MCC) that was used for this research is a proprietary design by J.A. Hoffer, Y. Chen, K.D. Strange and myself. It is a specially designed recording electrode capable of recording from multiple sites about a nerve. More details about the MCC cannot be provided here as we are in the process of writing a patent application. As opposed to a conventional nerve cuff with circumferential electrodes that record the aggregate activity of all nerve fibres within a nerve, the MCC is able to record activity from specific regions within the same nerve. A schematic example of a MCC with several representative electrodes is shown in Figure 3.1.

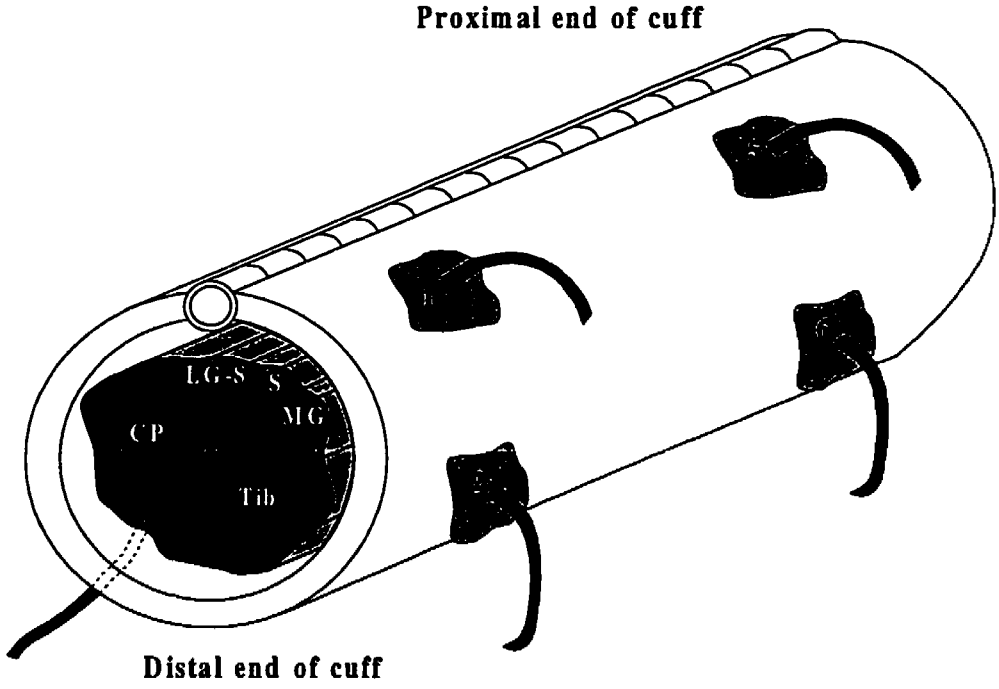

Figure 3.1: Example of a multi-contact cuff

Figure adapted with permission from a sketch by K.D. Strange

The MCCs used for this study had four pairs of recording electrodes placed around the circumference of the cuff. Each pair was aligned along the longitudinal axis of the nerve to record currents from action potentials traveling inside the cuff. Two

MCCs were implanted in the left forelimb of each of three cats to form an eight-channel recording array.

Longitudinal IntraFascicular Electrodes

The alternate recording array that was implanted into the forelimb of three other cats was of a quite different configuration. Four separate electrode pairs were sewn into each of the median and ulnar nerves at approximately the same locations where the MCCs were placed. The original design of the Longitudinal IntraFascicular Electrode (LIFE) is detailed in papers by Malagodi, Horch, and Schoenberg (1989) and Lefurge et al. (1991). The LIFEs used in this series of experiments were modified from the original design and constructed by K. Yoshida at the University of Alberta, Edmonton (personal communication, 1997). A diagram of a LIFE implanted in a nerve is shown below (see Figure 3.2). Each LIFE was composed of two separate wires each with a small unshielded platinum-iridium section about 0.5 mm long that were separated by about 2 mm. The LIFE approached the nerve entry point from the proximal end, left a large loop for strain relief, was sewn into the nerve in a distal to proximal direction, doubled back on itself, and then sutured at the entry point to prevent motion of the electrode in the nerve. The section of LIFE that was implanted within the nerve was about 6 mm long.

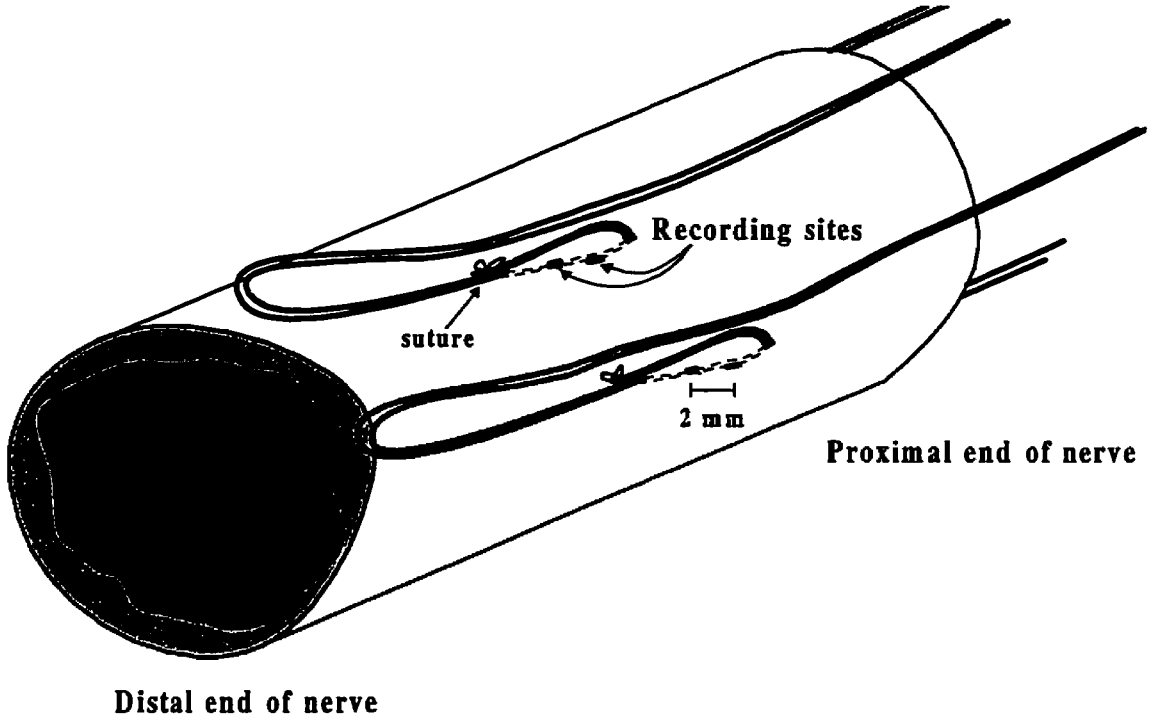

Figure 3.2: Longitudinal intrafascicular electrodes implanted in a nerve

Due to its small size and geometry, the LIFE had a very specific recording region. Typically, the LIFE recorded from a few axons within a single fascicle, so it provided a very selective recording. To obtain multiple sources of the ENG activity within a whole nerve, several LIFEs were implanted into the same nerve.

CHAPTER 4 : SELECTIVITY ANALYSIS

In order to quantify the results obtained with electrical or mechanical stimulation of nerve branches or digits, a technique was developed in our laboratory to measure the average selectivity of a particular experiment. When the electroneurographic (ENG) signals appearing at the sets of electrodes changed dramatically with different stimulated sources, a high degree of selectivity was achieved. A data set with optimal selectivity would have perfect separation between all of the source recordings and would be orthogonal, that is the dot product of any two different source vectors would be zero. On the other hand, a data set with an average selectivity of zero would have no separation between data vectors because they would all record the same signal. Thus, the term selectivity is analogous to the concept of orthogonality in linear algebra. In the following sections, I will describe how selectivity values were calculated.

Although other groups have developed their own methods to calculate selectivity indices (see Chapter 2: Background), we derived our own definition of a selectivity index that is based in linear algebra (Chen et al., 1997). Our selectivity measure uses the linear distance between two normalized vectors to give an impression of the level of selectivity of a recording set. The average distance between all pairs of recorded data then form the selectivity measure for a particular cuff or electrode array. In our method, a selectivity of 100 is the maximum possible and a selectivity of 0 implies that there is no discernible difference between any of the source recordings. The more selective a recording system is, the more likely is one able to discriminate recorded neural signals from various nerve branches, fascicles, digits, or other stimulated sites.

Data Vector Representation

A source data vector is comprised of a set of measurements, or features, taken from all of the N-recording electrodes of interest at the same moment of time after that source has been stimulated. These features include the peak-to-peak amplitude of the compound neural signal, the peak of the rectified and smoothed electroneurographic (ENG) signal, or the area of the rectified and smoothed ENG signal. The types of sources

in my project included individual sciatic nerve branches in the hindlimb and individual digits in the forelimb. An N-element data vector is represented mathematically by Equation 4.1 and a reduced two dimensional vector is represented graphically in Figure 4.1.

Equation 4.1: Data vector for source *i*

$v_i = \langle v_{i1} \quad v_{i2} \quad \cdots \quad v_{iN} \rangle$, where $1 \leq i \leq$ number of nerve branches, digits, or other sources and N is the number of electrodes in the array.

The axes e_1 and e_2 represent functions based on a combination of electrodes, for instance, e_1 may represent the sum of the features of the measurement from the median nerve and e_2 may represent the sum of the features taken from measurements on the ulnar nerve.

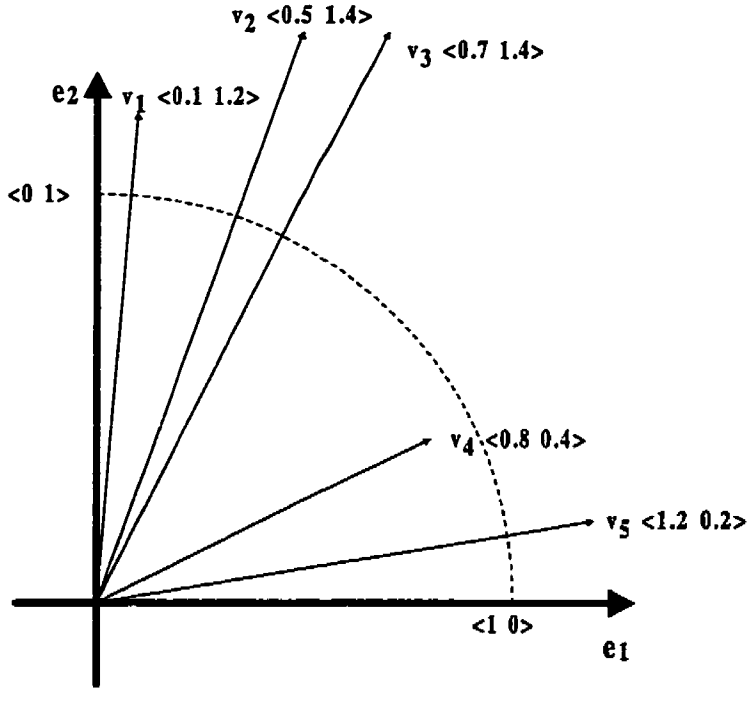

Figure 4.1: Geometrical representation of five data vectors

In order to compare selectivities between different subjects or from the same subject at different times, the data vectors were normalized. This normalization step was included to minimize the dominance of a large signal over smaller signals in the analysis and to reduce the effects of changes in electrode impedance that would change the

amplitudes of the recorded signals. From viewing the vectors in Figure 4.1, one can see that the average linear distance would be dominated by distances calculated from $\mathbf{v_2}$ and $\mathbf{v_3}$. By normalizing these vectors, all vectors in the recording session have the same influence. Equation 4.2 details the normalization step and Figure 4.2 show the normalized vectors from Figure 4.1.

Equation 4.2: Normalizing data vector *i*.

$$v_i' = \frac{v_i}{\|v_i\|}, \text{ where } \|v_i\| = \sqrt{v_{i1}^2 + v_{i2}^2 + \cdots + v_{iN}^2}$$

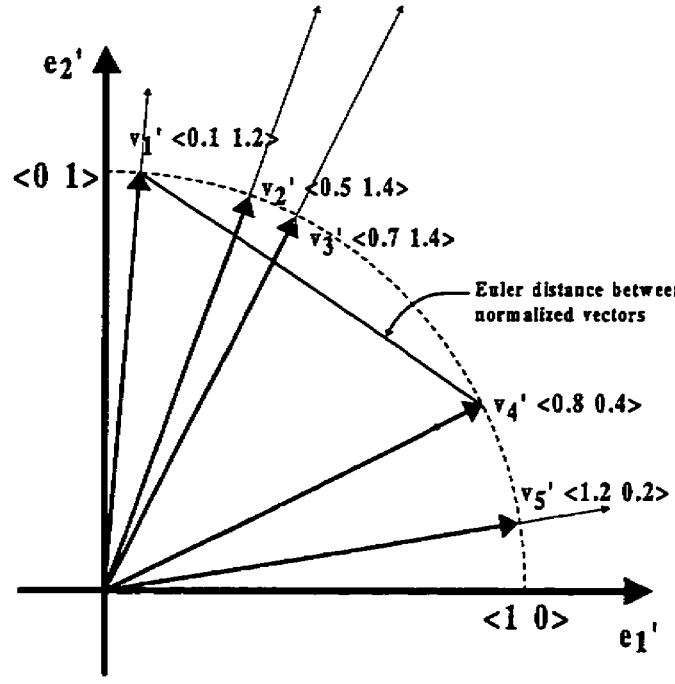

Figure 4.2: Geometrical representation of five normalized vectors

Calculation of the Selectivity Measurement

To calculate selectivity from the degree of separation of the various data vectors, the linear distance between each pair of the vectors is found. Because all of the vectors lie in the first quadrant, the maximum distance between two normalized vectors can be shown to be $\sqrt{2}$. To make the resulting intervector distance measures more readable, we

have further scaled this distance measure by multiplying the result by $100/\sqrt{2}$. This calculation is outlined in Equation 4.3.

Equation 4.3: Euler distance between each of the vectors.

$$d_{ij} = \left|v_i - v_j\right| = \left(\frac{100}{\sqrt{2}}\right) \cdot \sqrt{\sum_{k=1}^{N} (v_{ik} - v_{jk})^2}$$, where $1 \le i,j \le$ the number of nerve branches, digits, or other sources.

An alternate and more precise measure would be to calculate the angle between the normalized vectors. This would be achieved by taking the inverse cosine of the dot product of the normalized vectors and then scaling them by $100/\pi/2$. The angle method was not used because I did not discover the discrepancy in the measurement until much later. However, the error involved in using the Euler distance rather than the angular distance is minimal and probably less than that attributable to noise in the system.

After each of the vectors has been normalized and the Euler distance between each pair of vectors has been calculated and scaled, the average selectivity of a signal source may be calculated. The average selectivity for a signal source is calculated by averaging the linear distance from one vector to all other vectors (see Equation 4.4).

Equation 4.4: Selectivity for each source *i*.

$$S_i = \frac{1}{(M-1)} \sum_{j=1}^{M} d_{ij}$$, for $1 \le i \le$ M, where M is the number of sources.

Because the distance from any vector to itself is 0, the term (M - 1) rather than M is used to calculate the average selectivity for source *i*.

To obtain the overall average selectivity for all signal sources, the aggregate average is taken. In our technique, this is achieved by averaging all of the individual sources' average selectivities to obtain one average selectivity for the whole electrode array. Equation 4.5 shows how this is achieved.

Equation 4.5: Average selectivity for the multi-channel electrode array.

$$S = \frac{1}{M}\sum_{i=1}^{M} S_i$$

The selectivity measure presented in this chapter is the one that is referred to in later chapters of this thesis when discussing the selectivity of a recording. Any other selectivity measures will be noted appropriately.

CHAPTER 5 : ACUTE RECORDINGS FROM HINDLIMB NERVES

In the summer of 1996 we performed three terminal acute experiments under anesthesia to test two alternate Multi-Contact Cuff (MCC) designs as a preliminary stage to future chronic implantations (Chen et al., 1997). All protocols were approved in advance by the Simon Fraser University Animal Experimentation Ethics Committee. Although the details of the experiments differed slightly, the majority of the protocols of the experiments were the same. In each of the experiments, the sciatic nerve of the hindlimb of the cat was exposed and five to eight of its distal nerve branches were dissected free. These nerve branches included the common peroneal, tibial, lateral gastrocnemius-soleus, medial gastrocnemius, sural, perforant branch of biceps, and plantaris.

Recording Scenario

In all of the acute experiments performed, the left hindlimb was used. To prepare for the experiment the cat was sedated with ketamine, acepromazine and atropine, intubated, and anesthetized with halothane gas mixed with oxygen. The nerve branches from which recordings would take place were exposed and disconnected from their muscles to eliminate the effects that stimulation of the muscle may cause, such as contraction of the muscle causing electromyographic activity. The nerves were stimulated with either hook electrodes or a small bipolar stimulating cuff was implanted on each nerve branch. The MCCs were implanted in the mid-thigh region around the sciatic nerve as shown in the lateral view of the hindlimb in Figure 5.1.

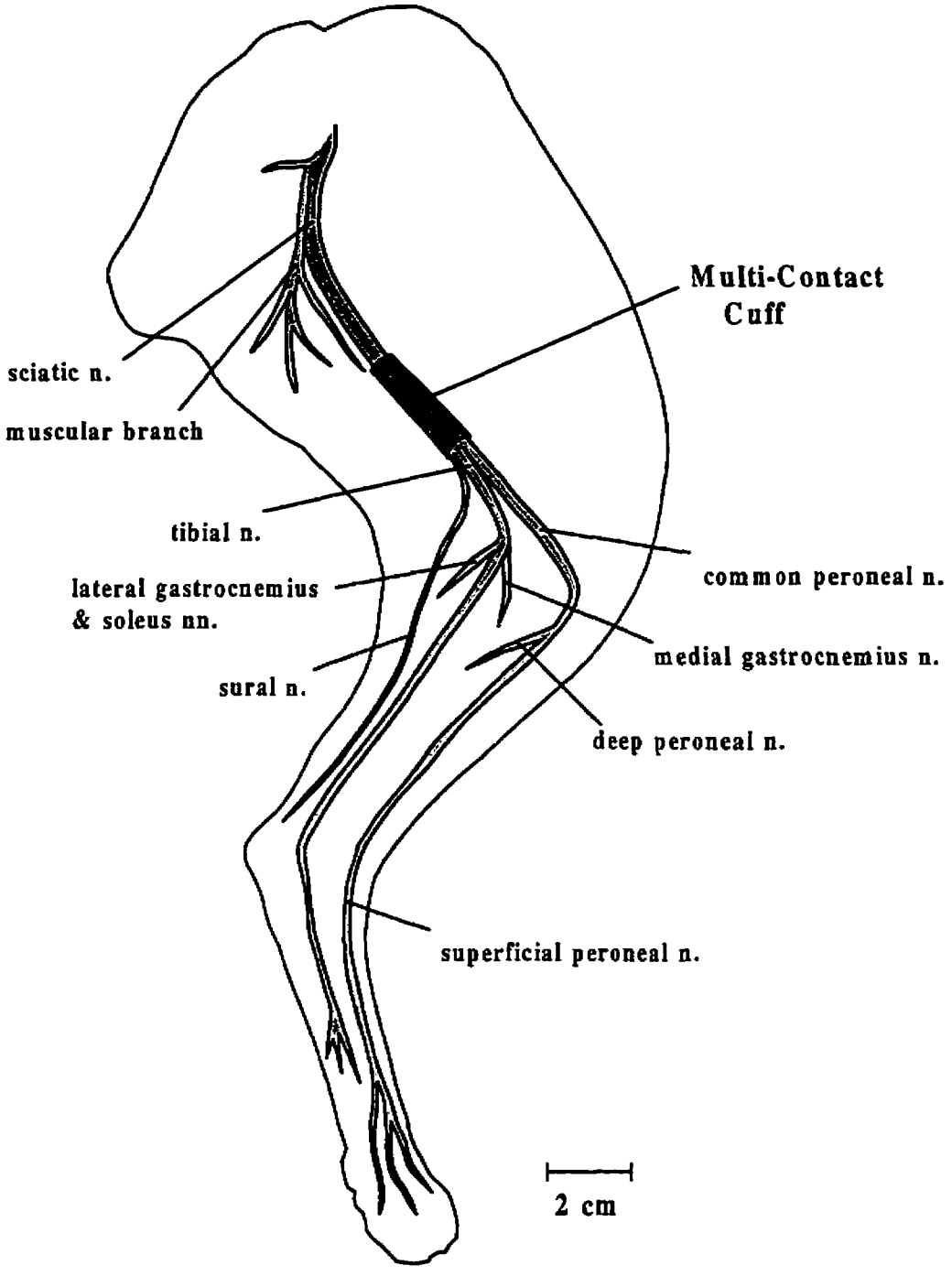

Figure 5.1: Location of multi-contact cuff in the hindlimb

When stimulating the individual nerve branches, current pulses of 50 μsec duration were delivered by an isolated biphasic stimulator with 1 pulse per second repetition rate controlled by a BAK Electronics BPG-2 Biphasic Pulse Generator (BAK Electronics, 1981a). The neural Compound Action Potentials (CAPs) arising from the stimulation, as detected by the electrodes in the MCC, were amplified 10,000 times by

chaining low-noise Leaf Electronics Dual QT-5B Preamplifiers (Leaf Electronics) (gain of 100) and BAK Electronics MDA-1 AC Differential Amplifiers (BAK Electronics, 1981b) (gain of 10x10), filtered between 500 Hz and 10 kHz by the amplifiers, and then stored onto FM tape with a Honeywell MD96C FM tape recorder (Honeywell, 1982). During the recording session, hard copies of the Tektronix TDS420 oscilloscope (Tektronix, 1993) screen displaying four channels of neural signals were printed. The same equipment described here was used in subsequent chronic experiments, only the gain settings on the BAK AC Differential Amplifiers were changed. When eight new low-noise high-gain amplifiers were developed later in the project, they replaced the four Leaf-BAK amplifier chains.

Measurements of the CAP peak-to-peak amplitudes were made later from the paper copies and eventually used in the selectivity analysis described in Chapter 4.

Experiment #1 - June 14, 1996

In this experiment, the first version of our MCC design was installed on the sciatic nerve and five nerve branches - the common peroneal, tibial, lateral gastrocnemius-soleus, medial gastrocnemius, and sural nerves - were dissected free and severed from their distal attachments about 2 - 8 cm from the recording cuff. Hook electrodes were used to stimulate each of the nerve branches and simultaneous recordings were made from the four contact pairs inside the MCC.

A plot of the selectivity of the MCC from Acute #1 is shown below. The selectivity indices that are shown in Figure 5.2 were calculated by the method presented by Sahin and Durand (1996) because we had not yet developed our selectivity measure at the time of this experiment. The degree of selectivity is shown by the amount of spread of the selectivity indices for a given contact set. If there were no selectivity, then each selectivity index would just be given by 100% divided by the number of stimulated nerve branches; in this case, 20%. In contrast, the spread seen in Figure 5.2 is quite large, indicating that the four electrode pairs recorded rather different signals.

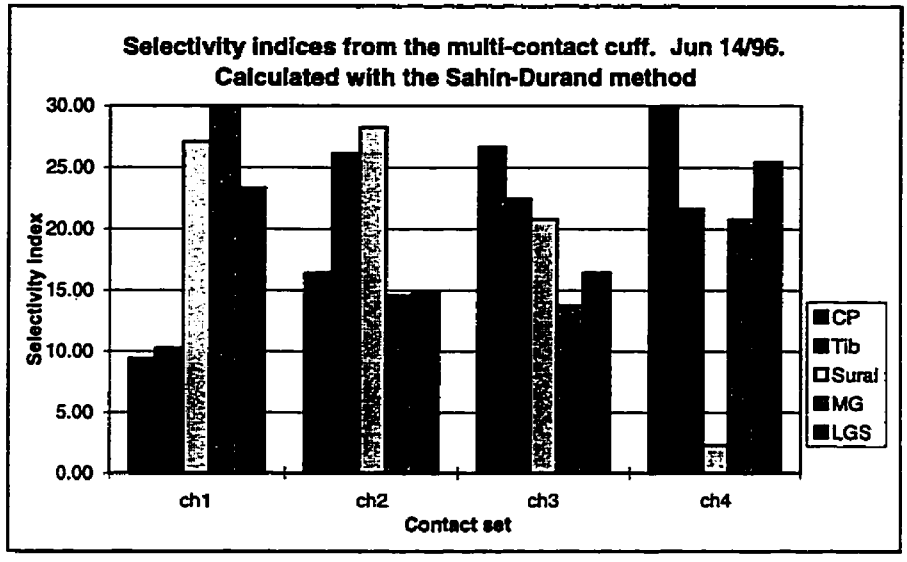

Figure 5.2: Selectivity indices from new MCC in Acute #1 calculated with the method presented by Sahin and Durand (1996)

Note for legend: CP - common peroneal; Tib - tibial; MG - medial gastrocnemius; LGS - lateral gastrocnemius-soleus.

A useful metric to analyze the spread of the results when presented in this fashion is to calculate the coefficient of variation, the standard deviation divided by the mean, of each of the contact sets and then average all of these values to get the coefficient of variation for the whole nerve cuff. For the data set shown, this value was found to be 40%. Figure 5.3 shows the results calculated with our selectivity analysis method. The average selectivity for each of the nerve branches and the overall average selectivity is displayed. The same abbreviations are used in Figure 5.2 and Figure 5.3. With our selectivity measure, the overall selectivity in this experiment was calculated to be 38% out of a theoretical maximum of 100.

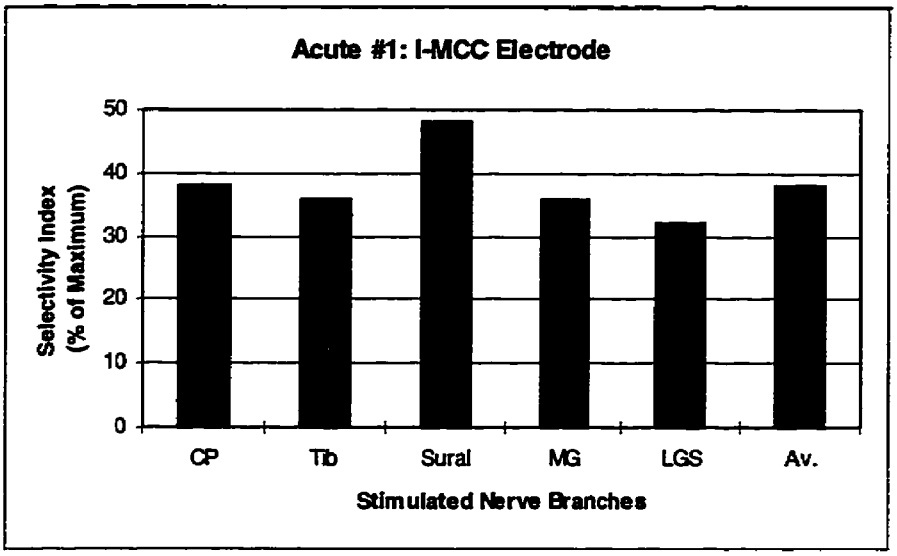

Figure 5.3: Selectivity indices from new MCC from Acute #1 calculated with our selectivity method

The results from this preliminary study showed that selective recordings can be made with our MCC as the different bipolar pairs were selective to specific nerve branches. Typically, the recording pair that was closest to the stimulated nerve branch gave the highest amplitude signal. Figure 5.4 shows the approximate location of the different nerve branches within the MCC. By comparing the results of the selectivity analysis with the position of nerve branches inside the MCC, one can see that the electrodes in the cuff usually produced the highest amplitude recordings for the branches that were closest to the electrode.

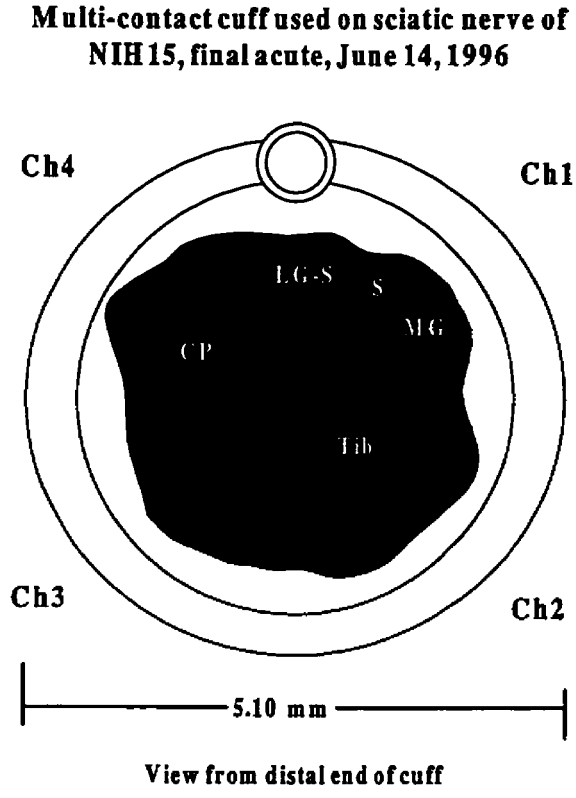

Figure 5.4: Cross section of sciatic nerve showing individual nerve branches within the new multi-contact cuff

Figure adapted with permission from a figure by K.D. Strange.

Experiment #2 - August 13, 1996

In the second experiment, a similar surgical protocol was followed, but this time eight branches of the sciatic nerve were exposed distally to the knee and stimulated. The common peroneal and tibial nerves were each divided into two branches and the perforant branch of biceps was also exposed. This time, stimulating cuffs were implanted onto each of the nerve branches to facilitate stimulation. In this set of experiments, we tested two alternative multi-contact cuff designs, an improved MCC and a conventional MCC (e.g., the design used by Lichtenberg and De Luca, 1979). The improved MCC design was tested three times and then the conventional MCC two times. The results of from one of the improved MCC tests and one of the conventional MCC tests are shown in Figure 5.5 below. Our selectivity measure calculated a value of 30 for the two trials on the improved cuff and the selectivity of the conventional MCC was calculated by our method to be 14.

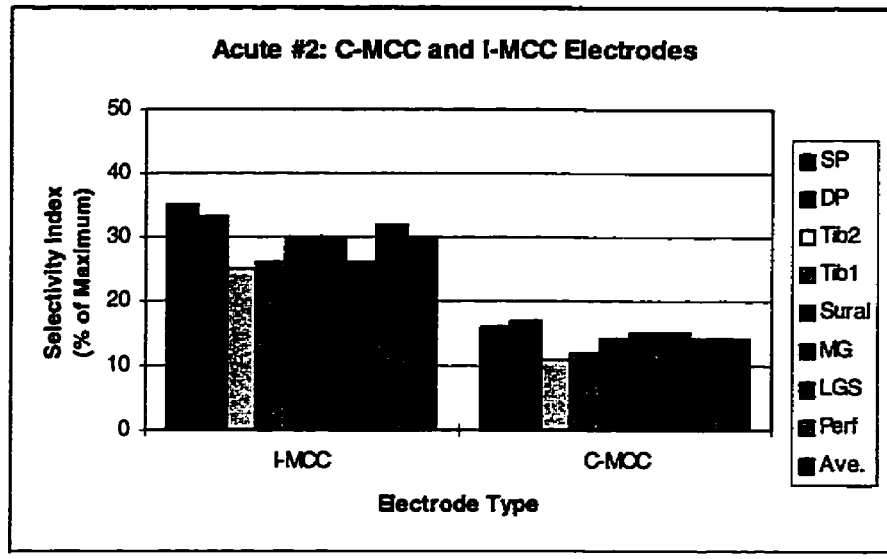

Figure 5.5: Selectivity indices from an improved MCC and a conventional MCC in Acute #2

Note for legend: SP - superficial common peroneal; DP - deep common peroneal; Perf - perforant branch of biceps; other abbreviations as in Figure 5.2.

Experiment #3 - September 12, 1996

After completing the second experiment, we realized that the results of this comparative study were inconclusive because we could not determine whether or not the improved selectivity was due solely to a better MCC design. We could not rule out that nerve conditions did not change over the course of the experiment that might have caused the selectivity to diminish with time. So, in a third set of experiments we alternated between using a conventional multi-contact cuff and an improved cuff. The first and third tests were performed with the conventional cuff and the second and fourth tests were performed with the improved cuff. By setting the experiment up in this manner we hoped to counter any effects that may have occurred if the health of the nerve changed over the course of the experiment and thus affected the measured selectivity. The results of the selectivity analyses for the four tests have been plotted in the following graphs in Figure 5.6.

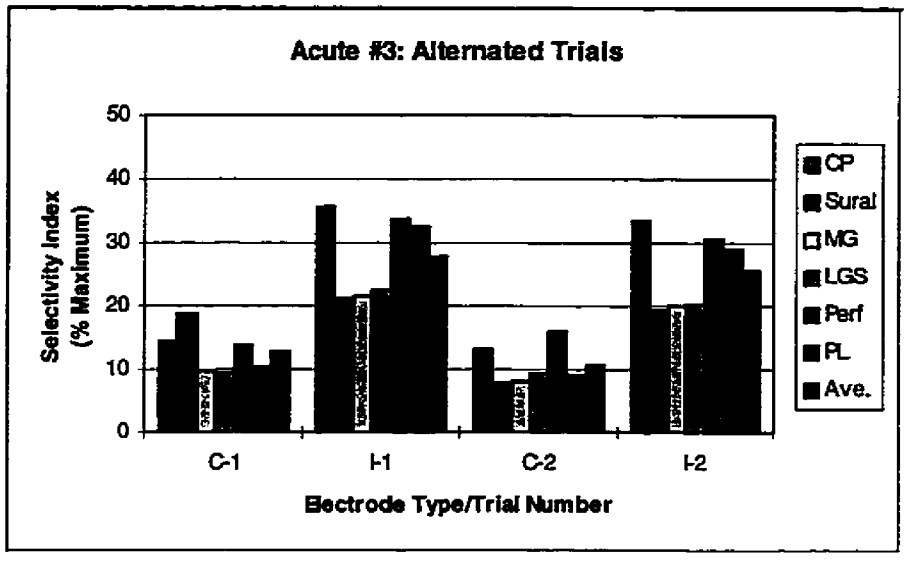

Figure 5.6: Selectivity indices from the improved MCC and conventional MCC in Acute #3

Note for legend: PL - plantaris; other abbreviations as in figures above.

One can see from the charts that the recordings made from the two cuffs are reproducible from test to test. For example, in test 2 and 4, which are the data from the improved cuff, the average selectivities are very similar for both tests and the overall selectivity remains constant. The results from tests 1 and 3 are similar too, but the selectivity of the sural branch changed. The change in individual selectivities may be due to the placement of the cuff changing relative to the nerve branches between the two tests. However, the overall selectivity is similar and remains lower than that observed in the improved cuff.

From the results of this experiment, we concluded that the changes that we made to the conventional multi-contact cuff design did improve the selectivity of recordings from nerve cuffs. We then decided to proceed with chronic implants using the improved MCC design.

CHAPTER 6 : ELECTRICAL STIMULATION OF FORELIMB DIGITS

After the acute experiments demonstrated that our Multi-Contact Cuff (MCC) would provide selective recordings from cat sciatic nerves, we proceeded with implanting similarly designed MCCs in chronic experiments to test how well the cuffs would perform over a six month implant period (Hoffer et al., 1997; Strange et al., 1997). A modified electrical stimulation protocol was used to test the selectivity of using a single MCC implanted on the median or ulnar nerve and the selectivity of using two MCCs on the two nerves. Longitudinal IntraFascicular Electrode (LIFE) arrays were implanted in the same nerves in different subjects and their selectivity was analyzed in the same manner (Hoffer et al., 1997; Strange et al., 1997). Figure 6.1 shows the approximate implantation sites for all devices.

To act as a comparative recording array, tripolar circumferential cuffs were implanted distal to the recording arrays on the median and ulnar nerves of all subjects. Stimulating the median and ulnar nerves with the proximally implanted bipolar circumferential cuffs and making recordings of the ENG activity in the distal cuffs and recording arrays was used as a means to monitor the general health of the nerve and the viability of the electrodes.

All protocols were approved in advance by the Simon Fraser University Animal Experimentation Ethics Committee.

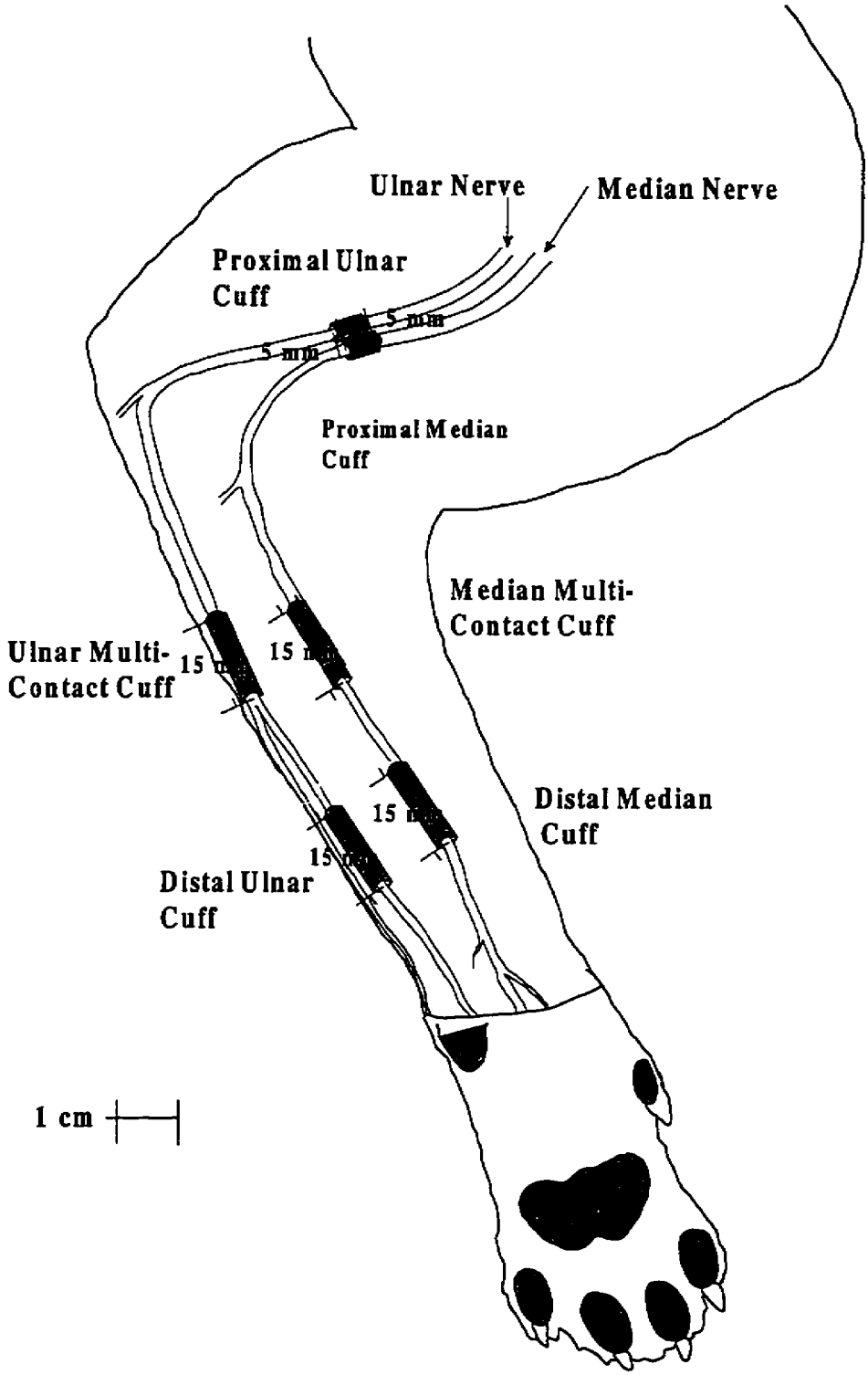

Figure 6.1: Location of devices implanted in forelimb

Adapted with permission from a figure by K.D. Strange

Recording Scenario

We used anesthetized subjects to perform the selectivity evaluation. Electrical stimulation of the digits was performed by placing a cuff around each individual digit with two circumferential electrodes placed 7 mm apart. A constant current stimulator provided 10 mA amplitude and 50 μs duration monophasic current pulses to the digit at a rate of 10 pulses/s. We found that an electrode - tissue impedance of approximately 10 kΩ was necessary to securely stimulate the nerve fibres in the digits and to generate a signal in the recording electrodes. If the impedance was too low, the current would shunt between the two electrodes without stimulating the digit. If the impedance was much higher, the stimulator would not be able to generate the necessary current.

The signals recorded by the two multi-channel arrays were amplified by a gain of 10,000, and stored to FM tape for archiving. Initially due to a limited number of available amplifiers, only four channels of ENG activity occurring on either the median or the ulnar nerve's four-channel recording array were recorded at any one time. The activity from the median and ulnar circumferential cuffs were amplified by a gain of 10,000 by chaining two BAK Electronics AC Differential Amplifiers together. Because electrical stimulation provided an invariant input, the recorded ENG activity did not change much between stimulations when recording activity from the median or ulnar nerves. This fact was verified by the simultaneous recordings from the median and ulnar circumferential cuffs that were made for all recording sessions. The amplitude of the ENG signals from the median and ulnar cuffs were used as controls between recordings from the median arrays and ulnar arrays on the same digit. After a set of eight new amplifiers was constructed, all eight channels of ENG activity occurring on both nerves' multi-channel arrays were recorded simultaneously.

To make off-line measurements of peak-to-peak ENG activity, the FM tape was played back and the signals from individual channels were displayed on the oscilloscope and averaged 10 times. Since the amplitude of uncorrelated noise decreased approximately by the square root of the number of samples used in the average, averaging was used to increase the signal-to-noise ratio. Measures of peak-to-peak amplitude of the compound signal that occurred between 1.5 and 4.0 ms after the stimulation of the digit

were recorded. At times less than 1.5 ms, a significant stimulus artifact was present; after 4 ms there was typically no ENG signal remaining. These measurements were obtained for each digit and then a selectivity analysis, as described in Chapter 4: Selectivity Analysis, was performed.

Figure 6.2 shows the results of an electrical stimulation experiment on NIH19 on day 0. The signals recorded on all eight channels from the two implanted MCCs after stimulating each digit are shown with their characteristic ENG patterns. The channels labeled 1 through 4 indicate the median MCC electrode recordings and channels 5 through 8 indicate the ulnar MCC recordings. From the figure, you can see that the median nerve was active when digits I through IV were stimulated and the ulnar nerve was active only after simulation on digits IV and V.

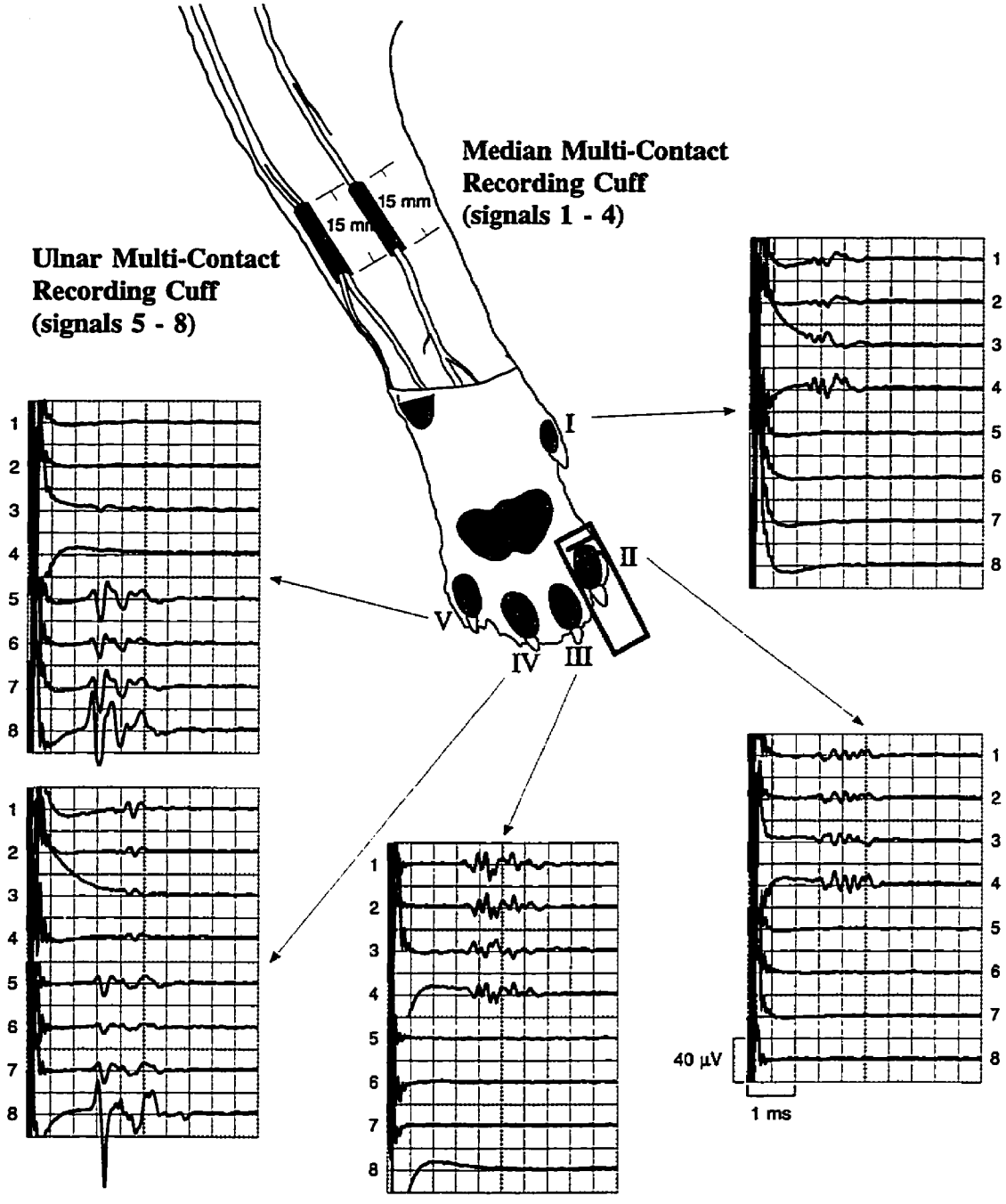

Figure 6.2: Compound neural signals obtained after stimulation of the individual digits. NIH19, Day 0.

Figure used with permission from K.D. Strange.

Results of Selectivity Analysis

There were three MCC implanted and three LIFE implanted cats; however, I only closely monitored two of each. The first NIH implant (NIH18) was disregarded for this project when the wires to the tripolar ulnar cuff were broken early in the experiment and therefore I could not determine the performance of the eight-channel system compared to the two-channel system. To balance the results, I only closely followed the last two LIFE implanted subjects.

The results of detailed selectivity analyses performed on four subjects are presented in the following tables (Table 6.1 to Table 6.4). The column labeled 8-channel refers to the recording array composed of either two MCCs or eight LIFEs implanted on the median and ulnar nerves. The column labeled 2-channel refers to the recording array formed from two circumferential tripolar cuffs implanted on the median and ulnar nerves. The selectivity values for these two columns was calculated after stimulation of all five digits. The 4-channel columns are for the MCC and LIFE recording arrays that were implanted on either of the nerves. The 4-channel median array had selectivities calculated after stimulation was provided to the median innervated digits I through IV, and the 4-channel ulnar array had selectivities calculated after stimulation was provided to digits IV and V.

Table 6.1: Summary of selectivity results using electrical stimulation of digits on NIH19

Day	8-channel (%)	2-channel (%)	4-contact MCC median nerve (%)	4-contact MCC ulnar nerve (%)
0	61		26	9
4	59		21	12
7	54	46	20	10
15	51	43	19	9
22	50	39	17	5
40	59	35	21	2
49	56	34	27	8
61	56	47	17	3
77	48[i]	40	7[i]	8
103	42	35	10	22
126	40[k]	33[k]	5[k]	28[k]
154	43	31	12	45
180	45*	30	21	36
mean ± s.d.	51.1 ± 6.8	37.5 ± 5.6	17.2 ± 6.6	15.2 ± 12.9

Notes: *first simultaneous 8-channel recording day; [i]broken wire on med3; [k]loss of ulncirc, uln1 & med3.

Table 6.2: Summary of selectivity results using electrical stimulation of digits on NIH21

Day	8-channel (%)	2-channel (%)	4-contact MCC median nerve (%)	4-contact MCC ulnar nerve (%)
0	55	46	10	8
2	55	48	9	29
14	49	45	15	5
35	55	48	14	13
63	47	42	11	6
84	46*	38	14	10
94	53	44	18	13
mean ± s.d.	51.4 ± 3.7	44.4 ± 3.3	13.0 ± 2.9	12.0 ± 7.5

Notes: *first simultaneous 8-channel recording day

Table 6.3: Summary of selectivity results using electrical stimulation of digits on NIH22

Day	8-channel (%)	2-channel (%)	4 LIFEs median nerve (%)	4 LIFEs ulnar nerve (%)
0	76	37	64	30
3	72	35	58	21
9	72	42	60	21
24	80	36	63	61
38	78	39	61	71
58	75*	31	63	8[f]
72	69	38	61	31[g]
mean ± s.d.	74.6 ± 3.5	36.9 ± 3.2	61.4 ± 1.9	34.7 ± 21.2

Notes: *first simultaneous 8-channel recording day; [f]problem with new amplifier N3, resulting in no signal for ulnar LIFE3; [g]problem with amplifiers on N1 and N2

Table 6.4: Summary of selectivity results using electrical stimulation of digits on NIH23

Day	8-channel (%)	2-channel (%)	4 LIFEs median nerve (%)	4 LIFEs ulnar nerve (%)
0	64	37	41	31
2	64	43	40	49
9	62	42	44	14
16	64	38	43	4
29	58*	38	30	15
43	49	36	29	20
mean ± s.d.	60.2 ± 5.4	39.0 ± 2.6	37.8 ± 6.0	22.2 ± 14.4

Notes: *first simultaneous 8-channel recording day

Summary of results

From a brief analysis of the results, one can see that there were similar selectivity values within the MCC and LIFE implanted subjects for the eight-channel electrode arrays. The MCC subjects, NIH19 and NIH21, had average selectivities of 51.1 and 51.4 and the LIFE subjects, NIH22 and NIH23, had average selectivities of 74.6 and 60.2. In all cases, the two-channel tripolar cuff arrays had fairly similar performances (37.5, 44.4, 36.9, and 39.0) in all of the subjects.

When reviewing the results for the eight-channel arrays, it became clear that the LIFE arrays outperformed the MCC arrays, sometimes by a large margin. This fact was probably due to their specific recording locations that allowed them to make very selective recordings. Using both multi-channel systems, the extra channels of information seemed to provide better selectivity over the two-channel system.

Looking at the single four-channel MCCs, we can see that they performed similarly in the subjects on both the median and ulnar nerves. The average selectivity values ranged from 12.0 to 17.2 which is a tight spread given the calculated standard deviations. The LIFEs were much more variable in their selectivity with values ranging from 22 to 61 and the ulnar nerve implanted LIFE arrays had larger standard deviations. In both of the LIFE implanted subjects, the median nerve selectivities were considerably higher than the ulnar nerve arrays.

Improvement of eight-channel over two-channel system

The eight-channel systems provided more selective recordings than the two-channel systems. This fact may be explained through the increased separation in multi-dimensional space of the median innervated digits. For example, in the two-channel system, the cuffs implanted about the median and ulnar nerves should see similar results if any of the first three digits are stimulated because theoretically only the median nerve would be active (i.e., data vector = < 1 0 >); therefore, the selectivity amongst those digits would be 0. The fourth digit is distinct because it would have similar levels of activity on the median and ulnar nerves (i.e., data vector = < 0.707 0.707 >). And the fifth digit is again distinct because it would have activity only on the ulnar nerve with little activity on the median nerve (i.e., data vector = < 0 1 >). Thus, the following theoretical selectivities could be expected:

Individual selectivities: $S_1 = 39$, $S_2 = 39$, $S_3 = 39$, $S_4 = 54$, $S_5 = 89$

Overall selectivity: $S = 52$

Because we did not have perfect all-or-none signals, the observed selectivity for the two-channel system was reduced.

On the other hand, the eight-channel system should be able to provide some extra distinction among the first three digits with little gained separation of the signals from the fourth and fifth digits. By improving the selectivity in the median innervated digits, the overall selectivity was increased.

Improvement of selectivity when using two nerves as opposed to one

The large improvement that is seen with the selectivity measures for the five-digit, eight-channel system versus the two- or four-digit four-channel system may be attributed to the fact that the overall spacing between data vectors in eight dimensional space became greater, even though the selectivity amongst the first three digits did not change significantly.

Drop in selectivity for single MCC in chronic compared to acute experiments

The apparent drop in selectivity values that was observed from the acute experiments to the chronic experiments may be explained by the fact that the nerves in the forelimb may not follow similar distinct branching as was observed in the sciatic nerve in the hindlimb. The nerve branches in the hindlimb were located on the surface of the nerve, were very distinct and could be separated easily, whereas the fascicles in the forelimb may be located more deeply as thus harder to make clear recordings by the electrodes. Another reason may be due to intermingling. At the site of the MCCs, a distance away from where most of the branching takes place in the paw, the fascicles may be less distinct due to the intermingling that occurs between various fascicles as they approach the spinal cord. A third reason may be that not all of the axons in a digital nerve branch were stimulated as they were in the acute experiments. The reduction in signal amplitude narrowed the margin between signal and noise and may have caused the lowered selectivity.

CHAPTER 7 : MECHANICAL STIMULATION OF FORELIMB DIGITS

Data Collection

Recording protocols

The mechanical stimulation experiments were performed directly after each electrical stimulation experiment, while the subject was still under anesthesia during a recording session. The wrist of the cat was atraumatically supported with a brace formed of plexiglass and tape to prevent the paw from drooping and the forearm was secured to the recording table with a half section of tubing and tape (see Figure 7.1). After the forelimb was secured, the manipulator (described below) was positioned under the forepaw. For normal input experiments, the tip of the lever arm was located a few millimetres below the digit pad; for slip inputs, the lever arm was raised to just indent the surface of the digit pad. The manipulator then went through its programmed sequence of stimulations.

Digit manipulator

The digit manipulator is a device that I designed capable of producing controlled mechanical stimulations in two dimensions to the individual digit pads of the forepaw of an anesthetized cat. Mechanical stimulation in the direction perpendicular to the digit pad was possible, as were stimuli tangential to the pad. The former stimulation is referred to as a normal input and the latter a slip input. These stimulations caused activity in sensory fibres, cutaneous and proprioceptive, which was recorded by electrodes placed around, by, or in forelimb nerves.

In the final version of the digit manipulator, five lever arms were aligned under the forepaw with one lever arm tip placed under each digit to produce inputs in one of two dimensions. The various manipulators were constructed in SFU's Science Technical Centre by Alex Szolnoki.

The single digit manipulator

The basic manipulator element was capable of perturbing one digit in one of two dimensions as shown in Figure 7.1, set up for a slip stimulation experiment. Solenoids were used in the design because they were easy to use, easy to control with a computer, and relatively inexpensive. The magnitude of the applied stimulation was controlled by limiting the solenoid's return to their resting position. For the slip input, a return spring and hard stop located at the rear of the lever arm were utilized. For the normal input, a special cylinder was constructed to stop the return of the piston in the vertical solenoid.

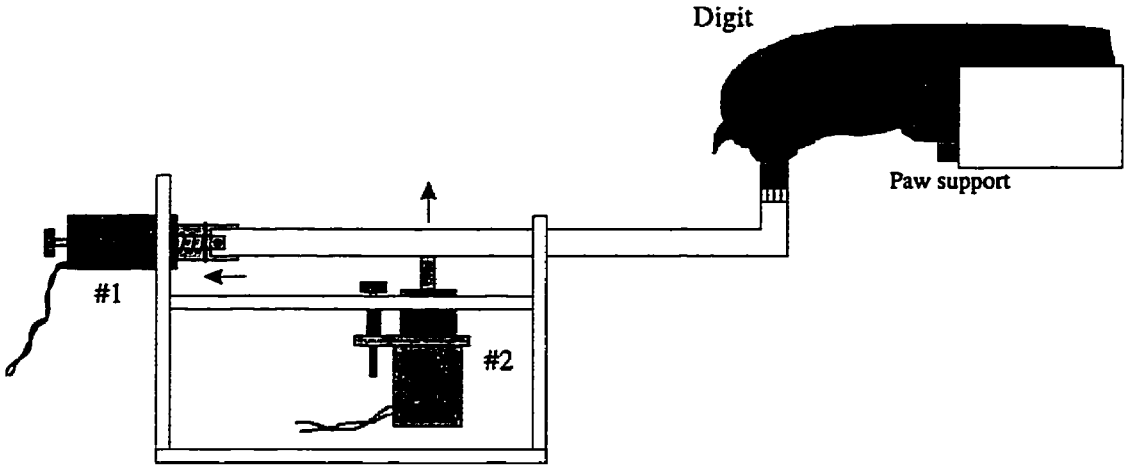

Figure 7.1: The single digit manipulator in position for a slip experiment

Solenoid #1 was a pull-type solenoid that was responsible for the slip input. When it was energized, the tip of the manipulator lever arm was pulled tangentially across the digit pad, creating a slip. When the solenoid was de-energized, a return spring pushed the manipulator's lever arm out of the solenoid and back against a hard stop. The position of the hard stop could be changed with a couple of small nuts and bolts located at the back of the arm, which controlled the length of the slip input.

Solenoid #2 was a push-type solenoid that was responsible for the normal input against the digit pad. When it was energized, the piston pushed the manipulator's lever arm up to contact the digit pad. Because the solenoid was located about half-way along the lever arm, the end of the arm traveled twice the distance of the piston. This was a good configuration for the solenoid because the solenoid was able to generate greater

force at a shorter stroke length. However, the amount of end point force of the solenoid was halved when used in this configuration.

The specifications of the single digit manipulator were as follows:

solenoid force (at 5 mm stroke length):	2 N
power:	up to 36W (12 V, 3A), DC power
size (LxHxW):	approximately 15 cm x 8 cm x 3 cm

The five-digit manipulator

At a later stage of the project, I designed a five-digit manipulator capable of perturbing any one of the digits. This design was based on the working version of the single-digit manipulator and included five copies of the single-digit manipulator placed side by side (see Figure 7.2). The manipulator was capable of delivering sequential inputs to any one of the five digits — either a slip stimulation along the long axis of the digit by energizing one of the outer solenoids or a normal stimulation against the digit pad by energizing one of the inner solenoids.

Because the manipulator was computer controlled, any sequence of individual stimulations could have been applied to the digits. I limited the experiments to series of slip inputs or series of normal inputs that were applied to the digits sequentially at a rate of one stimulation per digit per second (five stimuli/s distributed over five digits).

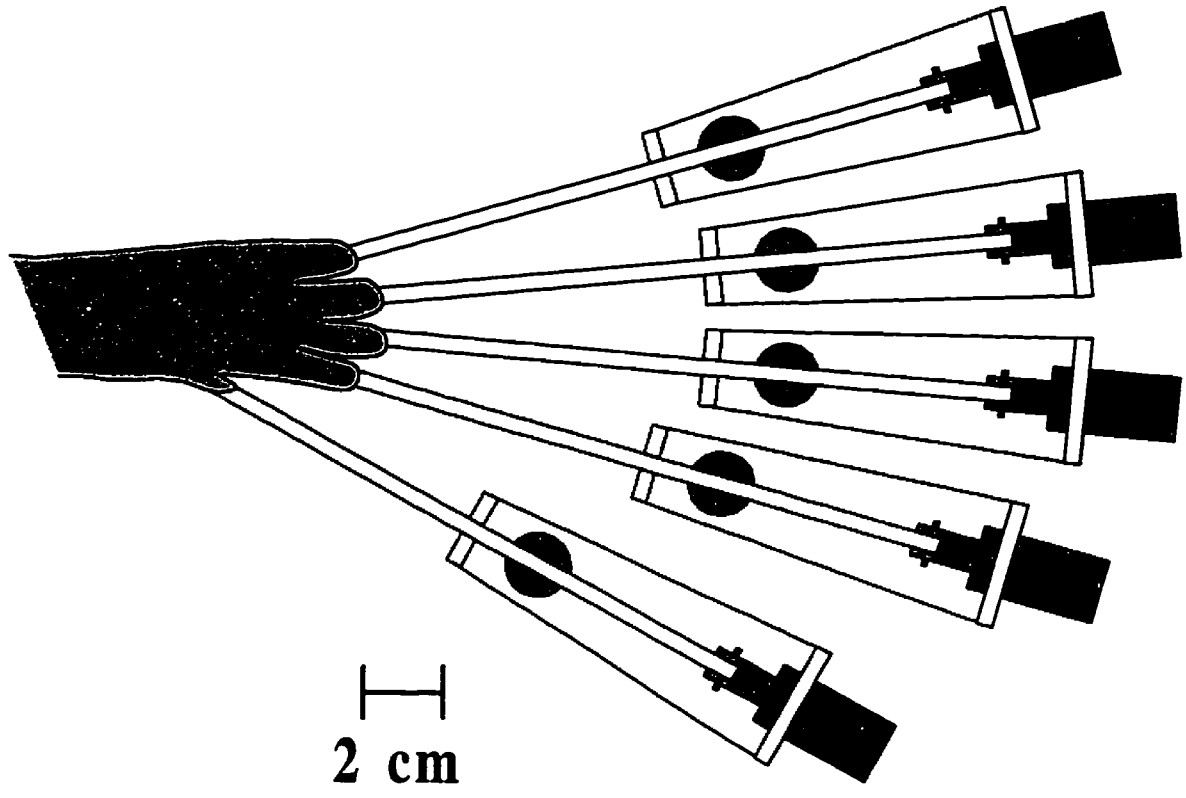

Figure 7.2: The five-digit manipulator in position

Data acquisition

Initially, recordings could only be made simultaneously from four recording channels using the chained Leaf and BAK amplifiers, so electroneurographic (ENG) activity was separately recorded from median and ulnar nerves. In later stages of the study, eight new amplifiers were constructed and the results from these recording sessions are provided below. The full recording scenario allowed better recordings to be made because all neural signals were recorded in parallel so the total activity in both of the nerves could be simultaneously monitored. As in the electrical stimulation cases, the median and ulnar circumferential cuffs were recorded concurrently by chaining two BAK amplifiers together.

Due to the very small amplitude of ENG signals, a gain of 100,000 was used to amplify the recorded ENG activity before recording the signal to FM tape. Even after amplification, a typical signal had a peak-to-peak amplitude of 300 mV which indicated a

neural signal of about 3 μV. The ENG was bandpass filtered between 500 Hz and 10 kHz to accentuate the neural response and remove high and low frequency electromagnetic interference.

After an experiment was completed, the data that was stored on the FM tape was played back, digitally sampled at 20,000 samples per second, and stored on writeable CD. The sampling rate was selected to be twice the bandwidth of the recording channels on the FM tape machine (i.e., 10 kHz) and approximately twice the highest frequency component of the filtered ENG signal. Storing the data digitally allowed for manipulation of the data off-line with various software packages.

Processing

Matlab processing and feature extraction

Due to the small amplitude and brief duration of the neural burst that occurred in the median and ulnar nerves after mechanical stimulation was applied to one of the digits, some signal processing was necessary in order to obtain useful features for further analysis. The processing included removing the DC offset found on the analog FM tape, further high-pass filtering the signal to remove 60 Hz interference, rectifying the neural signal, and low-pass filtering the signal with a Kaiser window Finite Impulse Response (FIR) filter with cutoff at 400 Hz to obtain the envelope of the ENG burst. The following block diagram (i.e., Figure 7.3) shows these steps. A Kaiser window filter was selected because it is a near-optimal FIR filter for a given mainlobe width and sidelobe area. A FIR filter has a constant delay of one half the window length that can be accommodated more easily when implementing hardware for real-time situations (Oppenheim and Schafer, 1989).

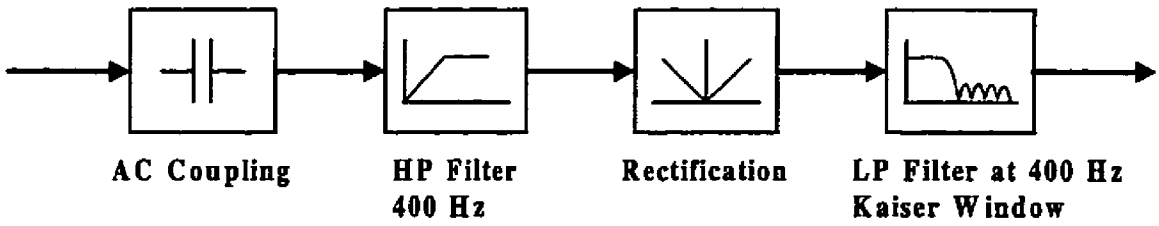

Figure 7.3: Steps used to filter recorded ENG activity after mechanical stimulation

Three features were extracted from the filtered signal: (1) the peak of the filtered ENG burst, (2) the time from the onset of the stimulation to the peak of the ENG burst, and (3) the area of the burst over a baseline level integrated over a 50 ms duration. Figure 7.4 shows these features on a filtered ENG burst.

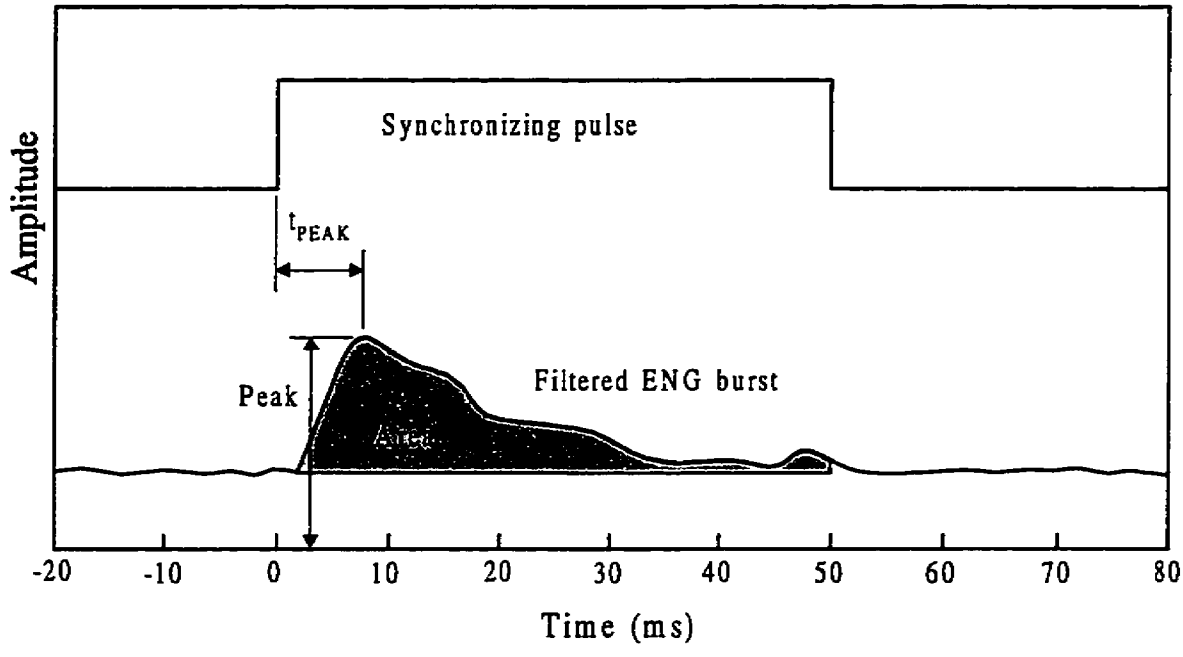

Figure 7.4: Filtered ENG burst showing peak, time to peak, and area features

Data from a normal stimulation experiment from both before and after processing is shown in Figure 7.5. For clarity only one channel is shown, along with the synchronizing pulse that shows when the solenoid was energized. The synchronizing pulse shows two pulses: (1) when the lever arm first made contact with the digit pad and (2) when the lever arm left the surface of the skin.

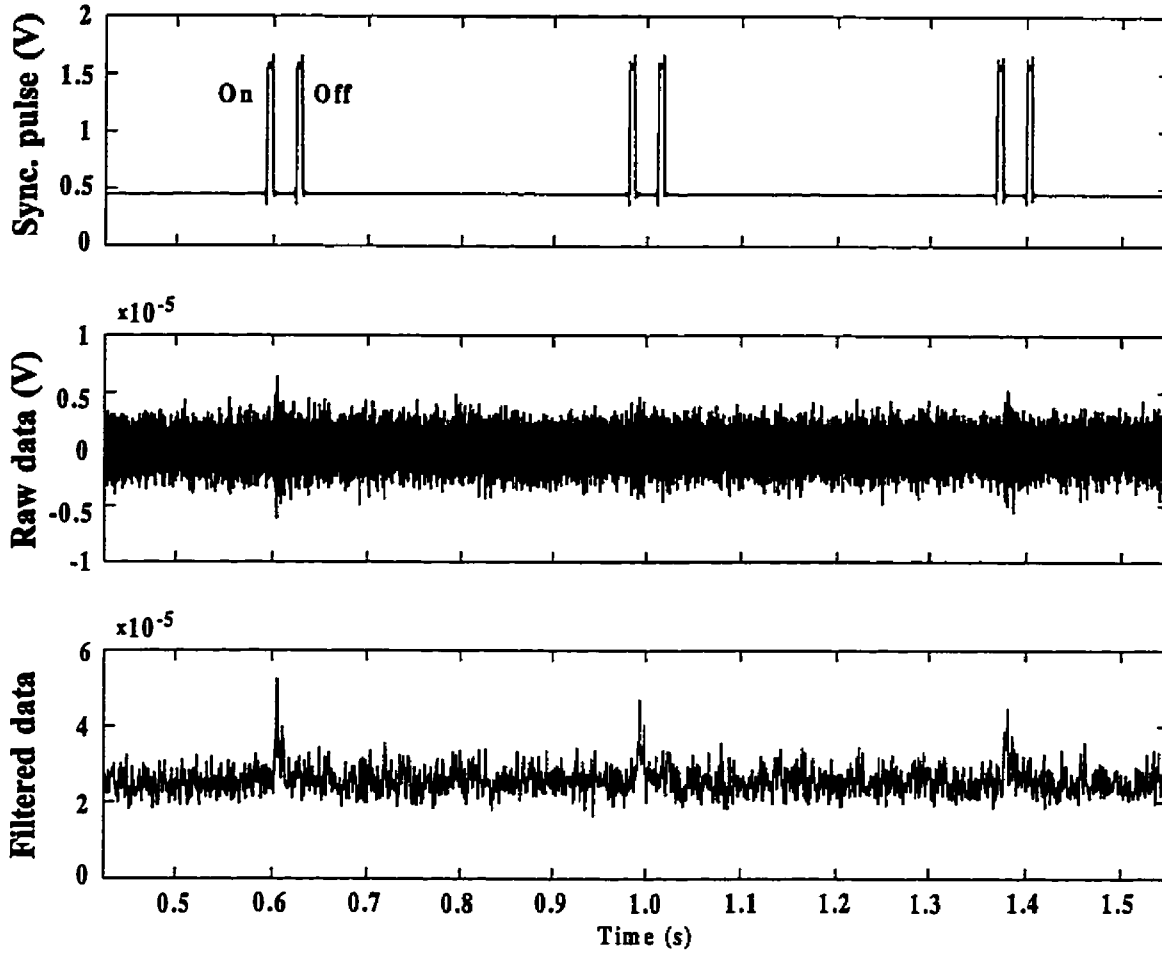

Figure 7.5: Sequence of processing on one channel of ENG data. Data recorded from NIH21 on day 99 using normal inputs applied to digit 3

In Figure 7.5, one can see that variability occurred from trial to trial. This variability may have been due to changes in the input, as the lever arm did not always provide an identical stimulus to the digit pad. Changes in the input may have been due to the solenoid tending to heat up with repeated use, the lever arm becaming slowed in the manipulator due to friction between the lever arm the guides, or the lever arm contacting a different part of the digit pad. Other sources of variability may have included changes in the mechanoreceptor electrochemical responses because some adaptation may have occurred with repeated presentations of the same mechanical input and the output response is not constant for every stimulus (Westling and Johansson, 1987).

Results

Selectivity analysis

Two features that were generated from the Matlab processing, ENG burst peak and area, were used in a selectivity analysis similar to the one used for responses to electrical stimulation of the digits. The full set of average selectivities collected with the single-digit and five-digit manipulators and analyzed with burst peak and area features appears in Appendix C. I chose the burst areas over the burst peaks because areas provided slightly better results than peaks. The results are provided in Table 7.1 for the four NIH subjects. I only included here the results obtained using the area features from normal and slip experiments that used the five-digit manipulator as an input device. The selectivity values for the eight- and two-channel arrays were calculated after mechanical stimulation of all five digits. The selectivity of the four-channel array on the median nerve was calculated for stimulation of the four median innervated digits, I through IV. The selectivity of the four-channel array on the ulnar nerve was calculated for stimulation of the fourth and fifth digits.

Table 7.1: Summary of mechanical selectivity results using ENG burst area features.

Subject	Day	8-channel selectivity (%)	2-tripolar selectivity (%)	4-channel array on median nerve (%)	4-channel array on ulnar nerve (%)
NIH19	154-S	16		15	2
(MCC)	180-N	14		4	2
	180-S	20		19	5
NIH21	84-N	14	6	5	10
(MCC)	84-S	6	4	3	1
	94-N	7	7	3	3
	94-S	9	5	7	5
	99-N	13	7	4	2
	99-S	7	5	2	4
NIH22	58-N	25	6	27	4
(LIFE)	58-S	28	10	34	6
	65-N	25	12	29	26
	65-S	28	8	34	11
	72-N	32	10	30	17
	72-S	28	6	30	9
NIH23	29-N	18	10	12	7
(LIFE)	29-S	18	8	9	9
	43-N	28	11	11	10
	43-S	17	10	11	4

Note: N - normal stimulation. S - slip stimulation

The average eight-channel MCC selectivities were 16.7 and 9.3 and the average LIFE selectivities were 28.5 and 20.3, both of which are better than the two-channel average selectivities obtained from the two tripolar cuffs located on the two nerves (5.7, 8.7, and 9.8). Of the two four-channel arrays, the results obtained on the median nerve (MCC: 12.7 and 4.0; LIFE: 30.7 and 10.8) were typically higher than the arrays implanted on the ulnar nerve (MCC: 3.0 and 4.3; LIFE: 12.2 and 7.5). In most cases, the LIFE recording arrays outperformed the MCC recording arrays.

Normally, the eight-channel selectivity was greater that either of the four-channel selectivity values. The relationship between the two four-channel arrays and the aggregate eight-channel array is not clear and would appear to be non-linear as is evidenced by the results of NIH22. For some cases, the four-channel array on the median

nerve has greater selectivity on the four digits than the full eight-channel system on the five digits. However, one should remember that for the different selectivity calculations, a different number of digits were used as the inputs. The eight-channel array measured the overall selectivity to identify five digits using information from the median an dulnar arrays, the four-channel median array measured the selectivity to identify the first four digits, and the four-channel array on the ulnar nerve measured the selectivity for the last two digits.

The modest mechanical stimulation selectivities, relative to the electrical stimulation selectivities, may be accounted by the larger variability in the ENG signals from variability in the input, variability in mechanoreceptor output, and the low signal-to-noise ratio that is seen with the neural bursts where the signal amplitude has a peak only about 3 times greater than the RMS amplitude of the background activity. The electrical stimulation experiments did not suffer from this variability as the electrical stimulation was essentially constant over all of the stimulated trials, the neural response to electrical stimulation was fixed, and the signal was about ten times larger than the noise that was observed.

Digit identification analysis

Discriminant analysis

A discriminant analysis classifies different individual cases based upon criteria that have been selected as the categorizing inputs. The individual cases in a discriminant analysis can be regarded as single points in multi-dimensional space. Unlike a cluster analysis that forms groups from the data without regard to relations that may occur in the data, a discriminant analysis classifies new cases into groups based on prior knowledge of the groupings. For the discriminant functions that were used in the analysis, it was assumed that the different groups had similar statistical properties of normal Gaussian distribution and equivalent covariance within groups. I made these assumptions because the same inputs were used on all digits and data was collected from all digits similarly, although these assumptions may not have been completely correct.

To perform the discriminant analysis individual samples are mapped from the N-dimensional measurement space (where N is the number of recording channels) to a reduced space spanned by K-1 orthogonal canonical functions (where K is the number of stimulated digits). Only K-1 lines, planes, or hyperplanes are necessary to separate K different groups (Cooley and Lohnes, 1971). The SPSS program derived the canonical functions to optimally separate the centroids of the K different groups by maximizing the ratio of between-groups sum-of-squares to the within-groups sum-of-squares (Norušis/SPSS, 1993). These functions were applied to sample cases and the individual cases were classified into the different groups based upon proximity of the case to each of the centroids. To test the accuracy of classification, a comparison was made between the predicted group classification to the actual grouping. Development of canonical functions used for discriminant analysis is discussed in detail in multivariate data analysis texts such as Cooley and Lohnes (1971).

Although not identical to the methods presented in the SPSS manual, Andrews (1972) and Young and Calvert (1974) provide good examples of how to develop linear discriminant functions and perform discriminant analyses. In these methods K linear discriminant functions are derived for the K groups.

When I ran the mechanical stimulation experiments, the stimulated digit was always coded in the synchronizing pulse train that was put onto FM tape. During Matlab processing, the pulse was decoded and the digit identification was stored with the extracted features for that digit. The actual stimulated digit information was entered into the discriminant analysis as the dependent grouping variable and the selected features were used as the independent categorizing variables.

Several analyses were performed to assess the performance of individual four-channel recording arrays operating on the individual nerves and associated digits and the overall performance of the eight-channel systems to identify all five digits. The first set of analyses determined the results of identifying which one-of-five digits was stimulated based on area, peak, and combined area and peak features from all of the eight recording electrodes. The second set of analyses evaluated the individual recording arrays on the median and ulnar nerves by identifying either one of digits I through IV based on features

collected for the median nerve or one of digits IV and V based on the features collected from the ulnar nerve array. Finally, the two-channel two tripolar cuff recording array was evaluated with the same three sets of features so that a comparison of the eight-channel system to the two-channel system could be made. Once all of these analyses were completed, the above analyses were reperformed using normalized data so that relations could be made between the digit identification accuracy and the selectivity data. The results from all of these canonical discriminant analyses are included in Appendix D.

Two different types of discriminant analyses were performed on the raw and normalized sets of data. A jackknife analysis technique was applied to the raw data to make predictions of group membership. The jackknife method, also known as a leave-one-out method, is used to determine how a single case would be classified based on the functions derived using the n-1 other data cases. By using raw data, the differences in the magnitudes of the source signals could be used to advantage to identify different groups. In the analysis method applied to the normalized data, all of the cases were left in to derive the canonical discriminant functions so that comparisons to the selectivity measures could be made. From reviewing the results in Appendix D, one can see that the results obtained from the two types of discriminant analyses are similar.

Summary of discriminant analysis results

The results of the discriminant analyses performed with the jackknife method on the raw data collected with the five-digit manipulator is provided in Table 7.2.

Table 7.2: Summary of digit identification accuracy using ENG burst area features and leave-one-out analysis

Subject	Day	8-channel accuracy (%)	2-channel accuracy (%)	4-channel array on median nerve (%)	4-channel array on ulnar nerve (%)
NIH19	154-S	76.3		94.4	50.0
(MCC)	180-N	76.7		41.5	70.4
	180-S	95.5		93.4	100
NIH21	84-N	79.7	43.6	80.2	87.0
(MCC)	84-S	72.2	40.6	59.0	35.2
	94-N	83.3	42.1	60.0	89.4
	94-S	89.5	67.7	84.8	96.4
	99-N	97.7	55.4	84.9	88.9
	99-S	92.5	50.0	84.9	100
NIH22	58-N	99.2	65.6	100	90.7
(LIFE)	58-S	99.2	63.6	98.1	90.9
	65-N	82.0	75.6	76.2	94.4
	65-S	97.0	61.8	91.4	100
	72-N	92.5	50.8	99.0	80.0
	72-S	99.2	56.9	100	100
NIH23	29-N	99.2	64.7	79.2	100
(LIFE)	29-S	100	62.4	85.8	96.3
		94.0	64.9	86.8	94.3
		96.2	61.5	88.6	77.8

Note: N- normal stimulation; S- slip stimulation

Table 7.2 shows that a high degree of accuracy was achieved using the canonical functions derived by the discriminant analysis. The eight-channel MCC array results averaged 82.8% and 85.8% and the LIFE results averaged array 94.9% and 97.4% for the four subjects tested. These results are considerably better than chance (i.e., 20%) and better than the results obtained using the two-nerve, two-channel systems (49.9%, 62.4%, and 63.4%). The four-channel systems also performed well with the median arrays averaging 76.4% and 75.6% for the MCCs and 94.1% and 85.1% for the LIFEs. The ulnar four-channel system also showed high accuracy (MCC: 73.5% and 82.8%; LIFE: 92.7% and 92.1%), although chance in this case was 50%.

Individual discriminant analysis results

The following tables and figures show the individual results from each subject from the discriminant analyses that provided the highest accuracy. The tables, also known as confusion matrices, show the predicted versus actual group classification for a single set of raw data in which a leave-one-out analysis had been performed. The correct identifications were placed on the diagonal with the off-diagonal elements representing the misgrouped cases. The figures show the group "clouds" of data that are formed after the individual cases had been transformed by the derived canonical discriminant functions and then plotted in two dimensions. The first two canonical functions (i.e., the x and y axes of the following figures) represent the greatest variability in the data with less variability accounted for with the third and fourth functions. On average 71.6% of the variability of the data was accounted for by the first canonical function and 94.7% was accounted for by adding the second function.

The standardized canonical discriminant function coefficients are the coefficients of the canonical functions after the variables have been standardized to a mean of 0 and a standard deviation of 1. The magnitude of the coefficients show how strongly a variable affects the output of the given function. In all of the cases, the coefficients are listed in order of the four median electrodes and then the four ulnar electrodes.

Table 7.3: Classification results for NIH19 on day 180 using ENG burst area features and slip inputs

		Predicted Group Membership					
	Digit	1	2	3	4	5	Total
Count	1	27	0	0	0	0	27
	2	0	24	2	0	0	26
	3	0	1	23	2	0	26
	4	0	0	1	26	0	27
	5	0	0	0	0	27	27
%	1	100.0	0.0	0.0	0.0	0.0	100.0
	2	0.0	92.3	7.7	0.0	0.0	100.0
	3	0.0	3.8	88.5	7.7	0.0	100.0
	4	0.0	0.0	3.7	96.3	0.0	100.0
	5	0.0	0.0	0.0	0.0	100.0	100.0

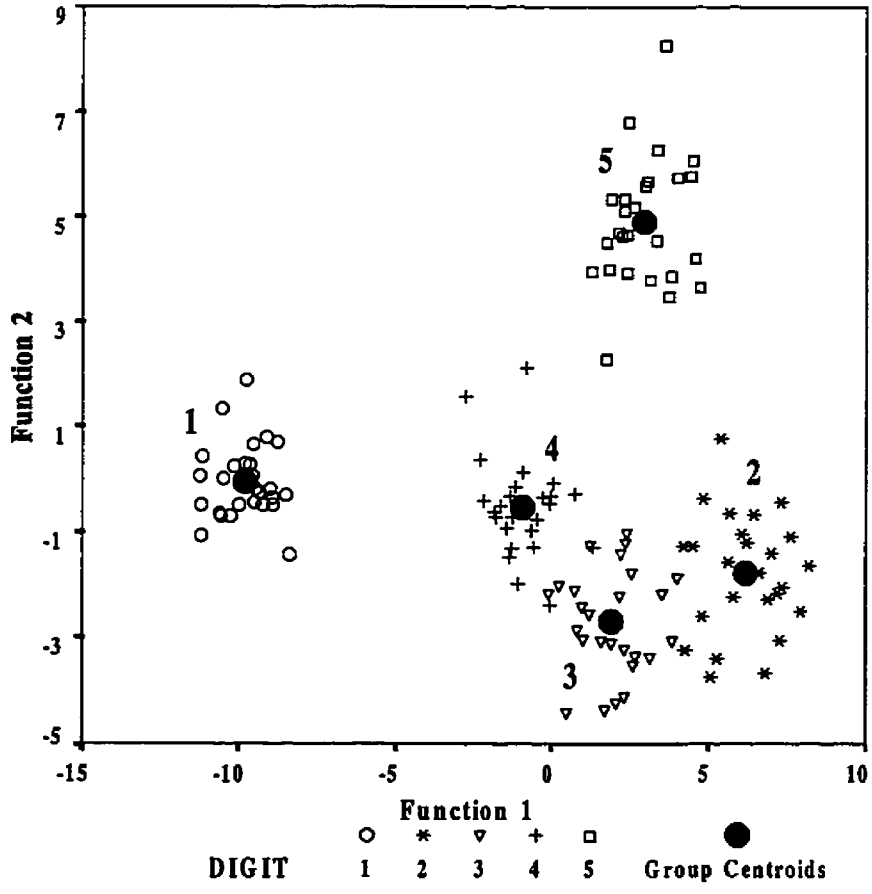

Figure 7.6: Scatter plot of ENG burst area feature data used in digit identification analysis for NIH19 on day 180 using slip inputs. 95.5% accuracy

Standardized canonical discriminant function coefficients:

F1:	0.420	0.549	0.092	0.182	0.078	0.189	0.180	0.277
F2:	-0.243	-0.193	0.012	-0.201	0.155	0.398	0.210	0.713

Table 7.4: Classification results for NIH21 on day 94 using ENG burst area features and slip inputs

		Predicted Group Membership					
	Digit	1	2	3	4	5	Total
Count	1	26	0	0	0	0	26
	2	0	23	3	0	0	26
	3	0	8	17	1	0	26
	4	0	0	0	26	1	27
	5	0	0	0	1	27	28
%	1	100.0	0.0	0.0	0.0	0.0	100.0
	2	0.0	88.5	11.5	0.0	0.0	100.0
	3	0.0	30.8	65.4	3.8	0.0	100.0
	4	0.0	0.0	0.0	96.3	3.7	100.0
	5	0.0	0.0	0.0	3.6	96.4	100.0

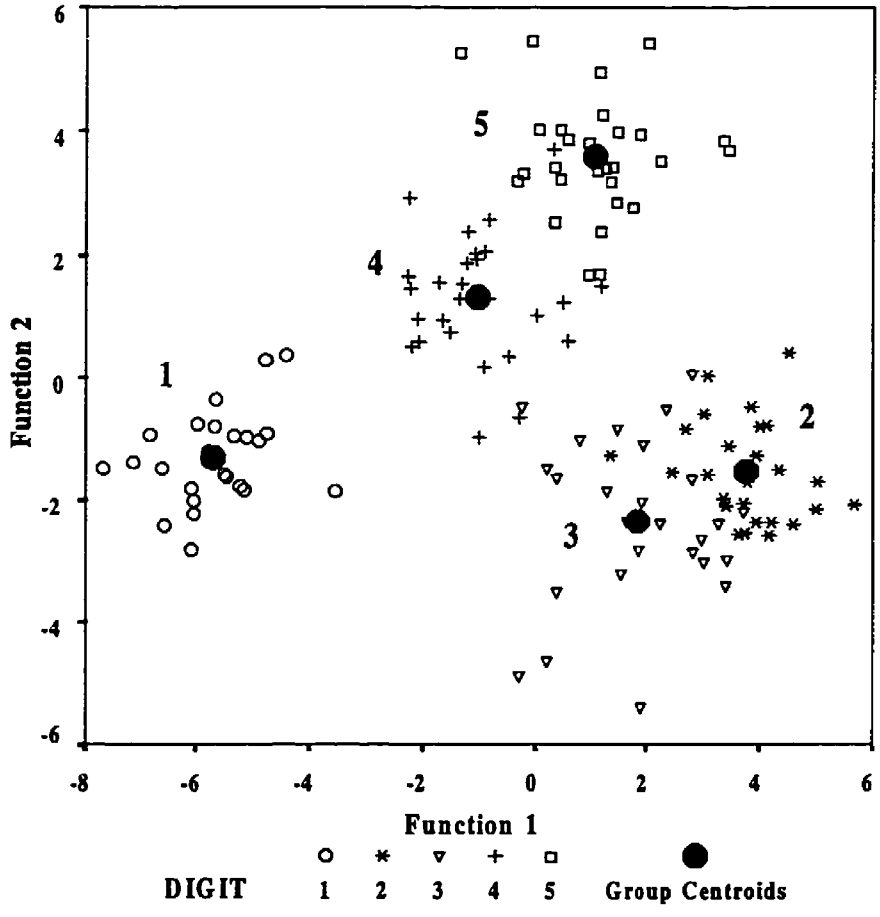

Figure 7.7: Scatter plot of ENG burst area feature data used in digit identification analysis for NIH21 on day 94 using slip inputs. 89.5% accuracy

Standardized canonical discriminant function coefficients:

F1: 0.762 0.294 -0.048 0.310 0.261 0.208 -0.047 0.086

F2: -0.457 0.008 -0.226 -0.206 0.514 0.155 0.247 0.653

Table 7.5: Classification results for NIH22 on day 58 using ENG burst area features and slip inputs

		Predicted Group Membership					
	Digit	1	2	3	4	5	Total
Count	1	27	0	0	0	0	27
	2	0	26	0	0	0	26
	3	0	0	25	0	0	25
	4	0	0	1	26	0	27
	5	0	0	0	0	28	28
%	1	100.0	0.0	0.0	0.0	0.0	100.0
	2	0.0	100.0	0.0	0.0	0.0	100.0
	3	0.0	0.0	100.0	0.0	0.0	100.0
	4	0.0	0.0	3.7	96.3	0.0	100.0
	5	0.0	0.0	0.0	0.0	100.0	100.0

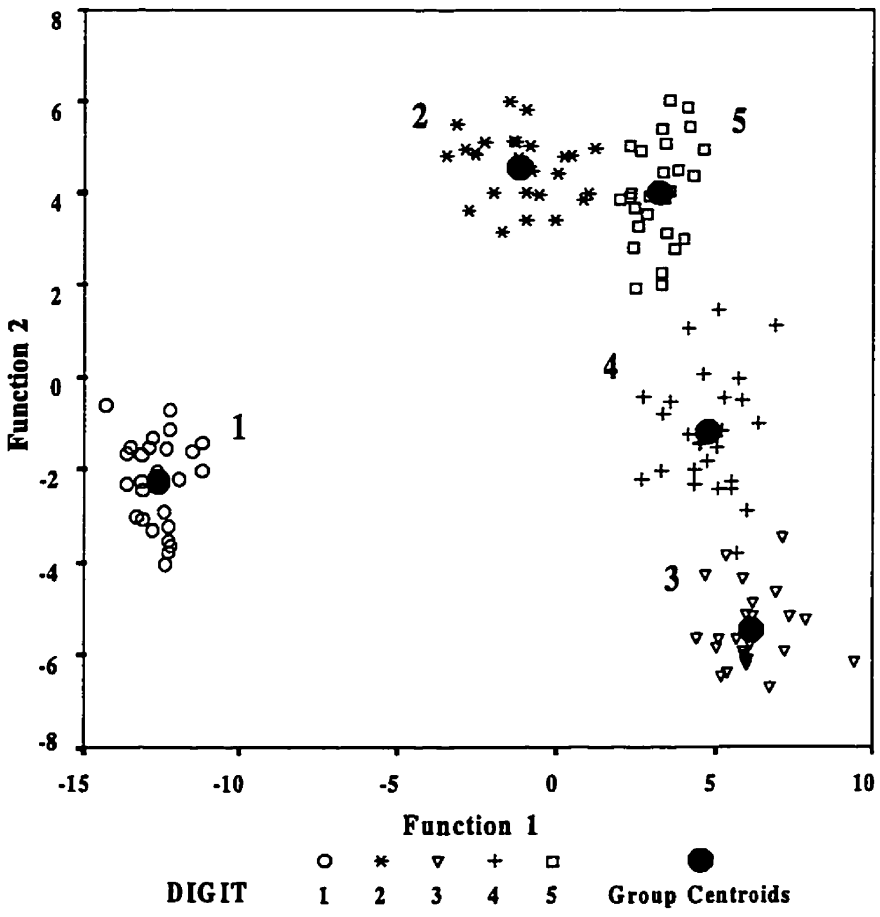

Figure 7.8: Scatter plot of ENG burst area feature data used in digit identification analysis for NIH22 on day 58 using slip inputs. 99.2% identification

Standardized canonical discriminant function coefficients:

F1:	0.642	0.159	0.057	-0.615	0.166	0.449	0.054	0.139
F2:	-0.185	0.152	0.090	0.715	-0.183	0.290	-0.011	0.791

Table 7.6: Classification results for NIH23 on day 29 using ENG burst area features from slip inputs

		Predicted Group Membership					
	Digit	1	2	3	4	5	Total
Count	1	26	0	0	0	0	26
	2	0	27	0	0	0	27
	3	0	0	26	0	0	26
	4	0	0	0	27	0	27
	5	0	0	0	0	27	27
%	1	100.0	0.0	0.0	0.0	0.0	100.0
	2	0.0	100.0	0.0	0.0	0.0	100.0
	3	0.0	0.0	100.0	0.0	0.0	100.0
	4	0.0	0.0	0.0	100.0	0.0	100.0
	5	0.0	0.0	0.0	0.0	100.0	100.0

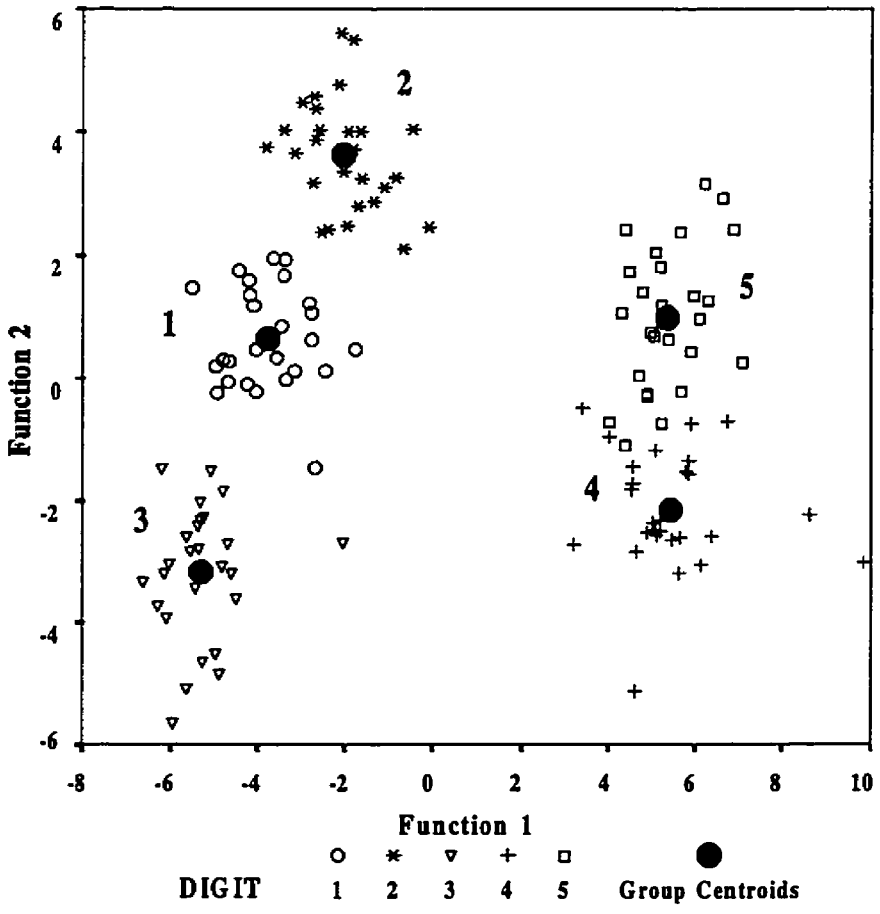

Figure 7.9: Scatter plot of ENG burst area feature data used in digit identification analysis for NIH23 on day 29 using slip inputs. 100% accuracy

Standardized canonical discriminant function coefficients:

F1:	-0.018	-0.058	0.005	-0.413	0.471	-0.067	0.579	0.091
F2:	0.316	-0.378	0.810	-0.006	0.783	0.209	-0.359	-0.076

Relation to Selectivity Index

In order to determine relations between the selectivity measure and the accuracy measure, it was necessary that the same data be used in both. Because the selectivity measure relied on normalizing the data vectors as one of its first steps, the discriminant analysis was recalculated with normalized values and all data were included in the classification. The results from the leave-all-in discriminant analysis performed with normalized data can be found in Appendix D. Table 7.7 shows the selectivity indices and digit identification accuracy for normalized ENG burst area feature data for the eight-channel and two-channel systems.

Table 7.7: Selectivity index and accuracy of identification using eight- and two-channel nerve recording arrays

Subject	Day	8-channel selectivity index (%)	8-channel accuracy (%)	2-channel selectivity index (%)	2-channel accuracy (%)
NIH19	154-S	16	76.3		
(MCC)	180-N	14	82.0		
	180-S	20	92.5		
NIH21	84-N	14	85.0	6	44.4
(MCC)	84-S	6	70.7	4	34.6
	94-N	7	77.2	7	39.8
	94-S	9	84.2	5	36.8
	99-N	13	88.7	7	33.8
	99-S	7	71.4	5	37.7
NIH22	58-N	25	100	6	49.6
(LIFE)	58-S	28	99.2	10	54.5
	65-N	25	87.2	12	56.5
	65-S	28	98.5	8	49.6
	72-N	33	95.5	10	51.5
	72-S	32	97.7	6	40.8
NIH23	29-N	18	99.2	10	52.6
(LIFE)	29-S	18	98.5	8	47.4
	43-N	28	95.5	11	56.5
	43-S	17	94.0	10	35.4

Note: N - normal stimulation; S - slip stimulations

Assuming a linear relationship between selectivity and accuracy, the correlation between eight-channel selectivity and eight-channel accuracy values using ENG burst area features was calculated to be 0.79. The plotted data are shown in Figure 7.10. This value indicated a moderately strong correlation, so the selectivity measure can be taken to be a good predictor of the expected accuracy of digit identification. The plot also indicates what level of selectivity would be necessary to achieve a desired level of accuracy in digit identification using canonical discriminant functions. It is apparent that mechanical selectivities of 25% will result in digit identification of about 95% accuracy. The correlation of two-channel selectivity to two-channel accuracy showed a moderate correlation of 0.71.

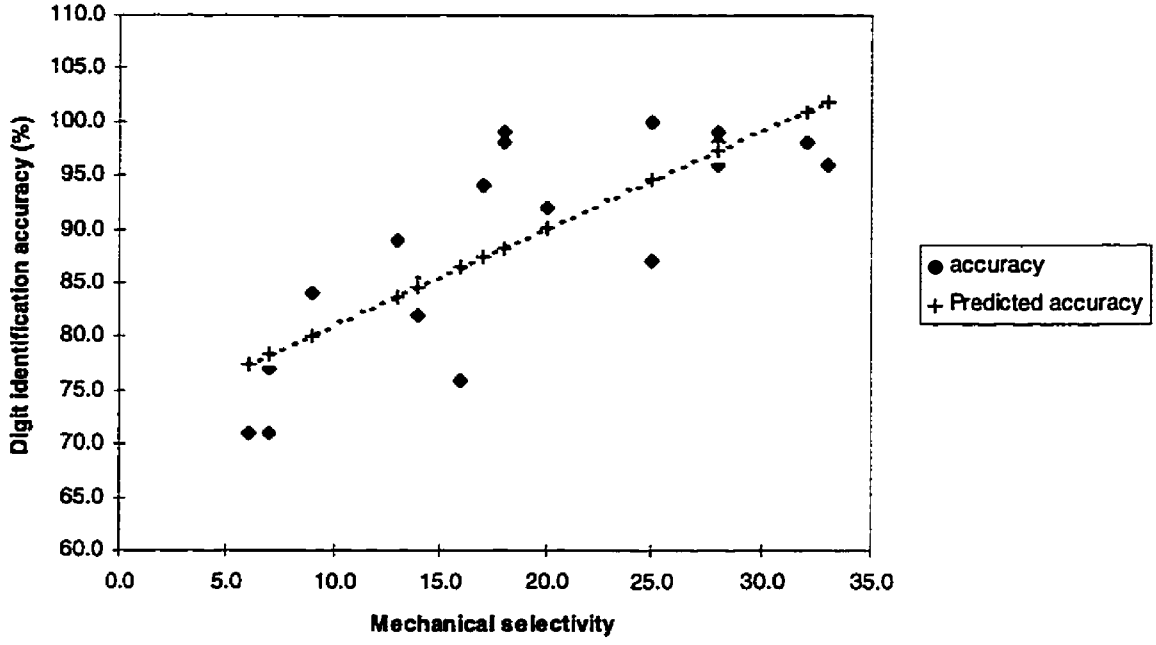

Figure 7.10: Scatter plot of relationship between selectivity and digit identification accuracy for eight-channel electrode arrays using ENG burst area features showing actual accuracy and predicted accuracy based on linear regression analysis.

A linear regression between the mechanical selectivity and percent correct digit identification showed that a minimum digit identification accuracy of approximately 72% would occur when there was no selectivity, and would be greater than 100% at full selectivity. This result is not expected in theory. Rather, a selectivity of 0 should indicate that the probability of correctly identifying a stimulated digit is chance or 20%, if there are five digits in the system. This observation indicates that a curvilinear relationship might

exist between the two variables, such as a line that started at (0, 20%) passed through (10, 90%) and then continued to (100, 100%).

Assuming that a non-linear relationship existed between mechanical selectivity and digit identification accuracy, I tested several alternative functions of the two variables and performed a regression analysis of the different combinations. The comparison of the results are shown in Table 7.8. The columns labeled $f(\bullet)$ represent the different functions that were applied to the selectivity and digit identification accuracy values. The column titled correlation coefficient using raw data shows the results of the regression analysis using the same data as in Figure 7.10. The last column shows the results of the regression analysis after two new data points were inserted to force the data through the points (1, 21%) and (100, 100%). The point (0, 20%) was not used because the logarithm of 0 does not exist.

Table 7.8: Comparison of relationships between selectivity and digit identification accuracy for eight-channel electrode arrays using ENG burst area features

f(Selectivity)	f(Accuracy)	Correlation coefficient using raw data	Correlation coefficient using increased data
selectivity	accuracy	0.80	0.48
selectivity	log(accuracy)	0.80	0.40
selectivity	$(\text{accuracy})^2$	0.80	0.54
log(selectivity)	accuracy	0.84	0.90
log(selectivity)	log(accuracy)	0.85	0.85
log(selectivity)	$(\text{accuracy})^2$	0.84	0.90
$(\text{selectivity})^2$	accuracy	0.74	0.26
$(\text{selectivity})^2$	log(accuracy)	0.73	0.20
$(\text{selectivity})^2$	$(\text{accuracy})^2$	0.74	0.31

From the table above, it appears that a logarithmic function would better describe the relationship between selectivity and accuracy.

CHAPTER 8 : OTHER ANALYSIS TECHNIQUES AND FUTURE DIRECTIONS

Other Analysis Techniques

Other techniques that can be used for classification and identification are presented here. Statistical classification relies upon prior knowledge of the system's parameters and is useful for systems that are not well characterized by theory but do have a lot of data that can be used to characterize the various groupings. Neural networks are used when a nonlinear mapping of inputs to outputs exists and a highly adaptive classification system is desired. Fuzzy expert systems require a programmer to derive a list of functions or rules that will lead to the proper identification. The relationship between these various classification techniques is shown in Figure 1.38 of Kasabov (1996, p. 67).

Statistical Classification

The discriminant analysis discussed in the previous chapter was a statistical classification scheme in which all of the groups' parameters were assumed to be uniformly distributed. If that is not the case or there is no known theoretical basis for the classification scheme, then more rigorous statistical approaches may be employed to classify the different cases into K distinct groups. A statistical classification scheme can be regarded as hypothesis testing in a system with K different means and K different distributions, where K is the number of groups to be classified. Unlike the discriminant function analysis which distinctly placed a case into a single group, a statistical approach allows the probability of a case to belong in any group. Prior to a Bayesian classifier being developed the conditional density functions (the probability of a case belonging to a particular group), costs for misclassification, and prior probabilities of any group occurring must be known for each group to determine the different decision regions. Young and Calvert (1974) provide a good discussion of the statistical approach to

classification. Most communication systems use statistical methods to identify different input signals.

The identification of new cases by a statistical classifier depends on the data that has been collected previously and their statistical distributions. No inferences are required about the data, just the probability of a certain group occurring and the probability that the new case belongs to a particular group. Figure 8.1 shows an example of a classification system that takes a new input, **x**, and classifies it based on the probability of a certain group being occurring, P_k, and the probability of the input belonging to a particular group ($P(x|D_k)$). The most probable outcome is selected as the predicted group or digit.

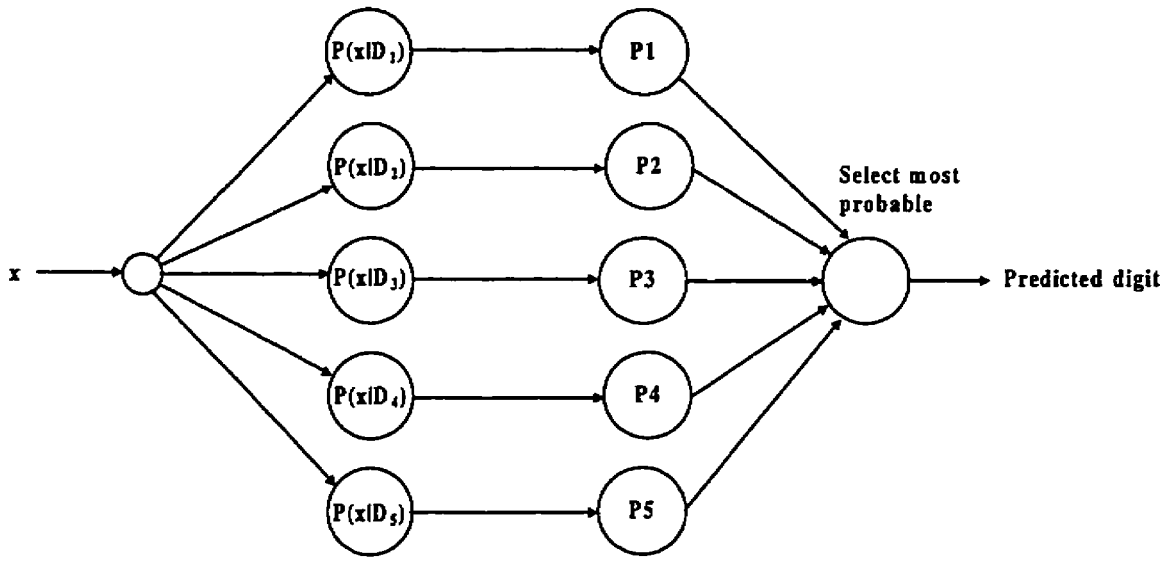

Figure 8.1: Example of a statistical classification system

Neural Networks

Neural networks are good classification systems to use when a non-linear mapping from the inputs to outputs exists. Not much prior knowledge about the relationship between the inputs and outputs is required as the relationship is generated by the neural net during its training session. Future cases are grouped based on the input-output relationship derived in the training sets. During training, the predicted group classification is compared to the actual group classification and the error rate is

determined. To reduce the error, back propagation techniques are used to change the weighting of the coefficients in the layers between the input stage and the output stage. A neural network that may have been used to analyze the eight recording channel and five digit classification is shown in Figure 8.2. Five different trees are constructed for the functions that identify the five digits. The tree that most likely identifies the input is selected as the predicted digit.

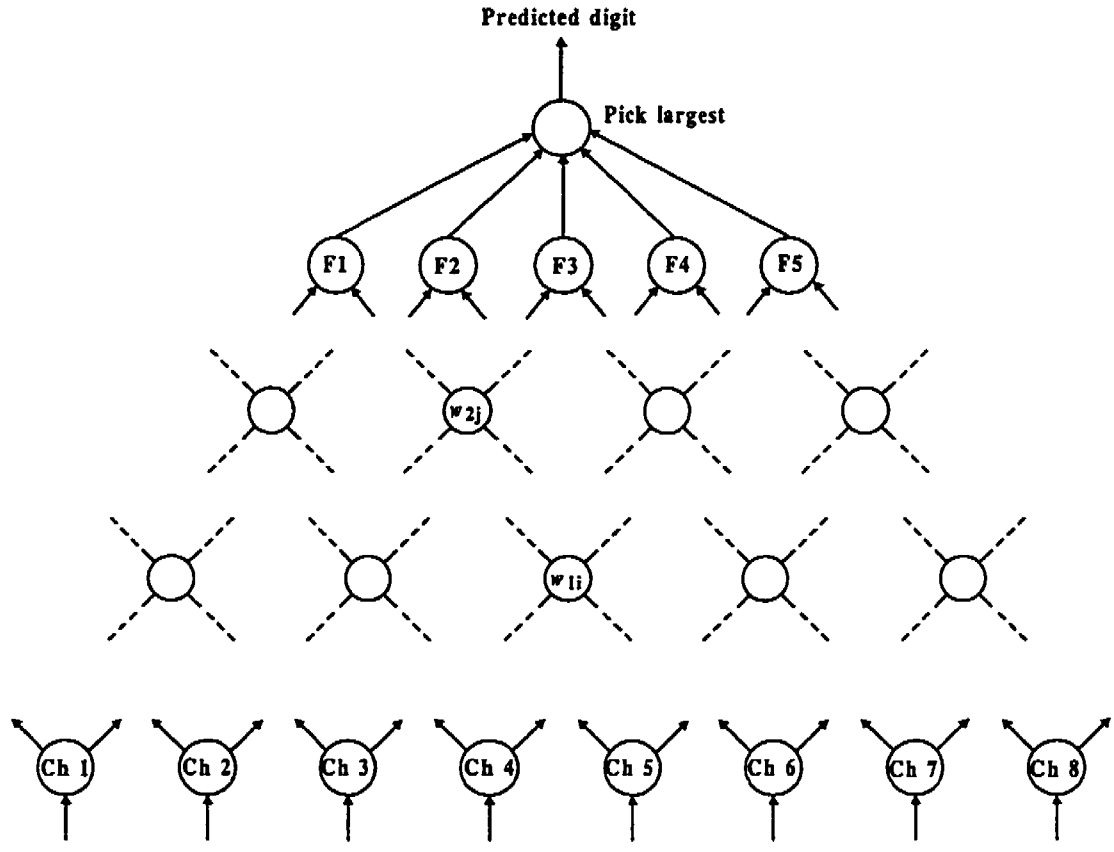

Figure 8.2: Neural network used to identify one-of-five digits from recordings from eight-channel recording array

Fuzzy Logic and Fuzzy Expert Systems

Fuzzy logic (Zimmermann, 1991) is based in the concept that a continuous distribution of possible inputs exists and then best matches the given input to an output; however, it is not based in probabilities (even though probabilistic theory is a subset of fuzzy theory) but possibilities or degrees of membership. A fuzzy logic system can be used when a known relationship between the inputs and the outputs is known or can be

assumed and expressed in words. Several rules can be made based on observations by an "expert" and these rules can be represented by mathematical functions that represent degrees of truth between 0 and 1, rather than strictly 0 or 1. Use of fuzzy systems assumes that the programmer knows most of the possible outcomes and that new cases can be accounted for through interpolation, therefore certain knowledge about the system must be known.

A series of IF - THEN statements, also known as fuzzy rules, are required to describe the system so that a proper identification can be made and then these can be represented graphically and algebraically. An example of fuzzy rules to describe a four-input, one-output system is shown below (Equation 8.1). The four input x_i's and the output y represent five different fuzzy variables defined on five different universes of discourse and high, medium, and low represent three different fuzzy sets to which the x_i's membership is calculated.

Equation 8.1: Fuzzy rules for a four-input one-output system

(1) IF (x1 is high) AND (x2 is medium) AND (x3 is low) AND (X4 is medium), THEN (y is approximately Group 1).

(2) IF (x1 is medium) AND (x2 is high) AND (x3 is medium) AND (x4 is low), THEN (y is approximately Group2).

(3) IF (x1 is low) AND (x2 is medium) AND (x3 is high) AND (x4 is medium), THEN (y is approximately Group 3).

(4) IF (x1 is medium) AND (x2 is low) AND (x3 is medium) AND (x4 is high), THEN (y is approximately Group 4).

An example of the fuzzy membership functions for the low, medium, and high functions are all plotted on the same axes in Figure 8.3 with the high membership function being highlighted. All of the functions have been normalized so that easy comparisons can be made between the various functions and variables. The figure shows the output of 0.4 corresponding to an input of 0.4 to the membership function high.

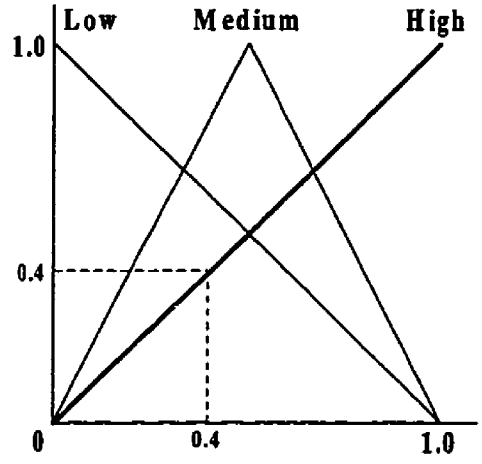

Figure 8.3: Membership functions for fuzzy sets low, medium, and high

The next figure shows all of the fuzzy rules for the four-input one-output system described by the IF-THEN rules in Equation 8.1. An input of <0.4 0.4 0.7 0.6> has been entered in the system. The first step in the analysis is to determine the degree of membership of the various variables for all of the rules. The degree of membership is calculated at the intersection of vertical dotted lines from the input line to each of the functions. Next, the AND part of the rules is calculated by taking the minimum of all of the membership functions for all of the variables. AND in fuzzy logic can be represented mathematically in various forms but it is typically represented by a minimum or a product. The degree of membership of the output y for the various rules is shown by the shaded regions in each of the possible outputs. In the final step, the union of all of the possible outputs is calculated and then the moment of the union is calculated. The final step (defuzzification) is to convert this fuzzy value 0.6 to one of the four possible outputs. If a linear distance measure is used, then it is closest to Group 3 for this example.

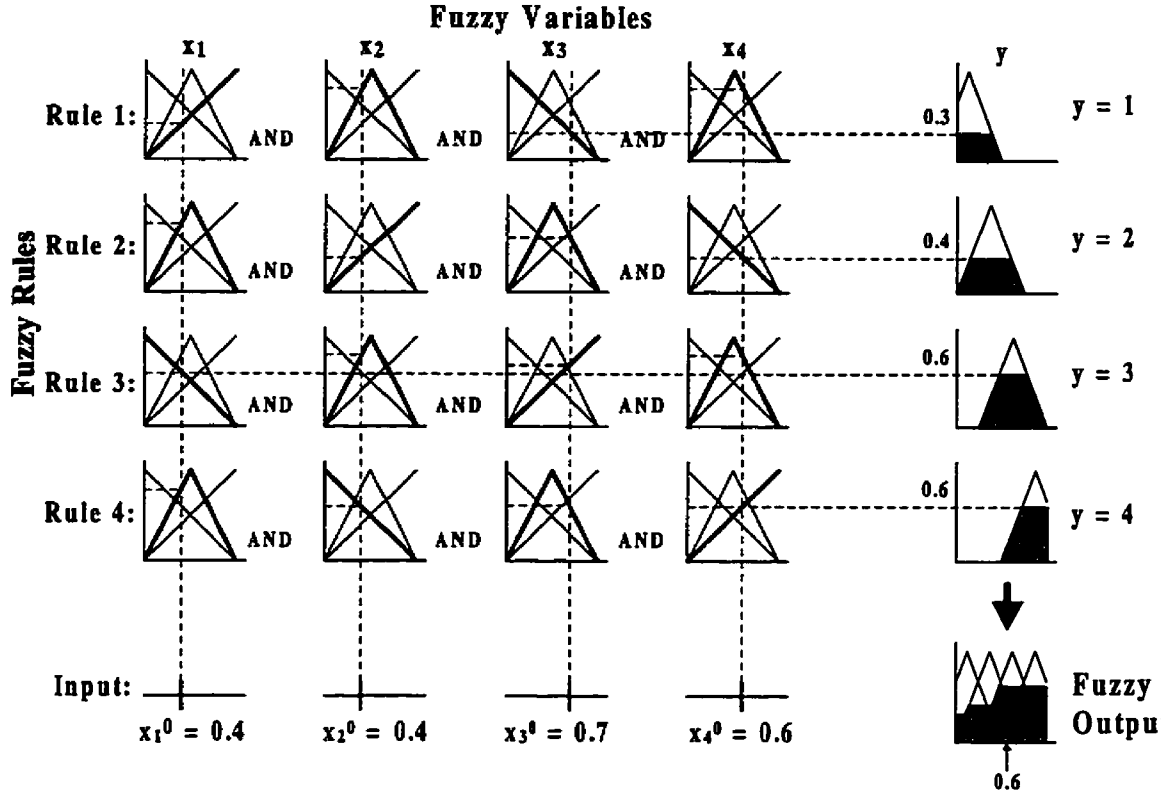

Figure 8.4: Plot of inference rules for an example of a four-input one-output fuzzy system

Zimmermann (1991), Ulieru (1996), and Kasabov (1996) all present methods to develop fuzzy sets, rules and inference methods and provide some applications of fuzzy theory.

Future Improvements

In order to increase the accuracy of source identification, a couple techniques that may be employed are improved feature selection and further nerve instrumentation. In the first, features more characteristic of the signals they represent can be used in the pattern recognition problem (see Chapter 2 of Andrews, 1972; Chapter 6 of Young and Calvert, 1974). Instead of using peak values or area values, different features may be used to greater effect. I calculated whether using both of these features for digit identification would increase the accuracy, but it did not seem affect the results too much. See the tables in Appendix D for more details.

Another way to increase the identification rate may be to instrument the radial nerve along with the median and ulnar nerves with multi-channel recording arrays. The radial nerve innervates the dorsal surface of the forelimb of the same digits as the median nerve. By using the information from the radial and median nerves, identification of digits I through IV may be improved and thus increase the overall identification rate. However by increasing the number of electrodes other problems may arise, such as the need to implant more wires and devices into the forelimb, the need for larger external connectors, and the identification system may become plagued with the "curse of dimensionality" (Andrews, 1972). The curse appears as the dimension of the system increases and the storage and processing needs increase. By reducing the number of electrodes per recording array, this curse may be avoided and a higher identification rate may still be achieved.

CHAPTER 9 : SUMMARY

Through the course of this thesis I have built the argument that the identification of digits from their specific neural patterns is possible. The work started with the development of a new Multi-Contact Cuff (MCC) and the selectivity analysis technique that was required to determine the efficacy of the recording cuff in acute and chronic situations. The studies in acute experiments showed that the MCC design performed well and that selective recordings could be made from different nerve branches. The electrical stimulation experiments of the forelimb digits in chronic experiments also showed that selective recordings could be made from both MCC and Longitudinal IntraFascicular Electrode (LIFE) arrays and thus individual source identification should be possible.

Because people are not usually presented with electrical shocks every time their finger tips touch or rub across a surface or their finger is moved out of place, a series of mechanical stimulation experiments was designed and executed to try to mimic two types of inputs that would occur in a natural setting – these were the normal and slip inputs discussed in the mechanical stimulation chapter. A selectivity analysis was performed and showed that selective recordings could be made although the selectivity values were rather low due to the variable nature of the input and the small amplitude ENG signal.

However, when the focus moved to identifying which were the mechanically stimulated digits, the results were promising. The digit identification rate when canonical discriminant functions were employed showed results that were considerably better than chance. The digit accuracy results from MCCs ranged from 70% to 90% depending upon the subject and the results from the LIFE subjects ranged between 80% and 100%. A relationship between mechanical selectivity and digit identification accuracy was found indicating there is a moderately strong correlation, although a plot of the data showed that the relationship might not be strictly linear.

In the next phase of the research, real-time digit identification will be attempted and if so, improved feature extraction may be necessary to increase the selectivity and identification rates and some other scheme to detect when a disturbance has taken place will need to be determined. Other pattern recognition and classification techniques such

as neural network analysis, fuzzy expert systems, and statistical methods may lead to improved results in the classification problem.

Because this thesis contained a series of controlled experiments with known inputs and simplified recording scenarios, the results of the experiments were easier to interpret and explain than might occur in awake recordings. Only five possible input sources were considered at any one time in the identification problem; however, in a real-life situation any number of the different digits could be stimulated at any time which would make identification of stimulated sources more complicated. Due to the specific recording regions of LIFEs and the binary-type of coding with these electrodes, one might expect the gap between the MCC and LIFE recording array digit identification rates to become wider. If more than one digit is stimulated and recorded with the LIFE array, one might expect the superimposed signals to indicate that two sources were stimulated. With the MCC recording array, it might be more difficult to identify how many sources were actually stimulated.

Contamination of the electroneurographic (ENG) signal may occur from electromyographic (EMG) activity that occurs with muscle motion, the stimulus artifact that occurs after stimulation of nerve or muscle, and other electromagnetic interference. EMG contamination can be removed with low-pass filtering techniques as the EMG has a lower frequency range than ENG. Specialized electrode configurations, such as tripolar electrode recordings, can also be used to remove EMG interference. The contamination due to stimulus artifact can be removed by blanking the inputs to the amplifiers during stimulation or recording only during intervals immediately preceding stimulation periods (Haugland and Hoffer, 1994). Other electromagnetic interference may also play a role in the contamination of the recorded neural signal and, if its frequency content does not overlap with the neural signal, may be removed by similar techniques as with EMG contamination.

Because the synchronizing pulse was recorded with the neural activity, there was no difficulty in determining when a stimulation was applied to one of the digits. In a real-life scenario, the onset of a disturbance is not known. To accommodate for the lack of a synchronizing pulse, the source identification may be calculated constantly with an extra

input to account for noise artifacts, thus requiring K+1 groups for the K possible sources and one extra for non-source signals. Another method could employ a trigger to start the identification calculation when the amplitude of the ENG activity is greater than some preset threshold or when the rate of rise of the filtered neural burst is greater than normal background activity.

Armed with the knowledge contained in this thesis, the field of functional electrical stimulation can benefit from knowledge that finer recordings are possible in the chronic situation. The selective recordings should allow more sophisticated Functional Electrical System (FES) controllers to be developed that can stimulate muscles more specifically. Hopefully, in the long run, paralyzed humans will benefit from these refined FES stimulation systems.

REFERENCES

Andrews, H.C. 1972. *Introduction to Mathematical Techniques in Pattern Recognition.* New York: Wiley-Interscience.

BAK Electronics Inc. 1981a. *Biphasic Pulse Generators: Model BPG-2.* Clarksburg, Maryland: BAK Electronics Inc.

BAK Electronics Inc. 1981b. *AC Differential Amplifiers: Model MDA-1.* Clarksburg, Maryland: BAK Electronics Inc.

Buckett, J.R., P.H. Peckham, and R.B. Strother. 1980. "Shoulder position control: An alternative control technique for motion impaired individuals," *Proc. Int. Conf. Rehab. Eng.*, Toronto, pp. 244 - 247.

Chen, Y., P.R. Christensen, K.D. Strange, and J.A. Hoffer. Accepted. "Multi-channel recordings from peripheral nerves: 2. Measurement of selectivity" in *Proc. 2nd Ann. Int. Func. Elec. Stim. Soc. Conf.*, Burnaby, 1997.

Christensen, P.R., Y. Chen, K.D. Strange, K. Yoshida, and J.A. Hoffer. Accepted. "Multi-channel recordings from peripheral nerves: 4. Evaluation of selectivity using mechanical stimulation of individual digits," in *Proc. 2nd Ann. Int. Func. Elec. Stim. Soc. Conf.*, Burnaby, 1997.

Cooley, W.W. and P.R. Lohnes. 1971. *Multivariate Data Analysis.* Toronto: John Wiley & Sons, Inc.

Crago, P.E., H.J. Chizeck, M.R. Neuman, and F.T. Hambrecht. 1986. "Sensors for use with functional neuromuscular stimulation," *IEEE Trans. Biomed. Eng.*, vol. 33, no. 2, pp. 256 - 268.

Crago, P.E., R.J. Nakai, and H.J. Chizeck. 1991. "Feedback regulation of hand grasp opening and contact force during stimulation of paralyzed muscle," *IEEE Trans. Biomed. Eng.*, vol. 38, no. 1, pp. 17 - 28.

Crouch, J.E. 1969. *Text-Atlas of Cat Anatomy.* Philadelphia: Lea & Febiger.

Franken, H.M., P.H. Veltink, and H.K. Boom. 1994. "Restoring gait in paraplegics by functional electrical stimulation," *IEEE Eng. Med. Biol.*, vol. , pp. 564 - 570.

Goodall, E.V., T.M. Lefurge, and K.W. Horch. 1991. "Information contained in sensory nerve recordings made with intrafascicular electrodes," *IEEE Trans. Biomed. Eng.*, vol. 38, no. 9, pp. 846 - 850.

Haugland, M.K. and J.A. Hoffer. 1994. "Slip information provided by nerve cuff signals: Application in closed-loop control of functional electrical stimulation," *IEEE Trans. Rehab. Eng.*, vol. 2, no. 1, pp. 29 - 36.

Haugland, M.K., J.A. Hoffer, and T. Sinkjaer. 1994. "Skin contact force information in sensory nerve signals recorded by implanted cuff electrodes," *IEEE Trans. Rehab. Eng.*, vol. 2, no. 1, pp. 18 - 28.

Hoffer, J.A. 1990. "Techniques to record spinal cord, peripheral nerve and muscle activity in freely moving animals," in *Neuromethods, Vol. 15: Neurophysiological Techniques: Applications to Neural Systems*, A.A. Boulton, G.B. Baker, and C.H. Vanderwolf, Eds. Clifton, New Jersey: The Humana Press Inc.

Hoffer, J.A. and M.K. Haugland. 1992. "Signals from tactile sensors in glabrous skin suitable for restoring motor functions in paralyzed humans," in *Neural Prostheses: Replacing Motor Function After Disease or Disability*, R.B. Stein, P.H. Peckham, and D.B. Popovic, Eds. New York: Oxford University Press.

Hoffer, J.A., K.D. Strange, Y. Chen, P.R. Christensen, and K. Yoshida. 1997. "Multi-channel recordings from peripheral nerves: 1. Properties of multi-contact cuff (MCC) and longitudinal intrafascicular electrode (LIFE) arrays implanted in cat forelimb nerves" in *Proc. 2nd Ann. Int. Func. Elec. Stim. Soc. Conf.*, Burnaby, 1997.

Hoffer, J.A., D. Crouch, K.Kallesøe, M. El Mouldi, S. Schindler, K. Strange, I. Valenzuela, and D. Viberg. 1994. *Sensory Feedback Signal Derivation from Afferent Neurons: Quarterly Progress Report #5.*

Honeywell Inc. 1982. *Technical Manual: Operator's Instructions for Model Ninety-Six Magnetic Tape Recorder/Reproducer System.* Denver, Colorado: Honeywell Inc.

Johansson, R.S. and G. Westling. 1984. "Roles of glabrous skin receptors and sensorimotor memory in automatic control of precision grip when lifting rougher or more slippery objects," *Exp. Brain Res.*, vol. 56, pp. 550 - 564.

Johansson, R.S. and G. Westling. 1987. "Signals in tactile afferents from the fingers eliciting adaptive motor responses during precision grip," *Exp. Brain Res.*, vol. 66, pp. 141 - 154.

Kandell, E.R., J.H. Schwartz, and T.M. Jessel. 1991. *Principles of Neural Science.* 3rd ed. New York: Elsevier Science Publishing Co., Inc.

Kasabov, N.K. 1996. *Foundations of Neural Networks, Fuzzy Systems, and Knowledge Engineering.* Cambridge, Massachusetts: A Bradford Book, The MIT Press.

Leaf Electronics, Ltd. *Leaf Dual QT-5B Preamplifiers.* Edmonton, Alberta: Leaf Electronics, Ltd.

Lefurge, T., E. Goodall, K. Horch, L. Stensaas, and A. Schoenberg. 1991. "Chronically implanted intrafascicular recording electrodes," *Ann. Biomed. Eng.*, vol. 19, pp. 197 - 207.

Lemay, M.A., P.E. Crago, M. Katorgi, and G.J. Chapman. 1993. "Automated tuning of a closed-loop hand grasp neuroprosthesis," *IEEE Trans. Biomed. Eng.*, vol. 40, no. 7, pp. 675 - 685.

Lichtenberg, B.K. and C.J. De Luca. 1979. "Distinguishability of functionally distinct evoked neuroelectric signals on the surface of a nerve", *IEEE Trans. BME*, vol. 26, no. 4, pp.228 - 237.

Malagodi, M.S., K.W. Horch, and A.A. Schoenberg. 1989. "An intrafascicular electrode for recording of action potentials in peripheral nerves," *Ann. Biomed. Eng.*, vol. 17, pp. 397 - 410.

McNaughton, T.G. and K.W. Horch. 1994. "Action potential classification with dual channel intrafascicular electrodes," *IEEE Trans. Biomed. Eng.*, vol. 41, no. 7, 609-616.

Milner, T.E., C. Dugas, N. Picard, and A.M. Smith. 1991. "Cutaneous afferent activity in the median nerve during grasping in the primate," *Brain Research*, vol. 548, pp. 228 - 241.

Nannini, N. and K. Horch. 1991. "Muscle recruitment with intrafascicular electrodes," *IEEE Trans. Biomed. Eng.*, vol. 38, pp. 769-776.

Nathan, R.H. 1993. "Control strategies in FNS systems for the upper extremities," *Crit. Rev. Biomed. Eng.*, vol. 21, no. 6, 485 - 568.

Norušis, M.J/SPSS, Inc. 1993. *SPSS for Windows: Professional Statistics, Release 6.1.* Chicago: SPSS, Inc.

Oppenheim, A.V. and R.W. Schafer. 1989. *Discrete-Time Signal Processing.* Englewod Cliffs, New Jersey: Prentice-Hall, Inc.

Palastanga, N., D. Field, and R. Soames. 1994. *Anatomy and Human Movement: Structure and Function. 2nd ed.* Toronto: Butterworth-Heinemann Ltd.

Rothwell, J. 1994. *Control of Human Voluntary Movement.* London, England: Chapman & Hall.

Sahin, M. and D.M. Durand. 1996. "Selective recording with a multi-contact nerve cuff electrode," *Proc. 19th Ann. Int. Conf. of IEEE EMBS*, Amsterdam, pp. ?.

Sinkjaer, T., M. Haugland, and J. Haase. 1994. "Natural neural sensing and artificial muscle control in man," *Exp. Brain Res.*, vol. 98, no. 3, pp. 542 - 545.

Srinivasan, M.A., J.M. Whitehouse, and R.H. LaMotte. 1990. "Tactile detection of slip: Surface microgeometry and peripheral neural codes," *J. Neurophys.*, vol. 63, no. 6, pp. 1323 - 1332.

Stein, R.B., M. Bélanger, G. Wheeler, M. Wieler, D.B. Popovic, A. Prochazka, and L.A. Davis. 1993. "Electrical systems for improving locomotion after incomplete spinal cord injury: An assessment," *Arch. Phys. Med. Rehabil.*, vol. 74, pp. 954 - 959.

Strange. K.D., P.R. Christensen, Y. Chen, K. Yoshida, and J.A. Hoffer. Accepted. "Multi-channel recordings from peripheral nerves: 3. Evaluation of selectivity using electrical stimulation of individual digits," in *Proc. 2nd Ann. Int. Func. Elec. Stim. Soc. Conf.*, Burnaby, 1997.

Struijk, J.J., M.K. Haugland, and M. Thomsen. 1996. "Fascicle selective recording with a nerve cuff electrode," *Proc. 19th Ann. Int. Conf. of IEEE EMBS*, Amsterdam, pp. ?.

Tektronix, Inc. 1993. *Programmer Manual: TDS Family Includes TDS 420, 460, 520, 540, 620, 640 Digitizing Oscilloscopes.* Beaverton, Oregon: Tektronix, Inc.

Ulieru, M. 1996. *Fuzzy Logic in Diagnostic Decision: Possibilistic Networks.* Dr-Ing Dissertation. Darmstadt University of Technology, Darmstadt, Germany.

Veltink, P.H., J.A. van Alste, and H.B.K. Boom. 1989. "Multielectrode intrafascicular and extraneural stimulation." *Med. Biol. Eng. Comput.*, vol. 27, pp. 19-24.

Westling, G. and R.S. Johansson. 1987. "Responses in glabrous skin mechanoreceptors during precision grip in humans," *Exp. Brain Res.*, vol. 66, pp. 128 - 140.

Young, T.Y. and T.W. Calvert. 1974. *Classification, Estimation and Pattern Recognition.* New York: American Elsevier Publishing Company, Inc.

Yoshida, K. and K. Horch. 1993. "Selective stimulation of peripheral nerve fibers using dual intrafascicular electrodes," *IEEE Trans. Biomed. Eng.*, vol. 40, no. 5, pp. 492-494.

Yoshida, K. and K. Horch. 1996. "Closed-loop control of ankle position using muscle afferent feedback with functional neuromuscular stimulation," *IEEE Trans. Biomed. Eng.*, vol. 43, no. 2, pp. 167-176.

Zimmermann, H.-J. 1991. *Fuzzy Set Theory – and Its Applications. 2nd Ed.* Boston: Kluwer Academic Publishers.

APPENDIX A : DIGIT MANIPULATOR CONTROLLER

Hardware

The next page contains the schematic for the hardware for the five-digit manipulator. The design shows the 74138 decoding chips that were used to select one of the ten LM1949 injector drive controllers from National Semiconductor. The transistors were high power TIP120s. The solenoids that are shown are TSP45-3V and TPO45-3V push- and pull-type solenoids purchased from Electro-Mechanisms of San Dimas, California.

Software

Single.c

This program was written to run the mechanical stimulation experiments with the five-digit manipulator.

```
/*      single2.c
 *
 *
 */
#include <stdio.h>
#include <nidaq.h>
#include <dos.h>
#include <conio.h>
#include <stdlib.h>
#include <ctype.h>


// AT-MIO-16F-5 acquisition board constants
#define       ATMIO_BASE    0x320         // Base address of the AT-MIO-16F-5
                                          //   acquision board on the EXCO machine

// The following registers have addresses w.r.t. the AT-MIO-16F-5 base
#define       EXT_STROBE_REGISTER 0x0E    // External strobe register address
#define       DIGOUT_REG          0x1C    // Digital outport register
#define       DIGIN_REG           0x1C    // Digital inport register
#define       PORTDIOA            0       // Digital port A
#define       PORTDIOB            1       // Digital port B
#define       Ton                 48      // 48 ms perturbation
//#define     Tstep               8       // 1/6th of Ton.  Necessary for
                                          //     triggering timing
#define       NumOfSources        5       // Number of Sources (i.e., digits)


int     brdCode;
int     brdNum = 1;


/*****************************************************************************/
/*             INIT                                                          */
/*                                                                           */
/* Initializes the interface port to initial values and configures the       */
/* digital and analog output channels.                                       */
/*****************************************************************************/
void Init ( void )
{
       clrscr();

       Init_DA_Brds (brdNum, &brdCode);
       DIG_Prt_Config (brdNum, PORTDIOB, 0, 1);
       DIG_Prt_Config (brdNum, PORTDIOA, 0, 1);

       DIG_Out_Port (brdNum, PORTDIOA, 0);      // Turn off trigger pulse
       DIG_Out_Port (brdNum, PORTDIOB, 15);     // Turn off all solenoid pulses


} /* Init */


/*****************************************************************************/
```

```
/*                    REFRESH                                                 */
/*                                                                            */
/******************************************************************************/
int SRQ ( void )
{
      int    continu = 0;
      int    option = 0;
      int    choice = 0;


      do
      {
            clrscr();

            printf ("Choose an option.\n"
                    "  1: Trigger one solenoid.\n"
                    "  2: Run the experiment.\n"
                    "  \n"
                    "  Q: Quit.\n");

            scanf("%s", &option);
            option = toupper(option);

            switch (option) {
              case '1':    choice = 1; continu = 1; break;
              case '2':    choice = 2; continu = 1; break;
              case 'Q':    choice = -1; continu = 1; break;
              default:     printf("Bug in SRQ!\n"
                                  "  %d was an illegal option.  Try again.\n",
option);  delay(2000); continu = 0; break;
            }
      }
      while (!continu);

      return (choice);


} /* SRQ */



/******************************************************************************/
/*           VALID SOLENOID ?                                                 */
/*                                                                            */
/******************************************************************************/
int validSolenoid ( int    solenoid )
{
      if ( (solenoid>0) && (solenoid<11) )
            return 1;
      else
      {
            printf ("You entered an invalid solenoid value (%d).  Try
again.\n", solenoid);
            printf ("Press any key to continue...\n");
            getch();
            return 0;
      }

} /* ValidSolenoid */



/******************************************************************************/
/*                    TURN ON SOLENOID                                        */
/*                                                                            */
/* This procedure turns on the solenoid given by the input parameters         */
/* 'source' and 'perttype'.  The source is normaly limited to one of the      */
```

```
/* five digits and the perttype is limited to either a normal perturbation  */
/* (perttype = 0) or a slip (perttype = 1).                                 */
/*                                                                          */
/* The trigger pulse is HIGH to signal the rising egde of the pulse and     */
/* HIGH (1)  at the end to signal the end of the pulse.  The length of the  */
/* first HIGH pulse signals which of the five soruces was signaled.  The    */
/* different trigger signals are listed here:                               */
/*                                                                          */
/* 1: 1-0-0-0-0-1                                                           */
/* 2: 1-1-0-0-0-1                                                           */
/* 3: 1-1-1-0-0-1                                                           */
/* 4: 1-1-1-1-0-1                                                           */
/* 5: 1-1-1-1-1-1                                                           */
/*                                                                          */
/**************************************************************************/
void TurnOnSolenoid ( int source, int perttype, int onTime, int offTime )
{
      int    solenoid;
      int    Tstep;


      solenoid = 2*(source-1) + perttype;
      Tstep = onTime/6;

      // Turn on trigger; turn on solenoid
      outport (ATMIO_BASE+DIGOUT_REG, ((16*solenoid)+0x0F));

      delay (source*Tstep);
      // Turn off trigger; leave solenoid on
      outport (ATMIO_BASE+DIGOUT_REG, (16*solenoid)+0);

      delay ((5-source)*Tstep);
      // Turn on trigger; leave solenoid on
      outport (ATMIO_BASE+DIGOUT_REG, ((16*solenoid)+0x0F));

      delay (Tstep);
      // Turn off trigger; turn off solenoid
      outport (ATMIO_BASE+DIGOUT_REG, 0xF0);

      // Leave off for specified time
      delay(offTime);

} /* TurnOnSolenoid */



/**************************************************************************/
/*            SETUP                                                       */
/*                                                                        */
/* This procedure is run when the user wishes to calibrate one of the     */
/* solenoids for an experiment.  The user is prompted for which solenoid to */
/* trigger and then that solenoid is triggered 'perts' times at a rate of */
/* 2 pulses per second to avoid burning out the solenoid.                 */
/*                                                                        */
/**************************************************************************/
void SetUp ( void )
{
      int    perts = 50;
      int    halt = 0;
      int    option = 'z';
      int    continu = 0;
      int    i;
      div_t x;
      int    digit;
      int    perttype;
      int    ylocation;
```

```
        clrscr();
        do
        {
                printf ("Pick a solenoid to calibrate (0 - 9) or 'Q' to quit.\n");

                scanf ("%s", &option);
                option = toupper(option);

                switch (option) {
                        case '0':
                        case '1':
                        case '2':
                        case '3':
                        case '4':
                        case '5':
                        case '6':
                        case '7':
                        case '8':
                        case '9':    option = option - '0'; continu = 1; halt = 0;
break;
                        case 'Q':    option = -1; continu = 1; halt = 1; break;
                        default:            printf("Bug in SetUp!\n"
                                                        "  %d was an
illegal option.  Try again.\n", option);  delay(2000); continu = 0; halt = 0;
break;
                }
        }
        while (!continu);

        if (!halt)
        {
                x = div(option,2);
                digit = (int)x.quot+1;
                perttype = (int)x.rem;

                // Draw markers indicating the number of perturbations to occur
                ylocation = wherey();
                gotoxy(1, ylocation+1);

                for (i=0; i<perts; i++)
                        printf(".");

                gotoxy(1,ylocation+1);

                // Allow the perturbations to begin.  Mark off the perts. as they
occur.
                i = 0;
                while ( (i<perts) & !kbhit() )
                {
                        TurnOnSolenoid(digit, perttype, Ton, (500-Ton));
                        printf ("*");
                        i++;
                }
        }

} /* SetUp */


/*****************************************************************************/
/*              RUN EXPERIMENT                                               */
/*                                                                           */
/* This procedure prompts the user for whether they wish to run a 'normal'   */
/* or a 'slip' perturbation experiment.  The digits are then perturbed one   */
/* at a time in a cycle so that each digit gets perturbed once per second.   */
```

```
/*                                                                          */
/**************************************************************************/
void RunExp ( void )
{
       int    perttype = -1;
       int    continu  = -1;
       int    halt         = -1;
       int    i,j;
       int    perts        = 50;
       int    digit;
       int    ylocation;


       do
       {
              clrscr();

              printf ("Pick a perturbation type.\n"
                             "   1: Normal\n"
                             "   2: Slip\n"
                             "   \n"
                             "   Q: Quit\n");

              scanf ("%s", &perttype);
              perttype = toupper(perttype);

              switch (perttype) {
                     case '1':
                     case '2':     perttype = perttype - '1'; continu = 1; halt =
0; break;
                     case 'Q':     perttype = -1; continu = 1; halt = 1; break;
                     default:            printf("Bug in RunExp!\n"
                                                                  "  %d was an
illegal option.  Try again.\n", perttype);  delay(2000); continu = 0; halt = 0;
break;
              }
       }
       while (!continu);

       if (!halt)
              // Draw markers indicating the number of perturbations to occur
              ylocation = wherey();
              gotoxy(1, ylocation+1);

              for (i=0; i<perts; i++)
                     printf(".");

              gotoxy(1,ylocation+1);

              i = 0;
              while ( (i<perts) & !kbhit() )
              {
                     for (digit=1; digit<=NumOfSources; digit++)
                            TurnOnSolenoid(digit, perttype, Ton, (200-Ton));
                     printf("*");
                     i++;
              }

} /* RunExp */



/**************************************************************************/
/*           MAIN                                                         */
/*                                                                        */
/**************************************************************************/
void main ()
```

```
{
        int             option;


        Init();

        do
        {
                option = SRQ();

                if (option == 1)
                        SetUp();

                if (option == 2)
                        RunExp();

        }
        while (option != -1);

        Init();
        exit(0);


} /* single2 */
```

APPENDIX B : MATLAB PROCESSING FILE

This is the Matlab .m file that I used to process the raw digitized data from the two tripolar, circumferential electrodes located on the median and ulnar nerves. The processing that was performed on the multi-channel electrode arrays was identical, except that there were more channels to process and plot, and from which to generate peak, area, and time-to-peak features.

Spitcirc.m

```
function spitcirc(newdr)
% an m-file to load the ascii data (*.vt) files, remove their DC offsets,
% rectify the signals, filter the data, decimate the data, and then spits
% out the peak amplitudes, the time of the peak amplitude, and the area of
% the neural activity burst.  The data is "spit out" to a file named s.dat,
% where s is the name of the directory for the data.  The data in s.dat is
% arranged in three groups of five columns.  The area data is in the first
% set of columns, peak data in the second group of five columns, and the
% timing data in the third set of columns.  The 1st - 4th columns contain
% the data from the 1st - 4th multi-electrode data.

olddir = cd
%newdr = input('Enter the new directory: ','s');
newdir = ['cd ',newdr]
eval (newdir)

decvalue = 10;                              % decimation value
filterlength = 44;                          % Kaiser window length
filterdelay = filterlength/2;
kw = kaiser(filterlength, 7.8573);          % Kaiser window with -80 dB sidelobes
                                            %    and cutoff frequency = 400Hz =
                                            %    0.04*pi
samprate    = 20000/decvalue;               % sampling rate = 20000/decvalue S/s
%ontime      = 0.050;                       % perturbation pulse width = 50 ms
%onsamp      = samprate*ontime;             % perturbation time in samples
%halfonsamp = onsamp/2;                     % half width of the perturbation
filtdelaysamp = filterdelay/decvalue;       % filter delay in decimated sample
                                            %     counts
%solenoid = 0.0023;                         % 2.3 ms to move the solenoid 3 mm
                                            %     (3mm/(0.35"/6.7ms) = 3mm/1.33m/s)
                                            %     in the vertical direction
solenoid = 0;                               % Set to 0 for slips; there is no
                                            %     movement delay for a slip input
transduction = 0.001;                       % 1 ms for transduction in the
                                            %     mechanoreceptor
conduction = 0.0005;                        % 0.5 ms conduction time in the nerve
                                            %     (100 m/s * 0.05 m)
conductdelay = (solenoid+transduction+conduction)*samprate;
                                            % total delay, not including filtering
                                            %     delays, in samples

Tstep = 0.008;                              % 8 ms
synctime = 6*Tstep*samprate;                % perturbation pulse width = 6*Tstep =
                                            %     about 48 ms

Wn = 0.04;                                  % Cutoff frequency in pi radians for the
                                            % High-pass Butterworth filter
```

```
[B,A] = butter(10, Wn, 'high');          % Coefficients for a 10th order,
                                         %     high-pass Butterworth filter

% Set the gains for the various channels.
medcircgain =100000;
ulncircgain =100000;

%figure;
clf;


% load the sync pulses and process it
load syncirc.vt;
syncdec = decimate(syncirc, decvalue);
syncdiff = diff(syncdec);
syncthresh = mean(syncdec);
clear syncirc;

% plot the sync pulse
subplot(3,1,1), plot(syncdec);
disp('syncirc loaded');


% process the tripolar data from the circumferential data from the median cuff
load medcirc.vt;
med1 = medcirc/medcircgain;
med1off  = med1-mean(med1);              % remove DC offset
med1off = filtfilt(B,A,med1off);         % filter out low-frequency interference
clear med1;
clear medcirc;
med1abs  = abs(med1off);                 % rectify the signal
clear med1off;
med1lp   = conv(med1abs, kw);            % low-pass filter the signal
clear med1abs;
med1dec  = decimate(med1lp, decvalue);
clear med1lp;
med1avg  = 0.75*mean(med1dec);

subplot(3,1,2), plot(med1dec);           % plot the median cuff data
disp('medcirc loaded');



% process the tripolar data from the circumferential data from the ulnar cuff
load ulncirc.vt;
uln1 = ulncirc/ulncircgain;
uln1off  = uln1-mean(uln1);              % remove DC offset
uln1off = filtfilt(B,A,uln1off);         % filter out unwanted noise
clear ulncirc;
clear ulncirc;
uln1abs  = abs(uln1off);                 % rectify the signal
clear uln1off;
uln1lp   = conv(uln1abs, kw);            % low-pass filter the signal
clear uln1abs;
uln1dec  = decimate(uln1lp, decvalue);
clear uln1lp;
uln1avg  = 0.75*mean(uln1dec);

subplot(3,1,3), plot(uln1dec);           % plot the ulnar cuff detail
disp('ulncirc loaded');


Yarray = [1e-4 max(med1dec) max(uln1dec)];
Ymax = max(Yarray);
Xlength = length(syncdec);
t = [1 Xlength];
```

```
subplot(3,1,1), set(gca,'Xlim', [0 Xlength]);
subplot(3,1,2), set(gca,'Xlim', [0 Xlength]), set(gca,'Ylim',[0 Ymax]), hold on,
plot(t,med1avg*ones(size(t)),'r');
subplot(3,1,3), set(gca,'Xlim', [0 Xlength]), set(gca,'Ylim',[0 Ymax]), hold on,
plot(t,uln1avg*ones(size(t)),'r');


% find the perturbation onset points and determine which digit was perturbed
perts = 0;
k = 1;
looplength = length(syncdiff)-synctime-filtdelaysamp-1;
datalength = synctime;

%for i=1:looplength,
i = 1;
while (i < looplength),
       if ( (syncdiff(i)>0.5) & (syncdec(i+5.5*Tstep*samprate)>0.5) ),
              onset = i;
              if ( (syncdec(i+4.5*Tstep*samprate) > 0.5) ),
                     digit = 5;

              elseif ( (syncdec(i+3.5*Tstep*samprate) > 0.5) ),
                     digit = 4;

              elseif ( (syncdec(i+2.5*Tstep*samprate) > 0.5) ),
                     digit = 3;

              elseif ( (syncdec(i+1.5*Tstep*samprate) > 0.5) ),
                     digit = 2;

              else
                     digit = 1;

              end;   % if syncdec


              if ( ((onset+filtdelaysamp+datalength) < looplength) &
((onset+filtdelaysamp) > 0) ),
                     med1array =
med1dec((onset+conductdelay+filtdelaysamp):(onset+filtdelaysamp+datalength))';
                     uln1array =
uln1dec((onset+conductdelay+filtdelaysamp):(onset+filtdelaysamp+datalength))';
                     perts = perts+1;

                     disp('channels chopped');


                     % calculates the areas, peaks, and time to peak information
for all of the
                     % nerve recordings
                     med1area = max(1e-15, (sum(med1array)-(datalength-
conductdelay)*med1avg));
                     [med1peak, med1index] = max(med1array);
                     med1time = (med1index-filtdelaysamp-conductdelay)/samprate;
                     med1data = [med1area med1peak med1time];
                     subplot(3,1,2), hold on,
plot(onset+filtdelaysamp+conductdelay+med1index,med1peak,'ro');

                     uln1area = max(1e-15, (sum(uln1array)-(datalength-
conductdelay)*uln1avg));
                     [uln1peak, uln1index] = max(uln1array);
                     uln1time = (uln1index-filtdelaysamp-conductdelay)/samprate;
                     uln1data = [uln1area uln1peak uln1time];
                     subplot(3,1,3), hold on,
plot(onset+filtdelaysamp+conductdelay+uln1index,uln1peak,'ro');

                     areadata = [med1area uln1area];
```

```
                    areadatan = areadata/norm(areadata);
                    peakdata = [med1peak uln1peak];
                    peakdatan = peakdata/norm(peakdata);
                    timedata = [med1time uln1time];

                    digit
                    areadata
                    peakdata
                    timedata
                    areadatan
                    peakdatan

                    alldata(k,:) = [digit areadata peakdata timedata areadatan
peakdatan];
                    k = k+1;
                    i = i+(1.5*synctime);

              end;   % if onset
              i = i+1;
       else
              i = i+1;

       end;   % if syndiff

end;   % while i


savefile = [newdr,'c.txt'];
savestuff = ['save ..\',savefile,' alldata -ascii -tabs'];
eval(savestuff);

perts

olddir = ['cd ',olddir]
eval (olddir)
```

APPENDIX C : MECHANICAL PERTURBATION SELECTIVITY RESULTS

NOTE: how to interpret these numbers

- All numbers give the average selectivity for a particular recording setup with the vector analysis or clustering method
- The four recording setups are as follows:

  column labeled 8-channel: 8 channel recordings on 5 stimulated digits

  column labeled median only: 4 channel recordings on 4 stimulated digits (I - IV)

  column labeled ulnar only: 4 channel recordings on 2 stimulated digits (IV & V)

  column labeled 2xTripolar: 2 channel recordings on 5 stimulated digits

- The first data element in the selectivity analysis columns represent the results using the peak feature of the rectified-smoothed-averaged neural burst; the second data element shows the results using the area feature of the rectified-smoothed-average neural burst. From 14 to 30 individual mechanical perturbations are averaged in the measure.
- The shaded sections of the 8-channel column indicates that days on which the 8-channel value was obtained by combining data from the two 4-channel recording sessions.
- A "-1" in the day column represents the selectivity value obtained after using the single-digit manipulator and a "-5" indicates the value obtained after using the five-digit manipulator.

Table C.1: Selectivity indices for NIH19: A Multi-Contact Cuff subject

Day	8-channel	median only	ulnar only	2xTripolar	Notes
22	[illegible]	10 / 12	8 / 33	11 / 26	normal only. ulnar nerve activity not recorded on digits I&II. Signal from dIII was used to fill in.
40	[illegible]	13 / 15	5 / 16	9 / 6	normal only
103	[illegible]	3 / 6	4 / 100	10 / 33	← bad uln3; normal only
126	[illegible] [illegible] [illegible]	/ 8 / 13 / 21	/ 4 / 14 / 17	/ 12 / 25 / 38	← normal perturbation ← slip perturbation (out; #1) ← slip perturbation (in; #2) Bad Ulnar circumferential
154	8 / 16	8 / 15	2 / 2	✣ / ✣	Slips only; very noisy signal on ulnar 1, gain set to 10,000 for that channel to avoid clipping on FM tape
180-1	15 / 14 9 / 11	7 / 7 5 / 6	3 / 1 3 / 2	✣ / ✣	● normal perturbation ● slip perturbation (out; #1) Bad Ulnar circumferential
180-5	14 / 14 10 / 20	5 / 4 8 / 19	2 / 2 5 / 5	✣ / ✣	← normal perturbation ● slip perturbation (out; #1) Bad Ulnar circumferential

Table C.2: Selectivity indices for NIH21, a MCC subject

Day	8-channel	median only	ulnar only	2xTripolar	Notes
14	[illegible]	7 / 14	1 / 10	5 / 13	normal only
35	[illegible] [illegible] [illegible]	7 / 29 4 / 38 7 / 23	5 / 23 3 / 6 3 / 16	5 / 29 5 / 28 4 / 33	← normal perturbation ← slip perturbation (out; #1) ● slip perturbation (in; #2)
84	12 / 14 4 / 6	7 / 5 5 / 3	13 / 10 1 / 1	7 / 6 2 / 4	← normal perturbation ← slip perturbation (out; #1)
94-1	5 / 7 5 / 8	2 / 2 3 / 4	4 / 5 2 / 4	4 / 5 2 / 5	● normal perturbation ← slip perturbation (out; #1)
94-5	3 / 7 3 / 9	2 / 3 3 / 7	2 / 3 3 / 5	5 / 7 3 / 5	← normal perturbation ← slip perturbation (out; #1)
99-1	8 / 8 11 / 8	7 / 6 7 / 7	2 / 4 5 / 3	3 / 5 2 / 4	● normal perturbation ● slip perturbation (out; #1)
99-5	8 / 13 4 / 7	4 / 4 2 / 2	2 / 2 7 / 4	5 / 7 3 / 5	← normal perturbation ← slip perturbation (out; #1)

Table C.3: Selectivity indices for NIH22, a LIFE subject

Day	8-channel	median only	ulnar only	2xTripolar	Notes
3	[illegible]	27 / 36	16 / 14	8 / 35	← normal perturbation
	[illegible]	36 / 57	12 / 24	5 / 52	← slip perturbation (out; #1)
	[illegible]	28 / 45	7 / 8	4 / 35	← slip perturbation (in; #2)
9	[illegible]	/ 46	/ 13	/ 23	← normal perturbation
	[illegible]	/ 55	/ 8	/ 20	← slip perturbation (out; #1)
	[illegible]	/ 56	/ 25	/ 39	← slip perturbation (in; #2)
24-1	22 / 23	21 / 20	9 / 13	3 / 4	slips only
58-5	21 / 25	21 / 27	7 / 4	5 / 6	← normal perturbation
	11 / 28	16 / 34	5 / 6	5 / 10	← slip perturbation (out; #1)
65-1	20 / 21	28 / 28	16 / 11	6 / 7	← normal perturbation
	14 / 22	25 / 32	5 / 3	4 / 6	← slip perturbation (out; #1)
65-5	16 / 25	20 / 29	19 / 26	10 / 12	← normal perturbation
	15 / 28	17 / 34	13 / 11	4 / 8	← slip perturbation (out; #1)
72-1	30 / 33	18 / 18	16 / 12	9 / 9	← normal perturbation
	25 / 31	15 / 20	4 / 8	4 / 6	← slip perturbation (out; #1) flakey amp for med1, uln1& uln2
72-5	22 / 32	23 / 30	11 / 17	8 / 10	← normal perturbation
	17 / 28	16 / 30	11 / 9	4 / 6	← slip perturbation (out; #1) flakey amp for med1, uln1& uln2

Table C.4: Selectivity indices for NIH23, a LIFE subject

Day	8-channel	median only	ulnar only	2xTripolar	Notes
29	17 / 18	12 / 12	11 / 7	9 / 10	← normal perturbation
	10 / 18	5 / 9	5 / 9	4 / 8	← slip perturbation (out; #1)
43-1	13 / 16	5 / 4	14 / 9	5 / 8	← normal perturbation
	16 / 17	11 / 7	12 / 15	2 / 4	← slip perturbation (out; #1)
43-5	19 / 28	7 / 11	11 / 10	9 / 11	← normal perturbation
	9 / 17	7 / 11	6 / 4	3 / 10	← slip perturbation (out; #1)

APPENDIX D : RESULTS OF DIGIT IDENTIFICATION ANALYSIS

NOTE: how to interpret the numbers in the following tables

- All numbers give the percentage of correctly identified digits from the mechanical stimulations.
- The four recording setups are as follows:

  row labeled 8: 8 channel recordings on 5 stimulated digits

  row labeled 2: 2 channel recordings on 5 stimulated digits

  row labeled 4m: 4 channel recordings on 4 stimulated digits (I - IV)

  row labeled 4u: 4 channel recordings on 2 stimulated digits (IV & V)

- Symbols used in this document:

  —: Not recorded

  ✤: High impedance signal; too noisy to be useful

Table D.1: Digit identification accuracy for NIH19 using leave-one-out analysis

Day		Raw data			Normalized			Perts
		Area (%)	Peak (%)	Area & Peak (%)	Area (%)	Peak (%)	Area & Peak (%)	
154S	8	76.3	63.2	86.0	72.8	56.1	71.1	23
	2	✤	✤	✤	✤	✤	✤	
	4m	94.4	74.4	92.2	85.6	65.6	85.6	
	4u	50.0	71.7	76.1	54.3	69.9	76.1	
180N-1	8	87.9	80.7	91.4	83.6	83.6	88.6	28
	2	✤	✤	✤	✤	✤	✤	
	4m	75.9	64.3	84.8	73.2	74.1	84.8	
	4u	83.9	100	100	100	100	100	
180S-1	8	82.9	77.1	81.4	81.4	72.1	78.6	28
	2	✤	✤	✤	✤	✤	✤	
	4m	67.0	61.6	64.3	75.9	65.2	75.0	
	4u	78.6	100	100	98.2	100	100	
180N-5	8	76.7	74.4	82.0	77.4	78.2	84.2	27
	2	✤	✤	✤	✤	✤	✤	
	4m	41.5	52.8	60.4	72.6	71.7	79.2	
	4u	70.4	59.3	64.8	98.1	92.6	100	
180S-5	8	95.5	76.7	97.7	90.2	77.4	88.0	27
	2	✤	✤	✤	✤	✤	✤	
	4m	93.4	65.1	94.3	84.9	70.8	83.0	
	4u	100	92.6	100	92.6	92.6	96.3	

Note: N-1 = stimulation provided by normal inputs with one-digit manipulator; N-5 = stimulation provided by normal inputs with five-digit manipulator; S-1 = stimulation provided by slip inputs with one-digit manipulator; S-5 = stimulation provided by slip inputs with five-digit manipulator.

Table D.2: Digit identification accuracy for NIH19 using leave-all-in analysis

Day		Raw data			Normalized			Perts
		Area (%)	Peak (%)	Area & Peak (%)	Area (%)	Peak (%)	Area & Peak (%)	
154S	8	81.6	71.9	93.9	76.3	63.2	84.2	23
	2	✤	✤	✤	✤	✤	✤	
	4m	95.6	77.8	98.9	87.8	71.1	91.1	
	4u	60.9	76.1	84.8	67.4	73.9	84.8	
180N-1	8	91.4	85.7	93.6	87.9	87.9	95	28
	2	✤	✤	✤	✤	✤	✤	
	4m	76.8	73.2	88.4	76.8	76.8	90.2	
	4u	76.8	100	100	100	100	100	
180S-1	8	87.1	82.1	92.1	85.7	77.9	86.4	28
	2	✤	✤	✤	✤	✤	✤	
	4m	67.9	67.0	75.0	78.6	69.6	83.9	
	4u	83.9	100	100	98.2	100	100	
180N-5	8	85.7	77.4	90.2	82.0	83.5	88.7	27
	2	✤	✤	✤	✤	✤	✤	
	4m	55.7	61.3	67.0	78.3	76.4	83.0	
	4u	72.2	64.8	74.1	100	96.3	100	
180S-5	8	98.5	84.2	98.5	92.5	79.7	95.5	27
	2	✤	✤	✤	✤	✤	✤	
	4m	96.2	67.0	98.1	87.7	78.3	89.6	
	4u	100	96.3	100	94.4	94.4	96.3	

Note: N-1 = stimulation provided by normal inputs with one-digit manipulator; N-5 = stimulation provided by normal inputs with five-digit manipulator; S-1 = stimulation provided by slip inputs with one-digit manipulator; S-5 = stimulation provided by slip inputs with five-digit manipulator.

Table D.3: Digit identification accuracy for NIH21 using leave-one-out analysis

Day		Raw data			Normalized			Perts
		Area (%)	Peak (%)	Area & Peak (%)	Area (%)	Peak (%)	Area & Peak (%)	
14N	8	—	—	—	—	—	—	14
	2	—	—	—	—	—	—	
	4m	63.1	70.8	66.2	46.2	67.7	58.5	
	4u	78.6	67.9	60.7	71.4	75.0	75.0	
35N	8	—	—	—	—	—	—	14
	2	—	—	—	—	—	—	
	4m	67.9	62.5	66.1	51.8	44.6	55.4	
	4u	82.1	78.6	85.7	57.1	75.0	67.9	
35S	8	—	—	—	—	—	—	14
	2	—	—	—	—	—	—	
	4m	35.7	33.9	48.2	41.1	41.1	53.6	
	4u	92.9	71.4	82.1	60.7	53.6	67.9	
84N	8	79.7	75.2	83.5	79.7	74.4	82.0	27
	2	43.6	45.9	47.4	43.6	36.8	40.6	
	4m	80.2	72.6	82.1	77.4	72.6	79.2	
	4u	87.0	87.0	87.0	87.0	85.2	85.2	
84S	8	72.2	30.1	68.4	60.2	31.6	59.4	27
	2	40.6	29.3	39.8	32.3	27.8	27.1	
	4m	59.0	35.2	61.9	53.3	38.1	57.1	
	4u	35.2	48.1	51.9	70.4	51.9	68.5	
94N-1	8	72.1	59.3	66.4	60.7	57.9	61.4	28
	2	43.4	37.7	40.9	32.1	28.3	32.1	
	4m	50	42.0	49.1	58.0	49.1	64.3	
	4u	73.2	71.4	76.8	66.1	69.6	67.9	
94S-1	8	76.4	69.3	80.0	70.7	65.7	70.7	28
	2	35.2	28.9	36.5	27.0	27.0	34.0	
	4m	58.0	52.7	59.8	70.5	52.7	76.8	
	4u	76.8	62.5	76.8	75.0	60.7	75.0	
94N-5	8	83.3	64.9	83.3	72.8	54.4	71.9	23
	2	42.1	42.1	48.1	39.1	35.3	42.9	
	4m	60.0	41.1	65.6	72.2	46.7	70.0	
	4u	89.4	80.9	93.6	76.6	66.0	70.2	
94S-5	8	89.5	60.2	88.7	78.2	48.1	77.4	26
	2	67.7	44.4	66.2	33.1	23.3	30.1	
	4m	84.8	50.5	85.7	70.5	48.6	76.2	
	4u	96.4	72.7	96.4	87.3	67.3	80.0	
99N-1	8	64.7	51.8	68.3	63.3	45.3	64.7	28
	2	30.8	27.6	28.8	35.3	26.3	29.5	

	4m	55.0	54.1	62.2	60.4	52.3	65.8	
	4u	67.3	43.6	72.7	70.9	41.8	78.2	
99S-1	8	70.7	68.6	71.4	59.3	61.4	62.1	28
	2	33.8	31.9	29.4	32.5	28.8	31.9	
	4m	74.1	70.5	77.7	64.3	71.4	70.5	
	4u	55.4	64.3	53.6	58.9	60.7	53.6	
99N-5	8	97.7	86.5	98.5	85.7	69.9	87.2	27
	2	55.4	42.3	52.3	31.5	34.6	26.9	
	4m	84.9	65.1	85.8	82.1	65.1	82.1	
	4u	88.9	79.6	87.0	79.6	59.3	83.3	
99S-5	8	92.5	63.9	89.5	63.9	50.4	66.2	26
	2	50.0	39.2	49.2	37.7	25.4	36.9	
	4m	84.9	62.3	85.8	65.1	45.3	69.8	
	4u	100	90.6	100	71.7	88.7	83.0	

Note: N-1 = stimulation provided by normal inputs with one-digit manipulator; N-5 = stimulation provided by normal inputs with five-digit manipulator; S-1 = stimulation provided by slip inputs with one-digit manipulator; S-5 = stimulation provided by slip inputs with five-digit manipulator.

Table D.4: Digit identification accuracy for NIH21 using leave-all-in analysis

Day		Raw data			Normalized			Perts
		Area (%)	Peak (%)	Area & Peak (%)	Area (%)	Peak (%)	Area & Peak (%)	
14N	8	—	—	—	—	—	—	14
	2	—	—	—	—	—	—	
	4m	69.2	75.4	78.5	52.3	69.2	72.3	
	4u	92.9	82.1	100	78.6	82.1	92.9	
35N	8	—	—	—	—	—	—	14
	2	—	—	—	—	—	—	
	4m	76.8	69.6	85.7	57.1	62.5	75.0	
	4u	92.9	92.1	96.4	64.3	82.1	82.1	
35S	8	—	—	—	—	—	—	14
	2	—	—	—	—	—	—	
	4m	46.4	48.2	64.3	48.2	57.1	64.3	
	4u	92.9	85.7	85.7	75.0	78.6	78.6	
84N	8	85.0	78.2	88.7	85.0	78.9	86.5	27
	2	46.6	47.4	54.1	44.4	44.4	46.6	
	4m	84.0	74.5	86.8	78.3	76.4	83.0	
	4u	88.9	87.0	88.9	87.0	88.9	90.7	
84S	8	80.5	45.9	86.5	70.7	45.1	72.2	27
	2	44.4	34.6	46.6	34.6	31.6	35.3	
	4m	64.8	41.0	70.5	61.0	43.8	61.0	
	4u	50.0	59.3	66.7	72.2	61.1	77.8	
94N-1	8	76.4	68.6	81.4	67.1	66.4	72.9	28
	2	45.3	40.3	48.4	34.0	30.8	39.0	
	4m	51.8	46.4	58.0	62.5	57.1	75.9	
	4u	80.4	75.0	83.9	69.6	71.4	75.0	
94S-1	8	85.0	72.9	90.0	77.1	68.6	82.9	28
	2	38.4	32.7	43.4	31.4	29.6	38.4	
	4m	64.3	59.8	70.5	75.0	57.1	83.0	
	4u	85.7	66.1	85.7	75.0	66.1	87.5	
94N-5	8	89.5	75.4	94.7	77.2	66.7	88.6	23
	2	44.4	46.6	51.9	39.8	38.3	48.1	
	4m	64.4	50.0	76.7	76.7	55.6	84.4	
	4u	93.6	80.9	95.7	80.9	74.5	85.1	
94S-5	8	93.2	66.9	95.5	84.2	55.6	85.7	26
	2	69.2	47.4	72.2	36.8	34.6	38.3	
	4m	89.5	61.0	89.5	74.3	54.3	81.9	
	4u	98.2	78.2	96.4	89.1	70.9	87.3	
99N-1	8	73.4	64.0	79.9	73.4	59.7	75.5	28
	2	35.3	30.1	34.6	38.5	28.2	36.5	

	4m	60.4	60.4	68.5	64.0	59.5	72.1	
	4u	67.3	56.4	80.8	80.0	56.4	83.6	
99S-1	8	80.7	75.0	83.6	64.3	69.3	70.0	28
	2	35.0	33.8	35.0	32.5	30.6	36.3	
	4m	75.0	73.2	83.0	68.8	73.2	75.9	
	4u	62.5	73.2	67.9	66.1	67.9	73.2	
99N-5	8	98.5	91.0	100	88.7	79.6	94.0	27
	2	56.2	43.8	56.2	33.8	36.2	38.5	
	4m	86.8	68.9	90.6	84.9	73.6	88.7	
	4u	94.4	79.6	96.3	79.6	63.0	90.7	
99S-5	8	94.7	71.4	97.0	71.4	60.9	82.7	26
	2	54.6	40.8	53.8	37.7	26.9	40.0	
	4m	86.8	67.0	89.6	67.0	47.2	75.5	
	4u	100	94.3	100	73.6	88.7	90.6	

Note: N-1 = stimulation provided by normal inputs with one-digit manipulator; N-5 = stimulation provided by normal inputs with five-digit manipulator; S-1 = stimulation provided by slip inputs with one-digit manipulator; S-5 = stimulation provided by slip inputs with five-digit manipulator.

Table D.5: Digit identification accuracy for NIH22 using leave-one-out analysis

Day		Raw data			Normalized			Perts
		Area (%)	Peak (%)	Area & Peak (%)	Area (%)	Peak (%)	Area & Peak (%)	
3N	8	—	—	—	—	—	—	14
	2	—	—	—	—	—	—	
	4m	94.4	74.1	94.4	90.7	79.6	92.6	
	4u	100	96.4	100	100	100	100	
3S	8	—	—	—	—	—	—	14
	2	—	—	—	—	—	—	
	4m	98.2	96.4	100	96.4	96.4	98.2	
	4u	100	100	100	96.4	100	96.4	
9N	8	—	—	—	—	—	—	14
	2	—	—	—	—	—	—	
	4m	94.6	89.3	94.6	91.1	82.1	92.9	
	4u	100	96.4	100	82.1	100	100	
9S	8	—	—	—	—	—	—	14
	2	—	—	—	—	—	—	
	4m	76.8	73.2	80.4	67.9	73.2	75.0	
	4u	92.9	85.7	92.9	60.7	85.7	75.0	
24S-1	8	99.3	91.3	98.7	98.7	89.3	97.3	30
	2	38.9	38.3	41.6	33.6	33.6	33.6	
	4m	79.2	73.3	80.8	94.2	80.0	97.5	
	4u	100	95.0	100	100	98.3	100	
58N-5	8	99.2	89.5	100	97.7	85.7	99.2	27
	2	65.6	61.1	79.4	48.9	43.5	48.9	
	4m	100	80.2	100	99.1	85.8	99.1	
	4u	90.7	83.3	87.0	100	90.7	100	
58S-5	8	99.2	78.2	99.2	99.2	74.4	99.2	27
	2	63.6	44.7	59.1	53.8	38.6	52.3	
	4m	98.1	81.0	95.2	99.0	77.1	99.0	
	4u	90.9	78.2	89.1	90.9	76.4	90.9	
65N-1	8	97.9	98.6	100	95.7	95.0	96.4	28
	2	51.6	50.9	57.9	40.9	43.4	44.7	
	4m	92.9	87.5	92.9	89.3	91.1	97.3	
	4u	100	100	100	100	100	100	
65S-1	8	92.9	97.9	100	93.6	95.0	97.9	28
	2	47.8	37.1	47.8	35.8	34.6	42.1	
	4m	82.1	82.1	84.8	81.3	97.3	95.5	
	4u	98.2	98.2	100	100	98.2	100	
65N-5	8	82.0	82.0	81.2	83.5	78.9	78.9	27
	2	75.6	62.6	76.3	50.4	53.4	50.4	

	4m	76.2	81.9	76.2	76.2	81.9	76.2	
	4u	94.4	96.3	94.4	98.1	96.3	98.1	
65S-5	8	97.0	83.5	99.2	97.7	85.0	98.5	27
	2	61.8	42.7	64.1	47.3	30.5	45.8	
	4m	91.4	83.8	95.2	99.0	85.7	99.0	
	4u	100	89.1	100	100	90.9	100	
72N-1	8	98.6	99.3	99.3	100	100	100	28
	2	49.4	46.9	52.5	44.4	43.8	47.5	
	4m	84.8	95.5	96.4	96.4	92.9	99.1	
	4u	100	100	100	100	100	100	
72S-1	8	99.3	98.6	100	97.9	100	100	28
	2	43.0	32.9	41.1	39.2	34.2	42.4	
	4m	83.9	92.9	95.5	92.0	89.3	97.3	
	4u	98.2	100	100	94.6	100	100	
72N-5	8	92.5	86.5	91.7	93.2	87.2	92.5	26
	2	50.8	53.8	58.5	50.8	40.8	53.8	
	4m	99.0	92.4	99.0	98.1	95.2	100	
	4u	80.0	80.0	76.4	76.4	76.4	74.5	
72S-5	8	99.2	82.0	99.2	97.7	81.2	98.5	27
	2	56.9	40.0	59.2	38.5	34.6	38.5	
	4m	100	77.4	99.1	97.2	77.4	94.3	
	4u	100	100	100	100	100	100	

Note: N-1 = stimulation provided by normal inputs with one-digit manipulator; N-5 = stimulation provided by normal inputs with five-digit manipulator; S-1 = stimulation provided by slip inputs with one-digit manipulator; S-5 = stimulation provided by slip inputs with five-digit manipulator.

Table D.6: Digit identification accuracy for NIH22 using leave-all-in analysis

Day		Raw data			Normalized			Perts
		Area (%)	Peak (%)	Area & Peak (%)	Area (%)	Peak (%)	Area & Peak (%)	
3N	8	—	—	—	—	—	—	14
	2	—	—	—	—	—	—	
	4m	94.4	77.8	100	94.4	79.6	98.1	
	4u	100	100	100	100	100	100	
3S	8	—	—	—	—	—	—	14
	2	—	—	—	—	—	—	
	4m	100	96.4	100	96.4	98.2	100	
	4u	100	100	100	96.4	100	100	
9N	8	—	—	—	—	—	—	14
	2	—	—	—	—	—	—	
	4m	98.2	92.9	96.4	94.6	87.5	98.2	
	4u	100	100	100	85.7	100	100	
9S	8	—	—	—	—	—	—	14
	2	—	—	—	—	—	—	
	4m	85.7	80.4	89.3	73.2	78.6	82.1	
	4u	100	92.9	100	78.6	92.9	92.9	
24S-1	8	100	92.7	100	98.7	92.7	98.7	30
	2	40.9	40.3	44.3	34.2	34.2	36.2	
	4m	81.7	75.8	86.7	95.0	85.0	99.2	
	4u	100	95.0	100	100	98.3	100	
58N-5	8	100	93.2	100	100	90.2	100	27
	2	65.6	62.6	84.0	49.6	44.3	49.6	
	4m	100	82.1	100	99.1	86.8	100	
	4u	92.6	90.7	94.4	100	92.6	100	
58S-5	8	99.2	82.7	99.2	99.2	81.2	99.2	27
	2	63.6	50.8	62.1	54.5	40.2	53.8	
	4m	98.1	84.8	99.0	99.0	79.0	99.0	
	4u	96.4	80.0	94.5	92.7	81.8	92.7	
65N-1	8	99.3	99.3	100	96.4	95.7	100	28
	2	52.8	52.2	61.0	40.9	45.3	47.8	
	4m	95.5	89.3	94.6	92.9	93.8	98.2	
	4u	100	100	100	100	100	100	
65S-1	8	95.0	98.6	100	96.4	96.4	99.3	28
	2	48.4	38.4	51.6	37.1	36.5	42.8	
	4m	84.8	82.1	85.7	83.0	98.2	96.4	
	4u	98.2	98.2	100	100	100	100	
65N-5	8	86.5	85.0	88.0	87.2	84.2	87.2	27
	2	77.1	62.6	80.9	56.5	55.0	56.5	

	4m	78.1	83.8	83.8	78.1	84.8	81.9	
	4u	96.3	98.1	100	100	98.1	100	
65S-5	8	99.2	90.2	100	98.5	89.5	99.2	27
	2	63.4	48.9	66.4	49.6	33.6	51.1	
	4m	93.3	88.6	97.1	99.0	86.7	99.0	
	4u	100	96.4	100	100	96.4	100	
72N-1	8	99.3	100	100	100	100	100	28
	2	50.0	49.4	57.5	45.6	45.0	51.3	
	4m	88.4	95.5	97.3	97.3	93.8	99.1	
	4u	100	100	100	100	100	100	
72S-1	8	99.3	100	100	99.3	100	100	28
	2	44.3	35.4	45.6	39.2	34.2	43.0	
	4m	84.8	95.5	97.3	92.0	91.1	97.3	
	4u	98.2	100	100	96.4	100	100	
72N-5	8	93.2	88.7	93.2	95.5	88.0	96.2	26
	2	50.8	54.6	61.5	51.5	40.8	54.6	
	4m	99.0	95.2	99.0	98.1	95.2	100	
	4u	83.6	80.0	81.8	81.8	78.2	85.5	
72S-5	8	99.2	85.0	100	97.7	85.0	99.2	27
	2	58.5	44.6	63.8	40.8	39.2	41.5	
	4m	100	79.2	100	98.1	80.2	98.1	
	4u	100	100	100	100	100	100	

Note: N-1 = stimulation provided by normal inputs with one-digit manipulator; N-5 = stimulation provided by normal inputs with five-digit manipulator; S-1 = stimulation provided by slip inputs with one-digit manipulator; S-5 = stimulation provided by slip inputs with five-digit manipulator.

Table D.7: Digit identification accuracy for NIH23 using leave-one-out analysis

Day		Raw data			Normalized			Perts
		Area (%)	Peak (%)	Area & Peak (%)	Area (%)	Peak (%)	Area & Peak (%)	
29N	8	99.2	94	99.2	98.5	93.2	98.5	27
	2	64.7	54.1	70.7	46.6	51.9	54.1	
	4m	79.2	75.5	79.2	96.2	91.5	97.2	
	4u	100	98.1	100	96.2	98.1	98.1	
29S	8	100	69.9	100	97.7	90.2	98.5	27
	2	62.4	38.3	60.9	45.9	42.1	45.1	
	4m	85.8	50.9	87.7	96.2	57.5	97.2	
	4u	96.3	81.5	98.1	100	79.6	100	
43N-1	8	88.6	84.3	93.6	84.3	81.4	92.9	28
	2	48.8	45.0	50.6	43.1	37.5	45.0	
	4m	51.8	51.8	61.6	67.9	75.9	86.6	
	4u	98.2	92.9	98.2	100	94.6	100	
43S-1	8	90.0	86.4	92.1	89.3	85.7	90.7	28
	2	34.0	27.0	35.8	25.8	25.8	31.4	
	4m	71.4	65.2	67.9	83.9	76.8	86.6	
	4u	100	89.3	100	100	98.2	100	
43N-5	8	94.0	84.2	94.7	95.5	88.0	95.5	27
	2	64.9	59.5	69.5	56.5	49.6	51.9	
	4m	86.8	68.9	83.0	97.2	86.8	97.2	
	4u	94.3	77.4	92.5	96.2	77.4	92.5	
43S-5	8	96.2	79.7	97.7	94.0	76.7	94.7	26
	2	61.5	38.5	59.2	30.8	26.9	29.2	
	4m	88.6	63.8	88.6	94.3	60.0	95.2	
	4u	77.8	75.9	83.3	77.8	75.9	81.5	

Note: N-1 = stimulation provided by normal inputs with one-digit manipulator; N-5 = stimulation provided by normal inputs with five-digit manipulator; S-1 = stimulation provided by slip inputs with one-digit manipulator; S-5 = stimulation provided by slip inputs with five-digit manipulator.

Table D.8: Digit identification accuracy for NIH23 using leave-all-in analysis

Day		Raw data			Normalized			Perts
		Area (%)	Peak (%)	Area & Peak (%)	Area (%)	Peak (%)	Area & Peak (%)	
29N	8	99.2	94.7	100	99.2	93.2	100	27
	2	66.9	57.1	74.4	52.6	52.6	57.1	
	4m	84.0	77.4	84.0	97.2	93.4	99.1	
	4u	100	98.1	100	100	98.1	100	
29S	8	100	76.7	100	98.5	92.5	100	27
	2	63.2	40.6	64.7	47.4	42.9	48.9	
	4m	86.8	57.5	91.5	97.2	61.3	98.1	
	4u	98.1	85.2	100	100	81.5	100	
43N-1	8	90.0	87.9	97.9	87.9	87.9	97.1	28
	2	53.1	46.3	55.6	43.1	39.4	47.5	
	4m	55.4	54.5	70.5	73.2	80.4	89.3	
	4u	98.2	94.6	100	100	96.4	100	
43S-1	8	93.6	90.7	95.7	94.3	89.3	96.4	28
	2	37.1	33.3	40.3	30.8	29.6	36.5	
	4m	73.2	70.5	75.0	89.3	81.3	90.2	
	4u	100	92.9	100	100	98.2	100	
43N-5	8	94.7	88.0	94.7	95.5	91.7	96.2	27
	2	67.2	59.5	73.3	56.5	51.1	59.5	
	4m	91.5	71.7	89.6	99.1	94.3	99.1	
	4u	94.3	79.2	98.1	96.2	83.0	96.2	
43S-5	8	98.5	85.7	99.2	94.0	81.2	97.0	26
	2	64.6	39.2	63.8	35.4	30.0	37.7	
	4m	91.4	68.6	91.4	96.2	65.7	96.2	
	4u	81.5	81.5	88.9	83.3	75.9	85.2	

Note: N-1 = stimulation provided by normal inputs with one-digit manipulator; N-5 = stimulation provided by normal inputs with five-digit manipulator; S-1 = stimulation provided by slip inputs with one-digit manipulator; S-5 = stimulation provided by slip inputs with five-digit manipulator.

IMAGE EVALUATION
TEST TARGET (QA-3)

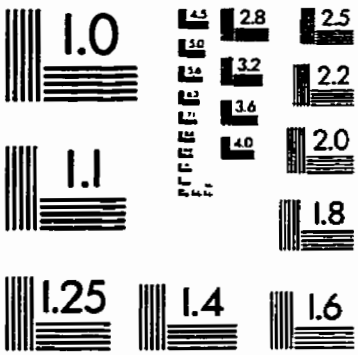

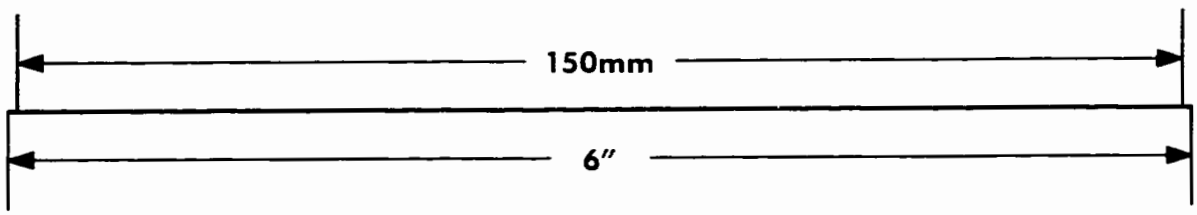

APPLIED IMAGE, Inc
1653 East Main Street
Rochester, NY 14609 USA
Phone: 716/482-0300
Fax: 716/288-5989